

การจัดกำมะถันในน้ำมันไฟโรไลซิสจากยางรถยนต์ใช้แล้วด้วยออกซิเดชันเร่งปฏิกิริยาเชิงแสง
โดยใช้ไทเทเนียมไดออกไซด์



นางสาว ผกากรอง ตรงแก้ว

ศูนย์วิทยทรัพยากร จุฬาลงกรณ์มหาวิทยาลัย

วิทยานิพนธ์นี้เป็นส่วนหนึ่งของการศึกษาตามหลักสูตรปริญญาวิทยาศาสตรมหาบัณฑิต

สาขาวิชาปิโตรเคมีและวิทยาศาสตร์พอลิเมอร์

คณะวิทยาศาสตร์ จุฬาลงกรณ์มหาวิทยาลัย

ปีการศึกษา 2553

ลิขสิทธิ์ของจุฬาลงกรณ์มหาวิทยาลัย

DESULFURIZATION OF PYROLYSIS OIL FROM WASTE TIRES VIA
PHOTOCATALYTIC OXIDATION USING TITANIUM DIOXIDE



Miss Phakakrong Trongkaew

ศูนย์วิทยทรัพยากร

A Thesis Submitted in Partial Fulfillment of the Requirements
for the Degree of Master of Science Program in Petrochemistry and Polymer Science

Faculty of Science

Chulalongkorn University

Academic Year 2010

Copyright of Chulalongkorn University

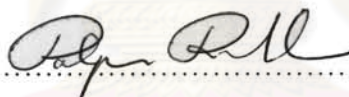
Thesis Title DESULFURIZATION OF PYROLYSIS OIL FROM
WASTE TIRES VIA PHOTOCATALYTIC OXIDATION
USING TITANIUM DIOXIDE
By Miss Phakakrong Trongkaew
Field of Study Petrochemistry and Polymer Science
Thesis Advisor Assistant Professor Napida Hinchiranan, Ph.D.
Thesis Co-Advisor Thanes Utistham, Ph.D.

Accepted by the Faculty of Science, Chulalongkorn University in Partial
Fulfillment of the Requirements for the Master's Degree



.....Dean of the Faculty of Science
(Professor Supot Hannongbua, Dr.rer.nat.)

THESIS COMMITTEE

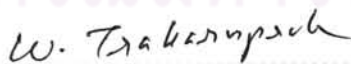


.....Chairman
(Professor Pattarapan Prasassarakich, Ph.D.)

.....Napida Hinchiranan.....Thesis Advisor
(Assistant Professor Napida Hinchiranan, Ph.D.)



.....Thesis Co-Advisor
(Thanes Utistham, Ph.D.)



.....Examiner
(Associate Professor Wimonrat Trakarnpruk, Ph.D.)



.....External Examiner
(Assistant Professor Chantip Samart, Ph.D.)

ผลการรอง ตรงแก้ว : การขจัดกำมะถันในน้ำมันไพโรไลซิสจากยางรถยนต์ใช้แล้วด้วย ออกซิเดชันเร่งปฏิกิริยาเชิงแสงโดยใช้ไทเทเนียมไดออกไซด์. (DESULFURIZATION OF PYROLYSIS OIL FROM WASTE TIRES VIA PHOTOCATALYTIC OXIDATION USING TITANIUM DIOXIDE) อ.ที่ปรึกษาวิทยานิพนธ์หลัก: ผศ.ดร.นพิตา นิชุทธิ์ระนันท์, อ.ที่ปรึกษาวิทยานิพนธ์ร่วม: ดร.ธเนศ อุทิศธรรม, 87 หน้า.

จุดประสงค์ของงานวิจัยนี้ คือ ศึกษาการขจัดกำมะถันในน้ำมันไพโรไลซิสจากยางรถยนต์ใช้แล้วด้วยโฟโตออกซิเดชันเร่งปฏิกิริยาเชิงแสงโดยใช้ไทเทเนียมไดออกไซด์ (TiO_2 หรือ Degussa-P25) ด้วยภาวะที่ไม่รุนแรง น้ำมันไพโรไลซิสจากยางรถยนต์ใช้แล้วมีปริมาณกำมะถัน 0.84% โดยน้ำหนัก กระบวนการโฟโตออกซิเดชันเกิดขึ้นภายใต้การใช้หลอดรังสีอัลตราไวโอเล็ตแบบปรอทความดันสูงขนาด 400 วัตต์ และใช้เวลาในการฉายแสง 1-7 ชั่วโมง กำมะถันที่ถูกออกซิไดซ์ถูกขจัดลงมาในวัฏภาคที่ใช้ในการสกัด ผลของปริมาณไทเทเนียมไดออกไซด์ (1-7 กรัม/ลิตร) อุณหภูมิในการเผาไทเทเนียมไดออกไซด์ ($400-800^\circ\text{C}$) อุณหภูมิที่ใช้ในการทำปฏิกิริยา ($30-70^\circ\text{C}$) อัตราส่วนน้ำมันต่อตัวทำละลายที่ใช้ในการสกัด (1/1-1/5 โดยปริมาตร) ชนิดของตัวทำละลายที่ใช้ในการสกัด (น้ำกลั่น เมทานอล และ อะซีโตไนไทรล์) อัตราการไหลของอากาศ ($0-150$ มิลลิลิตร/นาที่) ความเข้มข้นของไฮโดรเจนเปอร์ออกไซด์ ($0-30$ โดยน้ำหนัก) และจำนวนรอบในการขจัดกำมะถัน (1-3 รอบ) พบว่าประสิทธิภาพในการขจัดกำมะถันสูงสุดที่ 47.5% เมื่อใช้ไทเทเนียมไดออกไซด์ 7 กรัม/ลิตรที่ไม่ผ่านการเผา ในระบบที่มีน้ำมันไพโรไลซิส/อะซีโตไนไทรล์ 1/4 โดยปริมาตร ที่อุณหภูมิ 50°C ภายในเวลา 7 ชั่วโมง การออกซิเดชันของสารประกอบกำมะถันในน้ำมันไพโรไลซิสหลังการดีซัลเฟอไรเซชันเร่งปฏิกิริยาเชิงแสงถูกตรวจสอบด้วยแก๊สโครมาโทกราฟีชนิดเฟรมโฟโตเมตริกดีเทคเตอร์ (Gas Chromatography/Flame photometric detector, GC-FPD) และโครมาโทกราฟีของเหลวสมรรถนะสูง (High performance liquid chromatography, HPLC) ผลการทดลองแสดงให้เห็นว่ากระบวนการออกซิเดชันเร่งปฏิกิริยาเชิงแสงโดยใช้ไทเทเนียมไดออกไซด์มีประสิทธิภาพในการลดสารประกอบกำมะถันในน้ำมันไพโรไลซิส โดยเฉพาะกลุ่มเบนโซไทโอพีนโดยเปลี่ยนให้เป็นซัลโฟนหรือซัลฟอกไซด์ที่มีความเป็นขั้วเพิ่มขึ้น ซึ่งง่ายต่อการละลายในวัฏภาคของขั้นสกัด

สาขาวิชาปิโตรเคมีและวิทยาศาสตร์พอลิเมอร์ ลายมือชื่อนิสิต ตรงแก้ว ตรงแก้ว

ปีการศึกษา 2553 ลายมือชื่อ อ.ที่ปรึกษาวิทยานิพนธ์หลัก นพิตา น.

ลายมือชื่อ อ.ที่ปรึกษาวิทยานิพนธ์ร่วม ธเนศ

5172368323 : MAJOR PETROCHEMISTRY AND POLYMER SCIENCE

KEYWORDS : DESULFURIZATION / WASTE TIRE / PYROLYSIS /
PHOTOCATALYTIC OXIDATION / TITANIUM DIOXIDE

PHAKAKRONG TRONGKAEW : DESULFURIZATION OF
PYROLYSIS OIL FROM WASTE TIRES VIA PHOTOCATALYTIC
OXIDATION USING TITANIUM DIOXIDE. THESIS ADVISOR :
ASST. PROF. NAPIDA HINCHIRANAN, Ph.D., THESIS CO-ADVISOR
: THANES UTISTHAM, Ph.D., 87 pp.

The aim of this research was to study the desulfurization of waste tire pyrolysis oil via photo-oxidation catalyzed by titanium dioxide (TiO₂ or Degussa P-25) at mild reaction condition. The starting waste tire pyrolysis oil contained 0.84 wt% of sulfur content. The photo-oxidation of the pyrolysis oil was carried out by using a 400 W of high-pressure mercury lamp for 1-7 h. The oxidized sulfur compounds were then removed into the extracting phase. The effects of TiO₂ content (1-7 g/L), TiO₂-calcination temperature (400-800°C), reaction temperature (30-70°C), pyrolysis oil/extracting solvent (1/1-1/5 (v/v)), type of extracting solvent (distilled water, methanol and acetonitrile), air flow rate (0-150 mL/min) hydrogen peroxide concentration (0-30 wt%) and stages of the reaction (1-3 stages) on the %sulfur removal were also investigated. The maximum %sulfur removal at 47.5% was achieved when 7 g/L of uncalcined TiO₂ was loaded into the system containing 1/4 (v/v) of pyrolysis oil/acetonitrile at 50°C for 7 h after 3 stages of reaction. The oxidation of sulfurous compounds in the pyrolysis oil before and after photocatalytic desulfurization was detected by using gas chromatography equipped with a flame photometric detector (FPD) and high performance liquid chromatography (HPLC). The results indicated that the photocatalytic desulfurization using TiO₂ was effective to reduce the sulfurous compounds in the pyrolysis oil; especially, benzothiophenes by converting to sulfones or sulfoxides with higher polarity which was easier to be dissolved into the extracting phase.

Field of Study : Petrochemistry and Polymer Science Student's Signature Phakakrong Trongkaew

Academic Year : 2010

Advisor's Signature Napida Hinchiran

Co-Advisor's Signature Thanes Utistham

ACKNOWLEDGEMENTS

The author wishes to express greatest gratitude to her advisor, Assistant Professor Dr. Napida Hinchiranan, for her advice, assistance and generous encouragement throughout the course of this research. In addition, the author wishes to express deep appreciation to Dr. Thanet Utistham, Associate Professor Dr. Wimonrat Trakarnpruk, Assistant Professor Dr. Chanatip Samart, and Professor Dr. Pattarapan Prasassarakich for serving as the chairman and members of her thesis committee, respectively, for their valuable suggestions and comments.

Appreciation is also extended to Program of Petrochemistry and Polymer Science and the Department of Chemical Technology, Faculty of Science, Chulalongkorn University for granting financial support to fulfill this study and provision of experimental facilities.

The author is thankful to Center for Petroleum, Petrochemicals, Chulalongkorn University. The Institute for the Promotion of Teaching Science and Technology (The Project for the Promotion of Science and Mathematics Talented Teachers, PSMT) and Thailand Institute of Scientific and Technological Research for financial support throughout this research. The author wishes to express deep appreciation to Mr. Kriengkhai Boonkaruswong and Mr. Krisda Yotarak for his help. Finally, the author is very appreciated to her family and her best friends for their assistance and encouragement throughout her entire education.

CONTENTS

	PAGE
ABSTRACT (in Thai).....	iv
ABSTRACT (in English).....	v
ACKNOWLEDGEMENTS	vi
CONTENTS.....	vii
LIST OF TABLES	x
LIST OF FIGURES	xi
NOMENCLATURES	xiii
CHAPTER I: INTRODUCTION.....	1
1.1 The Statement of Problem	1
1.2 Objectives of the Research Work	3
1.3 Scope of the Research Work.....	4
CHAPTER II: THEORY AND LITERATURE REVIEWS	5
2.1 Tire.....	5
2.2 Vulcanization Process	6
2.2.1 Vulcanizing Agents.....	6
2.2.2 Sulfur Vulcanization	6
2.3 Waste Tire.....	7
2.4 Pyrolysis	8
2.5 Pyrolysis of Waste Tire.....	9
2.6 Sulfur Compounds in Petroleum Products and Waste Tire Pyrolysis Oil	12
2.7 Classification of Desulfurization Technologies.....	15
2.7.1 Catalysis Based HDS Technologies.....	17
2.7.2 Non-HDS Based Desulfurization Technologies	17
2.8 Photocatalytic Desulfurization	21
2.8.1 Titanium Dioxide or Titania (TiO ₂).....	22
2.8.2 Photocatalytic Process	24
2.8.3 Mechanisms of Photocatalytic Desulfurization	26
2.9 Literature Reviews.....	27

CONTENTS (continued)

	PAGE
CHAPTER III: EXPERIMENT AND CHARACTERIZATION.....	31
3.1 Materials	31
3.2 Experimental Procedures	31
3.2.1 Pyrolysis Process	31
3.2.2 Photocatalytic Desulfurization.....	32
3.3 Analytical Method	34
3.3.1 Characterization of Waste Tire Powder.....	34
3.3.2 Characterization of TiO ₂	34
3.3.2.1 X-Ray Diffractometry (XRD).....	34
3.3.2.2 Scanning Electron Microscopy (SEM).....	35
3.3.3 Type and Content of Sulfurous Compounds in the Pyrolysis Oil.....	35
3.3.3.1 Total Sulfur Content	35
3.3.3.2 Gas Chromatography –Flame Photometric Detector (GC-FPD).....	35
3.3.3.3 High Performance Liquid Chromatography (HPLC)	36
3.3.4 Quality of Pyrolysis Oil	36
CHAPTER IV: RESULTS AND DISCUSSION	37
4.1 Characterization of Waste Tire	37
4.2 Products Derived from Waste Tire Pyrolysis	38
4.3 Photocatalytic Desulfurization of Pyrolysis Oil Derived from Waste Tire.....	39
4.3.1 Influence of TiO ₂ Dosage on Degree of Sulfur Removal	39
4.3.2 Influence of Calcination Temperature on Degree of Desulfurization.....	40
4.3.3 Influence of Reaction Temperature on Degree of Sulfur Removal	42
4.3.4 Influence of Air Flow Rate on Degree of Sulfur Removal.....	43
4.3.5 Influence of H ₂ O ₂ Concentration on Degree of Sulfur Removal	44

CONTENTS (continued)

	PAGE
4.3.6 Influence of Extracting Solvent on Degree of Desulfurization ...	46
4.3.7 Influence of the Stage on Degree of Desulfurization.....	49
4.4 Characterization of Sulfurous Compounds Containing in Pyrolysis Oil.....	49
4.5 Quality of Oxidized Pyrolysis Oil.....	54
CHAPTER V: CONCLUSIONS	56
5.1 Conclusions.....	56
5.1.1 Characterization of Waste Tire and Its Pyrolysis Products	56
5.1.2 Photocatalytic Desulfurization of Pyrolysis Oil Derived from Waste Tire	56
5.1.3 Quality of the Photo-Oxidized Pyrolysis Oil	57
5.2 Recommendations.....	57
5.2.1 Enhancement of Titanium Dioxide Efficiency	57
5.2.2 Preparation of TiO ₂ Photocatalyst on Various Rigid Supports....	58
REFERENCES	59
APPENDICES	68
APPENDIX A: CALCULATION OF PRODUCT YIELDS	69
APPENDIX B: CALCULATION OF GROSS CALORIFIC HEATING VALUE	71
APPENDIX C: CALCULATION OF %SULFUR REMOVAL.....	73
APPENDIX D: DATA OF SULFUR REMOVAL EFFICIENCY	75
APPENDIX E: GC-FPD CHROMATOGRAMS OF STANDARD SULFUR COMPOUNDS, PYROLYSIS OIL AND OXIDIZED PYROLYSIS OIL	83
VITA.....	87

LIST OF TABLES

TABLE	PAGE
1.1 Comparison of tire pyrolysis oil with diesel, gasoline and crude oil (petroleum product)	2
2.1 The composition of a typical passenger tire by weight	5
2.2 Typical composition of the scrap tire feedstock	8
2.3 Some characteristics of crude oils	12
2.4 Types of organic sulfur	13
2.5 Studies on the adsorptive desulfurization	19
2.6 The properties of the anatase and rutile phase	23
3.1 Parameters and range of study for photocatalytic desulfurization of the waste tire pyrolysis oil using TiO ₂	33
4.1 Composition of waste tire feedstock.....	37
4.2 Gross calorific values of various materials.....	38
4.3 Yield of waste tire pyrolysis products	38
4.4 Effect of stage of reaction on sulfur reduction of waste tire pyrolysis oil.....	49
4.5 Gross calorific heating value of photocatalytic oxidation of sulfur in pyrolysis oil using TiO ₂ dosage 7 g/L	55
4.6 Viscosity, copper strip corrosion and gross calorific value of oils.....	55

ศูนย์วิทยทรัพยากร
 จุฬาลงกรณ์มหาวิทยาลัย

LIST OF FIGURES

FIGURE	PAGE
1.1 Reaction pathway for 3-methyl benzothiophene in acetonitrile by photoirradiation.....	3
2.1 The process of sulfur vulcanization	7
2.2 GC-FPD chromatograms for three transportation fuels.....	14
2.3 GC-FPD chromatograms of waste tire pyrolysis oil.....	15
2.4 Desulfurization technologies classified by nature of a key process to remove sulfur	16
2.5 Crystal structures of (a) anatase, (b) rutile, and (c) brookite..	22
2.6 Main process occurring on a semiconductor particle: (a) electron-hole generation; (b) oxidation of donor (D); (c) reduction of acceptor (A); (d) and (e) electron-hole recombination at surface and in bulk, respectively.	24
3.1 Schematic diagram of the fixed bed reactor for pyrolysis process.	32
3.2 Diagram of experimental apparatus for photocatalytic desulfurization of pyrolysis oil.....	33
4.1 Effect of TiO ₂ dosage on sulfur removal of pyrolysis oil derived from waste tire: 1 g/L (◆); 3 g/L (◻); 5 g/L (●); 7 g/L (▲) and 10 g/L (◇) (pyrolysis oil/distilled water = 1/1 (v/v); air flow rate = 150 mL/min and T = 30°C).....	39
4.2 Effect of calcination temperature on sulfur removal of waste tire pyrolysis oil: no calcined (✕); 400°C (■); 600°C (◇) and 800°C (●) (TiO ₂ / pyrolysis oil = 7 g/L; pyrolysis oil/distilled water = 1/4 (v/v) ; air flow rate = 150 mL/min and T = 30°C).....	40
4.3 SEM morphology of TiO ₂ (a) before and after calcination at (b) 400°C; (c) 600°C and (d) 800°C.....	41
4.4 XRD patterns of TiO ₂ (a) before and after calcination at (b) 400°C; (c) 600°C and (d) 800°C (A = anatase form and R = rutile form)	42
4.5 Effect of reaction temperature on sulfur reduction of waste tire pyrolysis oil: 30°C (◇); 40°C (●); 50°C (▲) and 70°C (◻) (TiO ₂ / pyrolysis oil = 7 g/L; pyrolysis oil/distilled water = 1/4 (v/v); air flow rate = 150 mL/min).....	43

LIST OF FIGURES (continued)

FIGURE	PAGE
4.6 Effects of air flow rate on sulfur reduction of waste tire pyrolysis oil: 0 mL/min (—◆—); 50 mL/min (—□—); 100 mL/min (—▲—) and 150 mL/min (—✱—) (TiO ₂ /pyrolysis oil = 7 g/L; pyrolysis oil/distilled water = 1/4 (v/v) and T = 50°C).....	44
4.7 Effect of adding H ₂ O ₂ on sulfur reduction of waste tire pyrolysis oil: with air flow rate 150 mL/min (—■—) and no air (—◆—) (TiO ₂ /pyrolysis oil = 7 g/L; pyrolysis oil/distilled water = 1/4 (v/v); T = 50°C and reaction time = 7h).....	45
4.8 Effects of the pyrolysis oil/distilled water (v/v) on sulfur reduction of waste tire pyrolysis oil: 1/1 (—■—); 1/2 (—□—); 1/3 (—▲—); 1/4 (—◆—) and 1/5 (—✱—) (TiO ₂ /pyrolysis oil = 7 g/L; air flow rate = 150 mL/min and T = 50°C).....	46
4.9 Effects of type used as extracting solvent on sulfur reduction of waste tire pyrolysis oil: distilled water (—◆—); methanol (—▲—) and acetonitrile (—■—) (TiO ₂ / pyrolysis oil = 7 g/L; pyrolysis oil/extracting solvent = 1/4 (v/v); air flow rate = 150 mL/min and T = 50°C).....	48
4.10 Appearance of pyrolysis oil in various extracting solvents: (a) distilled water; (b) methanol and (c) acetonitrile.....	48
4.11 GC-FPD Chromatograms of (a) pyrolysis oil and (b) photo-oxidized pyrolysis oil.....	51
4.12 HPLC Chromatograms of standard sulfur compounds and pyrolysis oil (a) before and (b) after photocatalytic desulfurization.	52
4.13 Reaction pathway for 3-methyl BT in acetonitrile by photoirradiation.....	53
4.14 Reaction pathway for DBT in acetonitrile by photoirradiation	53

NOMENCLATURES

A	:	Acceptor Species
BT	:	Benzothiophene
BR	:	Butadiene Rubber
cb	:	Conduction Band
CH ₄	:	Methane
C ₂ H ₄	:	Ethene
C ₃ H ₆	:	Propene
C ₄ H ₈	:	Butene
CLO	:	Commercial Light Oil
CO	:	Carbon Monoxide
CO ₂	:	Carbon Dioxide
COS	:	Carbonyl Sulfide
D	:	Donor Species
DBT	:	Dibenzothiophene
2,3-DMBT	:	2,3-Dimethyl Benzothiophene
3,6-DMDBT	:	3,6-Dimethyl Dibenzothiophene
4,6-DMDBT	:	4,6-Dimethyl Dibenzothiophene
DTDM	:	Dithiodimorpholine
e _{cb} ⁻	:	Electron in the Conduction Band
FCC	:	Fluid Catalytic Cracking
GC-FPD	:	Gas Chromatography/Flame Photometric Detector
GC-MS	:	Gas Chromatography/Mass Spectrometer
HDS	:	Hydrodesulfurization
H ₂ O ₂	:	Hydrogen Peroxide
HPLC	:	High Performance Liquid Chromatography
HO ₂ [•]	:	Hydroperoxyl Radical
H ⁺	:	Hydrogen Ion
h _{vb} ⁺	:	Hole in the Valence Band
H ₂ S	:	Hydrogen Sulfide
LGO	:	Light Gas Oil

NOMENCLATURES (continued)

4-MDBT	:	4-Methyl Dibenzothiophene
NR	:	Natural Rubber
$O_2^{\cdot-}$:	Superoxide Radical Anion
ODS	:	Oxidative Desulfurization
OH^-	:	Hydroxide Ion
OH^{\cdot}	:	Hydroxyl Radicals
$OH_2^{\cdot-}$:	Hydroperoxide Ion
RFCC	:	Residue Fluidized Catalytic Cracking
SBR	:	Styrene-Butadiene Rubber
SC	:	Semiconductor
SEM	:	Scanning Electron Microscopy
T	:	Thiophene
TiO_2	:	Titanium Dioxide
TMTD	:	Tetramethylthiuram Disulfide
2,3,5-TMBT	:	2,3,5-Trimethyl Benzothiophene
2,3,6-TMBT	:	2,3,6-Trimethyl Benzothiophene
2,3,7-TMBT	:	2,3,7-Trimethyl Benzothiophene
2,4,6-TMDBT	:	2,4,6-Trimethyl Dibenzothiophene
TNF	:	2,4,5,7-Tetranitro-9-Fluorene
TNs	:	Titanium Dioxide Nanotube Arrays
UV	:	Ultraviolet
vb	:	Valence Band
XRD	:	X-ray Diffraction

CHAPTER I

INTRODUCTION

1.1 The Statement of Problem

Nowadays, the world annually generates waste tires as 5×10^6 tons, representing 2% of total solid waste (Dall'Orso et al., 1999; Galvagno et al., 2002; Snyder, 1998). Since the waste tire is not biodegradable material and it also contains large amount of sulfur used as vulcanizing agents, it should be appropriately disposed instead of direct combustion. However, the waste tire has higher heating value (39.1 MJ/kg) (Qing et al., 2009) when compared to biomass such as palm (18-20 MJ/kg) (Vijaya, Chow, and Ma, 2004) or rice husk (13-15 MJ/kg) (Jenkins, 1989; Natarajan et al., 1998). Thus, it has been expected to replace the conventional fuels. To produce alternative fuels from solid waste, pyrolysis is the thermal degradation process to convert solid materials as solid carbon residue, a condensable oil and gases.

Tire pyrolysis is currently receiving renewed attention. Recycling of tires by pyrolysis offers an environmentally attractive method. The products of the tire pyrolysis process are solid char (30-40 wt%), condensable liquid (40-60 wt%), and gases (5-20 wt%). The solid residue contains carbon black and the mineral matter initially present in the tire. This solid char may be used as reinforcing filler in the rubber industry, activated carbon or smokeless solid fuel. The liquid product consists of various complex mixtures of organic components. Thus, the derived oils may be used directly as fuels, petroleum refinery feedstock or a source of chemicals. The gas fraction can be used as fuel in the pyrolysis process. According to the fact that the pyrolysis liquid product contains various organic compounds having 5–20 carbons with aromatics proportion (McNeill, 1989), the derived pyrolysis oils may be directly used as fuels or petroleum refinery feedstock. Unfortunately, a large amount of sulfur compounds found in the pyrolysis waste tire oil can cause environmental problems.

In petroleum products, sulfur-containing compounds in oil are converted to SO_x by combustion, which is one of the main sources of acid rain and air pollution. Legislation in Europe in 2005 limited the sulfur content in light oil as maximum as

50 ppm maximum. The United States has also set a limit of sulfur content in fuels used for highway to 15 ppm by the middle of 2006 (Zhao et al., 2007).

Some basic properties of tire pyrolysis oil were measured and compared to those of conventional petroleum fuel, as given in Table 1.1. The viscosity of tire pyrolysis oil is higher than that of diesel by about 1.5 times. The flash point and the fire point of the tire pyrolysis oil are closer to those of diesel. However, the sulfur content in tire pyrolysis oil is higher than that in the diesel fuel (Murugan, Ramaswamy, and Nagarajan, 2006). Hydrodesulfurization (HDS) is commonly applied to reduce the amount of sulfurous compounds in petroleum refinery. However, this process generally conducts under severe reaction conditions ($> 50 \text{ kg/cm}^3$ and $> 250^\circ\text{C}$) and consumes hydrogen gas to react with sulfur compounds in the presence of catalysts (Grassie, 1971). In addition, the sulfur-containing compounds in the light oil are difficult to be removed via HDS method (Madorsky, 1964).

To decrease energy and hydrogen consumption during desulfurization, photocatalytic desulfurization has been a new technique to decompose sulfurous compounds in oil using titanium dioxide (TiO_2) as a catalyst in recent years.

Table 1.1 Comparison of tire pyrolysis oil with diesel, gasoline and crude oil (petroleum product) (Murugan et al., 2006)

Property	Diesel	Gasoline	Crude oil ^a (petroleum product)	Tire pyrolysis oil
Density at 15 °C, kg/m ³	0.83	0.74	0.99	0.92
Kinematic Viscosity, cst at 40 °C	2.58	-	180	3.77
Net calorific value, MJ/kg	43.8	45.0	-	38.0
Flash point, °C	50.0	-42.8	Max.66	43.0
Fire point, °C	56.0	-48.9	-	50.0
Sulfur content, %	0.29	-	1.40	0.72
Ash content, %	0.01	-	0.10	0.31
Aromatic content, %	26.0	-	-	66.6 ^b
Non-aromatic content, %	74.0	-	-	33.4 ^b

^aData obtained for crude oil specifications (Available from: <http://www.Platts.com>)

^bLaresgoiti et al, (2004)

The previous research works revealed that the photocatalytic oxidation has potential to decrease the amount of sulfur derivatives (Laresgoiti et al., 2004; Mutsuzawa et al., 2002). Typically, this process involves two principle steps. In the first step, the sulfur-containing compounds are oxidized by photocatalysis. The oxidized sulfurous compounds could be classified as sulfoxides or sulfones resulting from oxygen donation to sulfurous compounds. The mechanism for photocatalytic desulfurization of 3-methyl benzothiophene is shown in Figure 1.1. In the second step, the oxidized sulfurous products with higher polarity can be readily extracted from the hydrocarbon fuel by dissolving in a polar solvent (Ali, Al-Malki, and Ahmed, 2009).

1.2 Objectives of the Research Work

The objectives of this research were stated as followed:

1. To study the photocatalytic desulfurization of the pyrolysis oil derived from waste tire.
2. To investigate the effect of reaction parameter: TiO₂ dosage, calcination temperature, type and content of extracting solvent, air flow rate, hydrogen peroxide (H₂O₂) content and stage of reaction on the %sulfur removal.

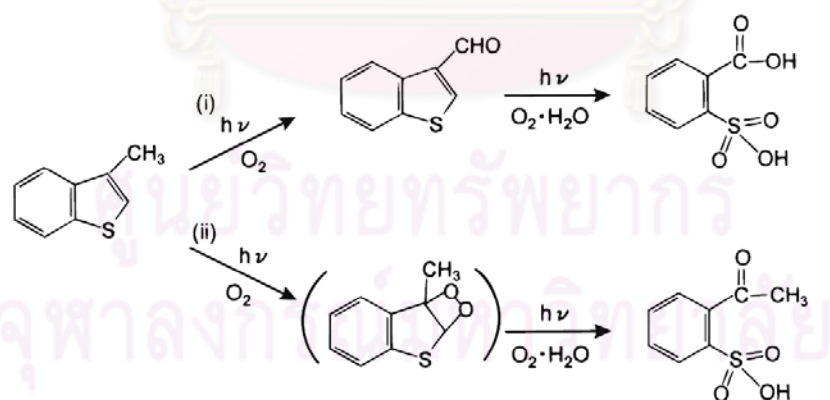


Figure 1.1 Reaction pathway for 3-methyl benzothiophene in acetonitrile by photoirradiation (Shiraishi et al., 1999).

1.3 Scope of the Research Work

The details of experimental procedure for this research were presented as followed:

1. Survey previous research literatures related to this work.
2. Prepare materials, design and construct the reactor for photocatalytic desulfurization.
3. Characterize the waste tire powder ($\phi = 355\text{-}425 \mu\text{m}$): proximate analysis, ultimate analysis, gross calorific value and sulfur content.
4. Prepare the pyrolysis oil from pyrolysis of waste tire powder in a fixed bed reactor at 400°C under nitrogen atmosphere with 0.1 L/min of flow rate for 15 min and then analyze its gross calorific value and total sulfur content.
5. Investigate the effect of reaction parameters used in photocatalytic desulfurization of pyrolysis oil on the %sulfur removal as following:
 - TiO_2 dosage: $1\text{-}10 \text{ g/L}$ of pyrolysis oil
 - Calcination temperature of TiO_2 : $400\text{-}800^\circ\text{C}$
 - Reaction temperature: $30\text{-}70^\circ\text{C}$
 - Pyrolysis oil/extracting solvent (v/v): $1/1\text{-}1/5$
 - Type of extracting solvent: distilled water, methanol and acetonitrile
 - Air flow rate: $0\text{-}150 \text{ ml/min}$
 - H_2O_2 concentration: $0\text{-}30 \text{ wt}\%$
 - Stage of the reaction: $1\text{-}3$ stages
7. Characterize the oxidized sulfurous compounds in the extracting solvents by using high performance liquid chromatography (HPLC)
8. Investigate type and content of remaining sulfurous compounds in the oxidized pyrolysis oil by using gas chromatography equipped with flame photometric detector (GC-FPD).
9. Summarize the results

CHAPTER II

THEORY AND LITERATURE REVIEWS

2.1 Tire (Dodds et al., 1983)

Tire is produced from vulcanization of rubbers such as styrene-butadiene rubber (SBR) and butadiene rubber (BR). Moreover, tire also consists of reinforcing textile cards, steel of fabric belts and steel-wire bead. Another important component in tire manufacturing is carbon black, which is used to strengthen the rubber and aid abrasion resistance. In addition, extender oil, a mixture of aromatic hydrocarbons, is added to soften the rubber and to improve workability. In the rubber vulcanization process, sulfur is used to crosslink the polymer chains within the rubber, and it also hardens and prevents excessive deformation at elevated temperature. The accelerator is typically an organosulfur compound which acts as a catalyst for the vulcanization process. The zinc oxide and stearic acid also control the vulcanization process and enhance the physical properties of the rubber vulcanizates. A typical composition for tire is shown in Table 2.1.

Table 2.1 The composition of a typical passenger tire by weight (Dodds et al., 1983)

Composition of tire	wt%
Styrene butadiene rubber (SBR)	62.1
Carbon black	31.0
Extender oil	1.9
Zinc oxide	1.9
Stearic acid	1.2
Sulfur	1.1
Accelerator	0.7
Total	99.9

2.2 Vulcanization Process

2.2.1 Vulcanizing Agents (Dick, 2001)

Sulfur is the most widely used vulcanizing agent in conjunction with activators (metal oxides and fatty acids) and organic accelerators. These are primarily used for general purpose rubbers such as natural rubber (NR), SBR and BR. They contain unsaturation (double bonds) as opposed to basically saturated rubbers (e.g., butyl, EPDM, etc.). Sulfur donors are used to replace parts or all of the elemental sulfur to improve thermal and oxidative aging resistance. They may also be used to reduce the possibility of sulfur bloom and to modify curing and processing characteristics. Two chemicals, which have been developed over the years to function as sulfur donors alone or in combination with sulfur, are tetramethylthiuram disulfide (TMTD) and dithiodimorpholine (DTDM). They provide significantly improved heat and aging resistance plus reduced heat build-up.

2.2.2 Sulfur Vulcanization (Mark, Erman, and Eirich, 2005)

Vulcanization of rubber is generally irreversible which is similar to other thermosets. This is contrast to thermoplastic processes (the melt-freeze process) which are the characteristic behavior of most modern polymers. The cross-linking in vulcanization is usually done by sulfur. The main polymers subjected to vulcanization are polyisoprene or NR and SBR, which are used for most passenger tires. The cure package is specifically adjusted for the substrate and the application. The reactive sites are allylic hydrogen atoms. These C-H bonds are adjacent to carbon-carbon double bonds. During vulcanization, some of these C-H bonds are replaced by chains of sulfur atoms linking with a cure site of another polymer chain. These bridges contain between one and eight sulfur atoms. The number of sulfur atoms in the crosslink strongly influences the physical properties of the final rubber vulcanizates. Short crosslinks give the rubber to have better heat resistance. The rubber vulcanizates containing crosslinks with higher number of sulfur atoms exhibit the good dynamic properties with lesser heat resistance. Dynamic properties are important for flexing movements of the rubber vulcanizates, e.g., the movement of a side-wall of a running tire. Without good flexing properties, these movements rapidly form cracks and, ultimately make the failure of rubber vulcanizates. The crosslink obtained from sulfur vulcanization process shown in Figure 2.1.

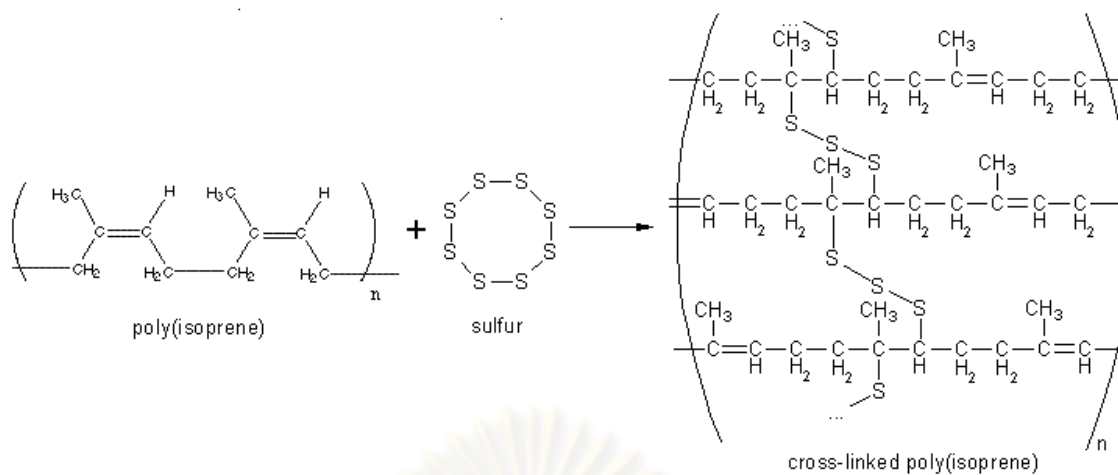


Figure 2.1 The process of sulfur vulcanization (Mark et al., 2005).

2.3 Waste Tire

Large quantities of waste tires are annually generated in the world. Their disposal represents an environmental and economic problem. Approximately, 5×10^6 tons/year of waste tires produced in the world were divided to be produced in Europe as 2×10^6 tons, in North America as 2.5×10^6 tons and in Japan 0.5×10^6 tons (Galvagno et al, 2002). Different alternatives for tire recycling such as retreading, reclaiming, incineration, grinding, etc., have been used. However all have significant drawbacks and limitations (Schnecko, 1994). Thus, it leads the environmental problem as well as economic problem of the disposal of an increasingly large mass of waste tires. The largest application of waste tires is; however, as a supplemental energy resource because tires mainly consist of natural rubber and synthetic rubbers with long hydrocarbon chains resulting in a high heating value. Pyrolysis can be considered as a non-conventional method for tire recycling and complex materials cannot be remolded. In the pyrolysis process, the organic volatile matter of tires (mainly the rubber polymers) is decomposed to low molecular weight products, liquids or gases, which can be used as fuels or a source of chemicals. The remaining inorganic components (mainly steel) and the non-volatile carbon black found in a solid residue can be recycled in worthwhile applications (Laresgoiti, 2000).

The composition of a typical scrap tire feedstock is shown in Table 2.2. According to high volatiles and fixed carbon contents, the scrap tires show high gross calorific value as 40 MJ/kg (Williams and Bottrill, 1995).

Table 2.2 Typical composition of the scrap tire feedstock (Williams and Bottrill, 1995)

Elemental composition (wt%)	Proximate analysis (wt%)	Gross calorific value (MJ/kg)
C 85.9	Volatiles 66.5	40.0
H 8.0	Fixed carbon 30.3	
N 0.4	Ash 2.4	
S 1.0	Moisture 0.8	
O 2.3		

Thus, the scrap or waste tires are interesting materials for using as an alternative energy resource. For this reason, both pyrolysis and combustion are currently receiving renewed attention. Pyrolysis offers an environmentally attractive method to decompose a wide range of wastes, including waste tires. In the pyrolysis process, the organic volatile matter of tires (ca. 60 wt%) is decomposed to obtain low molecular weight products, liquids or gases, which can be used as fuels or chemicals feedstock. The remaining non-volatile carbon black and the inorganic components (ca. 40 wt%) after pyrolysis can be also recycled for using in other applications. For combustion of tires to generate the electrical energy, the conditions applied in this process must be optimized to minimize the emissions (Juma et al., 2006).

2.4 Pyrolysis (Ashok, 2008)

Pyrolysis or thermal cracking can be generally defined as the decomposition of organic matters in the absence of oxygen or in an oxygen-starved atmosphere. The pyrolysis process may be endothermic, or exothermic, depending on the temperature of the reacting system. The steps of process include with drying and grinding the feed to sufficiently small particles for rapid reaction, pyrolysis reaction and the separation of products. The type of pyrolysis processes are listed as followed:

- **Slow Pyrolysis**

This is a conventional process whereby the heating rate keeps slow (approximately 5-7°C/min). This slow heating rate leads to higher char yields than the

liquid and gaseous products. Different kinds of biomass, such as wood samples, safflower seeds, sugarcane bagasse, sunflower seeds, municipal wastes, etc., are generally subjected to slow pyrolysis to produce the solid fuels.

- **Fast Pyrolysis**

Fast pyrolysis is considered as a better process than the slow pyrolysis. The heating rate for fast pyrolysis is high as 300-500°C/min to get the higher liquid yield. Fluidized-bed reactors are suitable for this process since they can provide the high heating rates and rapid devolatilization. They are also easy to operate. The reactor types such as entrained flow reactors, circulating fluidized-bed reactors, rotating reactors, etc. are used for this purpose.

- **Flash Pyrolysis**

This is an improved version of fast pyrolysis to obtain the desired high reaction temperature within a few seconds. The heating rates are very high (ca.1000°C/min). The flash pyrolysis process is carried out at atmospheric pressure. The entrained flow and fluidized-bed reactors are appropriate reactors for this process.

2.5 Pyrolysis of Waste Tire (Juma et al., 2006)

Tire pyrolysis (thermal decomposition in an oxygen-free environment) is currently receiving renewed attention. Recycling of tires by pyrolysis offers an environmentally attractive method. The products of the tire pyrolysis process are: solid char (30-40 wt%), liquid residue (40-60 wt%) and gases (5-20 wt%). The solid residue contains carbon black and the mineral matters initially presented in the tire. This solid char may be used as reinforcing filler in the rubber industry, as activated carbon or as smokeless fuel. The liquid product consists of a very complex mixture of organic components. Thus, the derived oils may be directly used as fuels, petroleum refinery feedstock or a source of chemicals. The gas fraction can be used as fuel in the pyrolysis process.

Pyrolysis is one of recycle methods for waste tire to supply the market for pyrolysis products. For this reason, characterization of pyrolysis products and possibilities of their application in other processes are very important. The details of pyrolysis products from waste tire pyrolysis are given below:

- **Solid Residue**

The solid residue contains carbon black and some mineral matters for vulcanization process. Several studies have reported the production of chars and activated carbon from waste tires via pyrolysis process (Edward et al., 2004; Zabaniotou et al., 2004). These activated carbons have been used to adsorb organic substances such as phenol, basis dyes, butane and natural gas. It is also adsorbed heavy metals for waste water treatment. The activated carbon obtained from solid product of pyrolysis is produced by activation with an activating gas at 800-1000°C. Carbon characteristics (especially specific area) are greatly influenced by the degree of the activation, nature of activating agent (steam or CO₂) and process temperature. Based on the current technology and literature results, the activated carbon from waste tire which is activated below 700°C looks impractical. The particle size of the tire rubber also affects the porosity of the resultant activated carbon generated from steam activation (Edward et al., 2004).

- **Liquid Product**

The liquid phase is the most important product of tire pyrolysis. There are several literatures that studied the characteristics of the pyrolysis liquid products derived from waste tire (Laresgoiti et al., 2004; Williams and Brindle, 2003). Gas chromatography/Mass spectroscopy (GC/MS) is the most often method to analyze chemical species in both liquid and gas yields from pyrolysis and products of char combustion. Laresgoiti et al. (2004) characterized the liquid products obtained from waste tire pyrolysis at 300, 400, 500, 600, and 700°C and reported in terms of GC/MS analysis, elemental analysis, gross calorific values and distillation data. It was found that the liquids derived from waste tire pyrolysis were complex mixtures of C₆-C₂₄ organic compounds, containing a lot of aromatics (53.4–74.8%), some nitrogenated (2.47–3.5%) and oxygenated compounds (2.29–4.85%). Their gross calorific value (42 MJ/kg) was higher than that specified for commercial heating oils.

However, the sulfur content (1–1.4%) was close to or slightly over the limit value. Significant quantities of valuable light hydrocarbons such as benzene, toluene, xylene, limonene, etc. were obtained. The concentration of these compounds increased when reaction temperature was reached to 500°C and then decreased. The concentration of the important portion of polycyclic aromatics such as naphthalenes, phenanthrenes, fluorenes, diphenyls, etc. also significantly increased with increasing the reaction temperature. Pakdel et. al. (2001) reported that the vacuum pyrolysis of used tires produced approximately 55 wt% of pyrolysis oil. This oil typically contained 20-25 wt% of naphtha fraction with a boiling point lower than 200°C. It was observed that *dl*-limonene (20-25 wt%) was found in the naphtha fraction. Williams and Taylor (1993) also found that the pyrolysis oil obtained from waste tire had molecular weight in the range from a nominal 50 to 1200.

- **Gaseous Product**

The yield of the gas fraction produced from waste tire pyrolysis via different systems showed important variations. For example: Laresgoiti et al. (2000) studied the pyrolysis of waste tire under nitrogen atmosphere at 400-700°C. They found that the pyrolyzed gases consisted of carbon monoxide (CO), carbon dioxide (CO₂), hydrogen sulfide (H₂S) and hydrocarbons such as methane (CH₄), ethene (C₂H₄), propene (C₃H₆), butene (C₄H₈), and their unsaturated derivatives. Berrueco et. al. (2005) analysed the temperature influence on the global yields and the gas composition. They observed that the liquid yield increased with increasing the temperature to 400-500°C. However, this liquid yield remained almost constant when the pyrolysis was operated at higher temperature. The gas yield showed a growth from 2.4 wt% to 4.4 wt% and the main gases produced by this system were hydrogen (H₂), CO, CO₂ and hydrocarbons: CH₄, C₂H₄, C₃H₆ and C₄H₈. Roy et al. (1990) studied the vacuum pyrolysis of waste tire. The gaseous product also mainly composed of H₂, CO, CO₂ and a few hydrocarbon gases. Thus, it was concluded from previous literatures that the pyrolysis gases from waste tire were consisted of H₂, H₂S, CO, CO₂, CH₄, C₂H₄, C₃H₆ and other light hydrocarbons (Juma et al., 2006).

2.6 Sulfur Compounds in Petroleum Products and Waste Tire Pyrolysis Oil


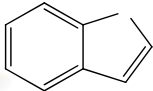
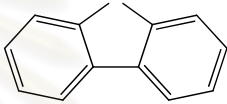
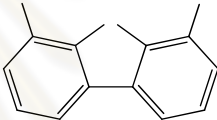
(Wauquier, 1995)

Sulfur compounds are the most influential heteroatomic components that are found in crude oils (Table 2.3). Total sulfur in crude oils can vary from 0.04 wt% for light crude oils to about 8.0 wt% for heavy crude oils. In addition, the total amount of sulfur compounds depends on the sources of crude oils. In general, the higher density of crude oil with the lower API gravity has the higher sulfur content. There are many varieties of sulfur compounds in crude oils in both inorganic and organic forms such as elemental (S), H₂S and carbonyl sulfide (COS) including thiophene derivatives as shown in Table 2.4. However, the prevailing conditions during formation, maturation, and even in situ alternation may dictate only preferred types exist in any particular crude oils. Moreover, the types of sulfur in crude oils depend on geological environment of sources, depth of the individual well, time and substrates to form crude oil.

Table 2.3 Some characteristics of crude oils (Wauquier, 1995)

Crude oil	Origin	Visc. mm ² /s	Asph. wt%	O wt%	N wt%	S wt%	Ni ppm
Batiraman	Turkey	1180	22.1	0.53	0.49	7.04	99
Boscan	Venezuela	595	14.1	0.79	0.74	5.46	125
Lacq.sup.	France	81.7	13.2	0.57	0.42	4.94	19
Chauvin Source	Canada	28	6.0	0.48	0.66	2.80	35
Bellshill Lake	Canada	7.9	2.2	0.34	<0.3	1.97	11
Emeraude	Congo	113	1.7	1.10	0.65	0.57	64
Anguille	Gabon	14.1	1.2	0.92	0.26	0.82	115
Duri	Sumatra	51	0.7	0.65	0.47	<0.1	39
Pematang	Sumatra	10.2	0.1	0.51	0.26	<0.1	15
Edjeleh	Algeria	5.3	0.1	0.73	0.34	<0.1	1.5
Hassi Messaoud	Algeria	2.32	0.1	1.93	0.38	<0.1	<0.2

Table 2.4 Types of organic sulfur (Wauquier, 1995)

Sulfur compound	Structure
Thiols (mercaptan)	R-S-H
Sulfides	R-S-R'
Disulfides	R-S-S-R'
Thiophene	
Benzothiophene	
Dibenzothiophene	
4,6-Dimethyldibenzothiophene	

Nevertheless, the compositions of sulfur compounds in different fractions of petroleum are not same because each type of sulfur compounds has different boiling range. Ma et al. (2002) reported that the major sulfur compounds that exist in commercial gasoline were thiophene, 2-methylthiophene, 3-methylthiophene, 2,4-dimethylthiophene and benzothiophene. Major sulfur compounds existing in JP-8 were 2,3-dimethylbenzothiophene, 2,3,7-trimethylbenzothiophene, 2,3,5-trimethylbenzothiophene and/or 2,3,6-trimethylbenzothiophene. The sulfur compounds commonly found in commercial diesel fuel were alkyl benzothiophenes and alkyl dibenzothiophene. The major compounds were dibenzothiophene derivatives with alkyl groups at 4 and/or 6-position including 4-methyldibenzothiophene (4-MDBT), 4,6-dimethyl dibenzothiophene (4,6-DMDBT), 3,6-dimethyl dibenzothiophene (3,6-DMDBT) and 2,4,6-trimethyl dibenzothiophene (2,4,6-TMDBT). In addition, Yin et al. (2002) studied the distribution of sulfur compounds in naphthas of china fuels which were obtained from fluid catalytic cracking (FCC) and residue fluidized catalytic cracking (RFCC). They found that the amount of mercaptan and disulfide were comparatively low. The sulfide content was ca. 25 wt% of total sulfur and the largest component of sulfur compounds was thiophenic derivatives.

Ma et al. (2001) showed chromatograms obtained from gas chromatography equipped with flame photometric detector (GC-FPD) of gasoline, diesel and jet fuel as shown in Figure 2.2. The FPD detects only sulfur compounds. It was reported that the major sulfur compounds in commercial gasoline were 3-methyl thiophene (3-MT), benzothiophene (BT), thiophene (T), 2-methyl thiophene (2-MT) and 2,4-dimethyl thiophene. The major sulfur compounds existing in jet fuel were 2,3,7-trimethyl benzothiophene (2,3,7-TMBT) and 2,3-dimethyl benzothiophene (2,3,-DMBT) with the minor species of 2,3,5-trimethyl benzothiophene (2,3,5-TMBT) and 2,3,6-trimethyl benzothiophene (2,3,6-TMBT). The sulfur compounds commonly found in the diesel fuel were 4-methyl dibenzothiophene (4-MDBT), 4,6-dimethyldibenzothiophene (4,6-DMDBT), 2,4,6-trimethyldibenzothiophene (2,4,6-TMDBT), 3,6-dimethyldibenzo thiophene (3,6-DMDBT), dibenzothiophene (DBT), 2,3,7-trimethylbenzothiophene (2,3,7-TMDBT), 2,3,5-trimethylbenzothiophene (2,3,5-TMBT), 2,3-dimethylbenzo thiophene (2,3-DMBT) and others. Among them, the 4,6-DMDBT and the dibenzothiophenes with two alkyl substituents at 4- and 6-positions still remained even after deep hydrodesulfurization (Kim et al., 2006).

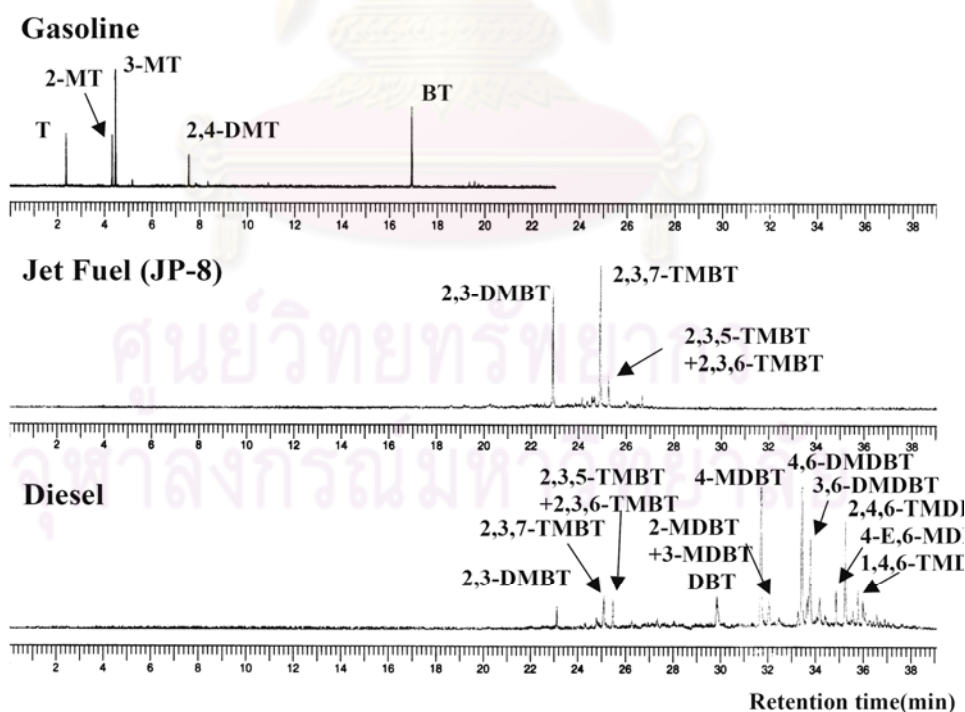


Figure 2.2 GC-FPD chromatograms for three transportation fuels (Ma et al., 2001).

For the pyrolysis oil derived from waste tire, Williams and Bottrill (1995) showed GC-FPD chromatograms of pyrolysis waste tire oil (Figure 2.3). It indicated that the major sulfur compounds in the waste tire pyrolysis oil were benzothiophene, dibenzothiophene and its derivatives: methyl, dimethyl, trimethyl and tetramethyl dibenzothiophene. It also contained naphthothiophenes, benzonaphthothiophene and their methyl derivatives. Moreover, the waste tire-derived pyrolysis oil had the complex nitrogen and sulfur containing species (Mirmiran et al., 1992).

2.7 Classification of Desulfurization Technologies (Babich and Moulijn, 2003)

Desulfurization processes can be classified as two groups: hydrodesulfurization (HDS) based and non-HDS based, depending on the role of hydrogen in removing sulfur. In HDS based processes, hydrogen is used to decompose organosulfur compounds and eliminate sulfur from refinery streams, while non-HDS based processes do not require hydrogen. Different combinations of refinery streams: pre- or post-distilling treatments with hydrotreating to maintain desired fuel specifications can also be assigned as HDS based processes since HDS treatment is one of the key steps. The two above-mentioned classifications overlap to some extent. Most sulfur elimination processes with the exception of selective oxidation are HDS based. The separation processes of organosulfur compounds are usually used in non-HDS based treatment since they do not require hydrogen if concentrated sulfur-rich streams are not subsequently hydrotreated.

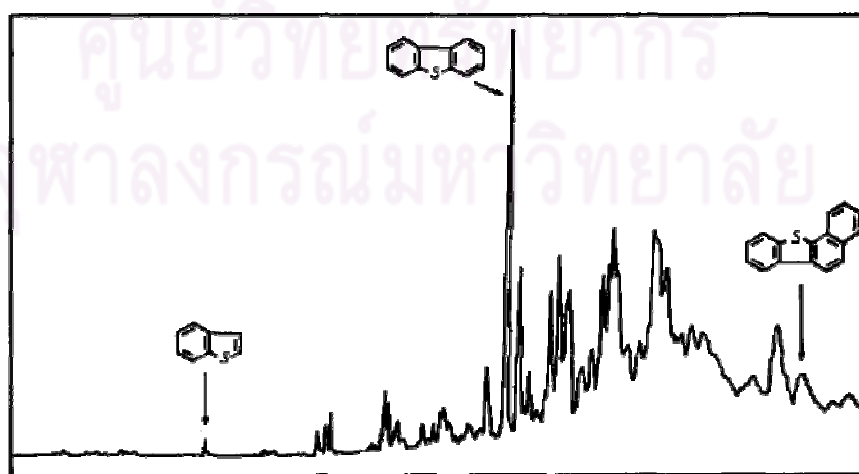


Figure 2.3 GC-FPD chromatogram of waste tire pyrolysis oil (Williams and Bottrill, 1995).

The desulfurization processes can also be classified based on the nature of the key physico-chemical process used for sulfur removal (Figure 2.4). The most developed and commercialized technologies are those which catalytically convert organosulfur compounds. Such catalytic conversion technologies include conventional hydrotreating, hydrotreating with advanced catalysts and/or reactor design, and a combination of hydrotreating with some additional chemical processes to maintain fuel specifications. The main feature of the technologies of the second type is the application of physico-chemical processes which are different in nature from catalytic HDS to separate and/or to transform organosulfur compounds from refinery streams. Such technologies include as a key step distillation, alkylation, oxidation, extraction, adsorption or combination of these processes.

Currently, there are several available processes and technologies to reduce sulfur compounds in refinery. Each process has different advantages, disadvantages, and limitations to remove sulfur compounds. The following approaches are considered to be attractive for attaining high levels of sulfur removal separation by catalytic HDS and non-HDS based desulfurization technologies:

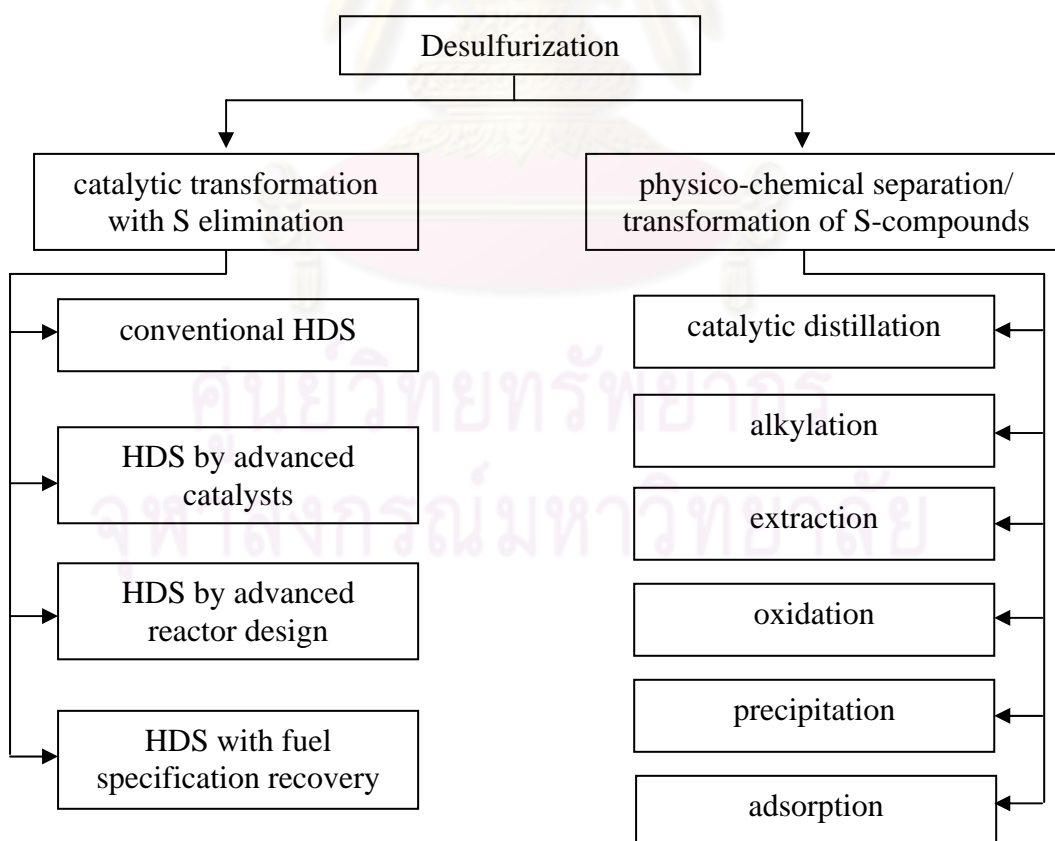


Figure 2.4 Desulfurization technologies classified by nature of a key process to remove sulfur (Babich and Moulijn, 2003).

2.7.1 Catalysis Based HDS Technologies

Catalytic HDS of crude oil and refinery streams is carried out at elevated temperature and hydrogen partial pressure to convert organosulfur compounds as H_2S and hydrocarbons. The conventional HDS process is usually conducted over sulfided $CoMo/Al_2O_3$ and $NiMo/Al_2O_3$ catalysts (Topsoe, Clausen, and Massoth, 1996). Their performance in terms of desulfurization level, activity and selectivity depends on the properties of the specific catalyst used (active species concentration, support properties, synthesis route), the reaction conditions (sulfiding protocol, temperature, partial pressure of hydrogen and H_2S), nature and concentration of the sulfur compounds in the feed stream, and reactor and process design. The reactivity of organosulfur compounds is widely varied depending on their structure and local sulfur atom environment. The low-boiling crude oil fraction mainly contains the aliphatic organosulfur compounds: mercaptans, sulfides, and disulfides. They are very reactive in conventional hydrotreating processes and easily be completely removed from the fuel. For higher boiling crude oil fractions such as heavy straight run naphtha, straight run diesel and light fluid catalytic cracking naphtha, the organosulfur compounds pre-dominantly contain thiophenic rings. These compounds include thiophenes and benzothiophenes with their alkylated derivatives. These thiophenes are more difficult than mercaptans and sulfides to convert via hydrotreating. The heaviest fractions blended to the gasoline and diesel pools bottom FCC naphtha, coker naphtha, FCC and coker diesel mainly contain alkylated benzothiophenes, dibenzothiophenes and alkyldibenzothiophenes, as well as polynuclear organic sulfur compounds, i.e. the least reactive sulfur compounds in the HDS reaction.

2.7.2 Non-HDS Based Desulfurization Technologies

Technologies without the use of hydrogen for catalytic decomposition of organosulfur compounds are discussed here as non-HDS based desulfurization. The following approaches are considered to be attractive for attaining high levels of sulfur removal by decomposition via oxidative desulfurization, adsorption and precipitation.

- **Oxidative Desulfurization** (Huang et al., 2008)

Oxidative desulfurization (ODS) has received much attention as an alternative new method for deep desulfurization of light oils because of its attractive features such as lower reaction temperature, milder pressure conditions and lower cost of operation. Oxidation of organosulfur compounds leads to the formation of their sulfoxides/sulfones, which are highly polar, and thus can be easily removed by extraction into polar solvents or by adsorption. Several researchers have reported the catalytic oxidation of organic sulfur compounds using molecular sieves as catalyst under mild conditions. Vanadosilicates were used as the catalyst for the desulfurization of light oil. Three types of vanadosilicates having different structures and pore size distributions, such as VS-1, VS-2, and VHMS, were used for investigations. In the presence of W-containing layered double hydroxide as catalyst, the organic sulfides and thiophene derivatives could be effectively oxidized using hydrogen peroxide (H_2O_2) as oxidizing agent. The nano WO_x/ZrO_2 catalyst was also an effective catalyst for oxidation of dibenzothiophene (DBT). Moreover, the supported Pd, Cr_2O_3 , unsupported manganese oxides and a commercial Co–Mo/ Al_2O_3 were used as catalysts for oxidation of a mixture of thiophene, benzothiophene and DBT in the presence of H_2O_2 .

- **Adsorptive Desulfurization** (Zhou, 2007)

Desulfurization by adsorption is based on the ability of a sorbent to selectively adsorb sulfur compounds from fossil fuels. Based on the mechanism of the sulfur compound interaction with the sorbent, it can be divided into two groups: adsorptive desulfurization and reactive adsorption desulfurization. Adsorptive desulfurization employs physical adsorption of sulfur compounds on the sorbent surface. Regeneration of the sorbent is usually performed by flushing the spent sorbent with a desorbent resulting in a high concentration of sulfur compounds in the exit flow. Reactive adsorption desulfurization is based on chemical interaction of the sulfur compounds and the sorbent. Sulfur is fixed in the sorbent, usually as sulfide. The S-free hydrocarbon is released into the purified fuel stream. Regeneration of the spent sorbent results in sulfur elimination as H_2S , S, SO_x , or sulfur-compounds

depending on the process applied (Babich and Moulijn, 2003). The efficiency of the desulfurization is mainly depended on the sorbent properties: its adsorption capacity, selectivity for the sulfur compounds, durability and regenerability (Babich and Moulijn, 2003). There has been an ongoing effort to develop new sorbents to remove the sulfur compounds from liquid fuels as summarized in Table 2.5.

During the past decade, several results have been published on the use of adsorption for liquid fuel desulfurization. Commercially available sorbents (i.e., zeolites, activated carbon and activated alumina) were used in this purpose (Salem and Hamid, 1997, Weitkamp et al., 1991, King et al., 2000 and Jayne et al., 2005). However, it is reported that currently available commercial sorbents were not suitable for the adsorptive desulfurization (Takahashi et al., 2002).

Table 2.5 Studies on the adsorptive desulfurization (Babich and Moulijn, 2003)

Reference	Sorbents	Treated fuels	Remarkable results
Salem and Hamid (1997)	Activated carbon Zeolite 5A Zeolite 13X	Naphtha (550 ppmw S)	Zeolite 13X as well as activated carbon showed much higher sorption capacities for S compounds.
Takahashi et al. (2002)	Zeolites, Activated carbon Modified activated Alumina	Thiophene, Benzene	The sorbent capacities for thiophene at low pressure: Cu-Y, Ag-Y >> Na-ZAM-5 > activated carbon > Na-Y > modified alumina, H-USY.
Hernandez-Maldonado and Yang (2003)	Zeolites	Thiophene, Benzene, n-Octane	The sorbent capacities for thiophene: Cu-Y > H-Y > Na-Y > Ag-Y.
Ma et al. (2005)	Cu(I)-Y, Ni-based sorbent	Commercial gasoline (305 ppmw S)	Cu(I)-Y and Ni-based adsorbent showed the sorbent capacities of 0.22 and 0.37 mg S/g of sorbent at room temperature, respectively.
Hernandez-Maldonado and Yang (2005)	Cu(I)-Y	Diesel, Gasoline, Jet fuel	The sorbent capacities of 0.395 And 0.278 mmol S/g of sorbent for jet fuel and diesel, respectively.

Initial results on sorbents based on π -complexation for desulfurization were reported by Yang et al. (2003). It showed that Cu(I)-Y, γ -Al₂O₃/Cu(I)-Y, Ag-Y, and Ni-based sorbent were superior to all previously reported sorbents in this application. For desulfurization, they used transition-metal ion exchanged zeolites to selectively remove organo-sulfur molecules from commercial diesel and gasoline.

Ma et al. (2005) recently synthesized various adsorbents including metal, metal halides, metal oxides, metal sulfides and modified zeolites and evaluated their desulfurization efficiency for gasoline and jet fuels. It was found that the selectivity of sulfur removal was occurred via a direct sulfur-adsorbent interaction rather than π -complexation.

- **Desulfurization by Precipitation** (Babich and Moulijn, 2003)

Desulfurization by precipitation is based on the formation and subsequent removal of insoluble charge-transfer complexes. Preliminary experiments were reported for a model organosulfur compound (4,6-DMDBT, referred as DBT) in hexane and gas oil using 2,4,5,7-tetranitro-9-fluorene (TNF) as the most efficient p-acceptor (Meille et al., 1998; Milenkovic et al., 1999). A suspension of the p-acceptor and sulfur containing gas oil was stirred in a batch reactor where insoluble charge transfer complexes between p-acceptor and DBT derivatives were formed. The consecutive steps include filtration to remove the formed complex from gas oil and the recovery of the excess p-acceptor by using a solid adsorbent. However, the efficiency of the process was very low. The results indicate that the sulfurous compounds were removed in the removal of only 20%. Moreover, there was a competition for complex formation between DBT compounds and other non-sulfur aromatics resulting to low selectivity for DBT removal. Moreover, a large overstoichiometric amount of TNF was used to provide good complexing and its excess should be removed from the oil stream afterwards. This was interesting to introduce a complexing agent into a solid organic or inorganic matrix. This would simplify the process since the filtration and p-acceptor recovery steps should be avoided.

2.8 Photocatalytic Desulfurization

Catalytic hydrodesulfurization (HDS) is commonly used for sulfur removal from fuels. This process involves high temperatures above 300°C with elevated hydrogen pressures of over 2 MPa (Yang, Hernandez-Maldonado, and Yang, 2003; Kim et al., 2006). This process also requires precious metal catalysts and large reactor size. DBT derivatives; especially, 4 and/or 6 alkyl-substituted DBT, are difficult to be removed by using the HDS process unless an energy-intensive process is applied. To reduce the energy needed for desulfurization, a large number of non-HDS processes, such as adsorption and oxidation have been investigated (Babich and Moulijn, 2003; Ito and Rob van Veen, 2006; Song and Ma, 2003; Song, 2003). Adsorption desulfurization has some problems to be solved. When the selectivity is low, the adsorbents are often to be regenerated. However, the use of adsorbent with high selectivity is possibly difficult to be regenerated (Hernandez-Maldonado and Yang, 2004; Salem and Hamid, 1997; Hernandez-Maldonado, Stamatis, and Yang, 2004).

To save energy and reduce operating costs, an alternative desulfurization process needs to be developed. Photocatalytic desulfurization is a new technology to degrade sulfur-containing compounds in oil, and has received much attention as a new technology for the deep desulfurization of light oil. In these reactions, the process comprises two stages. The first stage consists of the transfer of sulfur-containing compounds in light oil to a polar extraction solvent (Zhao et al., 2007). Then, it is followed by the photooxidation to decompose the sulfur-containing compounds by photons from the light source and a catalyst (Hermann, 1999). In most of these experiments, light at wavelengths longer than 280 nm, emitted from a high-pressure mercury lamp or a Xe–Hg lamp with a relatively high output power, e.g., 300 W, is used under oxidizing atmosphere. However, at the present stage, the extractive photocatalytic desulfurization process is far from being widely applied in industry, and there are a number of problems that need to be solved to make the process technically and economically feasible (Babich and Moulijn, 2003).

2.8.1 Titanium Dioxide or Titania (TiO_2) (Carp et al., 2004)

The example of catalyst for photocatalytic process is TiO_2 , zinc oxide (ZnO), cadmium sulfide (CdS) and ferrous oxide (Fe_2O_3). The selection of catalyst is depended on the reaction. For TiO_2/UV systems, they have been successfully developed for decomposition of various chemical species (Legrini et al., 1993).

The configuration of TiO_2 is divided as 3 types: anatase, rutile and brookite (EPA, 1998). The rate of hydroxyl radical formation depends on the crystalline forms of TiO_2 (EPA, 1998). Figure 2.5 shows the crystal structures of TiO_2 . Many research works reported that the anatase form had the highest level of photoconductivity with a band gap of 3.2 electron volts (EPA., 1998; Munter et al., 2007). Rutile is considered much less photoreactive than anatase (Bahnemann, 1999; Munter et al., 2001). However, it has higher efficiency for recombination of the electron-hole pair and a smaller surface area (Munter et al., 2001).

Some research revealed that the optimum ratio of rutile and anatase form exhibited high photocatalytic efficiency (Oillis and Turchi, 1990). Degussa P25 is commercially TiO_2 which is accepted as a standard photocatalytic form of TiO_2 (Bahnemann, 1999; Hoffiman et al., 1995; Legrini et al., 1993). Some important properties corresponding to their structures were showed in Table 2.6.

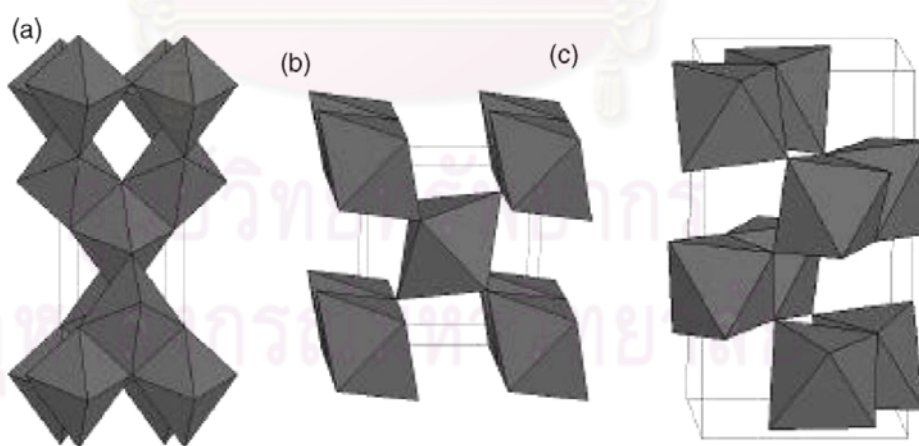


Figure 2.5 Crystal structures of (a) anatase, (b) rutile, and (c) brookite

Table 2.6 The properties of the anatase and rutile phase (Fujishima, Hashimoto, and Watanabe, 1999)

Properties	Anatase	Rutile
Crystalline form	Orthorhombic	Orthorhombic
Band gap energy (eV)	3.20	3.03
Band gap wavelength (nm)	384	411
Hardness (Mohs)	5.5 – 6.0	6.0 – 7.0
Density (g/cm ³)	3.894	4.250
Gibbs free energy, ΔG_f^0 (kcal/mole)	-211.4	-212.6
Lattice constant, a(A ⁰)	3.784	4.593
Lattice constant, c(A ⁰)	9.515	2.959
Melting point	Changes to rutile at high temperature	1858

Both crystal structures, anatase and rutile, are commonly used as photocatalyst, with anatase showing a greater photocatalytic activity for most reactions. It has been suggested that higher photoreactivity of anatase form is related to the slightly higher Fermi level with lower capacity to adsorb oxygen and higher degree of hydroxylation (i.e., the number of hydroxy groups on the surface). Furthermore, there are also reported that TiO₂ containing a mixture of anatase (70–75%) and rutile (30–25%) is more active than TiO₂ with only anatase form. The disagreement of the results may lie in the intervening effect of various coexisting factors, such as specific surface area, pore size distribution, crystal size, and preparation methods, or in the way the activity is expressed. The behaviour of Degussa P25, commercial TiO₂ photocatalyst, consisting of an amorphous state together with a mixture of anatase and rutile in an approximate proportion of 80/20, exhibits higher active than the pure crystalline phases. The enhanced activity arises from the increased efficiency of the electron–hole separation due to the multiphase nature of the particles.

2.8.2 Photocatalytic Process (Litter, 1999)

The basic principles of heterogeneous photocatalysis can be summarized shortly as followed. The semiconductor (SC) is the unique material which is consisted of an electronic band with the highest occupied energy band called as a valence band (vb) and the lowest empty band called as a conduction band (cb). These are separated by a bandgap, i.e. a region of forbidden energies in a perfect crystal. When a photon with higher or equal energy compared to the bandgap energy is absorbed by a semiconductor particle, an electron from the vb is promoted to the cb (e_{cb}^-) with simultaneous generation of a hole in the vb (h_{vb}^+) (Eq. 2.1). The e_{cb}^- and h_{vb}^+ can recombine on the surface or in the bulk of the particle in a few nanoseconds to generate heat (Eq. 2.2) or can be trapped in surface states where they can react with donor (D) (Eq. 2.3) or acceptor (A) species (Eq. 2.4) adsorbed or close to the surface of the particle (Robertson, 1996). The schematic photocatalytic reaction mechanism is proposed as shown in Figure 2.6 (Mills and Le Hunte, 1997). The efficiency of a photocatalyst depends on the competition of different interface transfer processes involving electrons, holes and their deactivation by recombination.

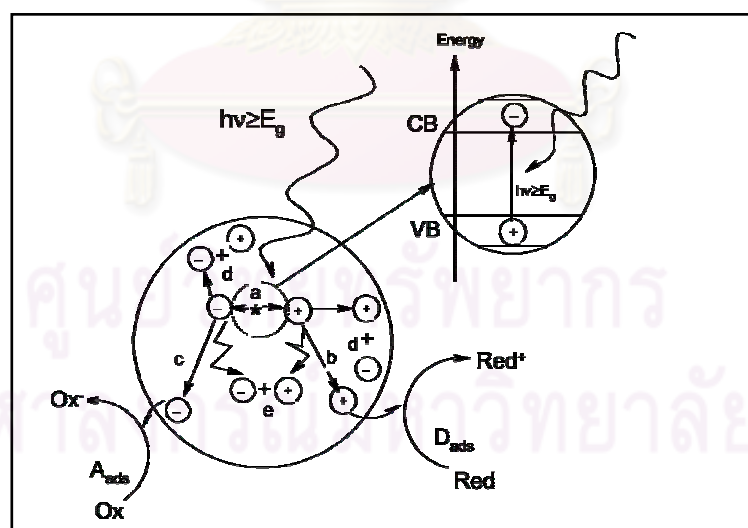
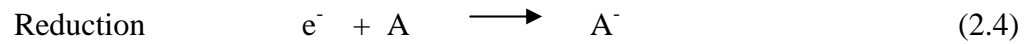
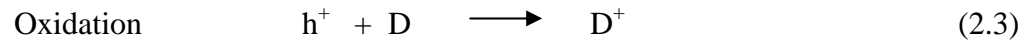
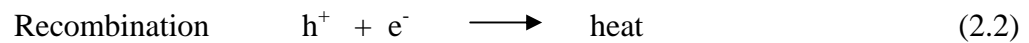
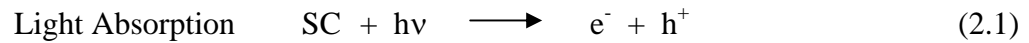
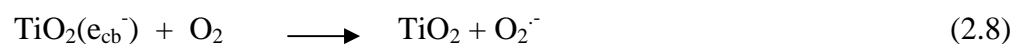
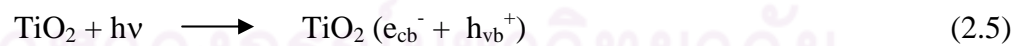


Figure 2.6 Main process occurring on a semiconductor particle: (a) electron-hole generation; (b) oxidation of donor (D); (c) reduction of acceptor (A); (d) and (e) electron-hole recombination at surface and in bulk, respectively. (Mills and Le Hunte, 1997)

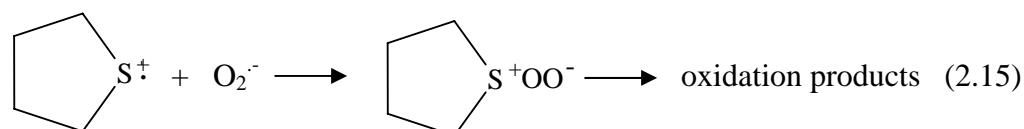
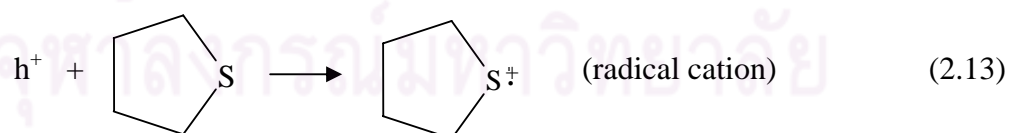
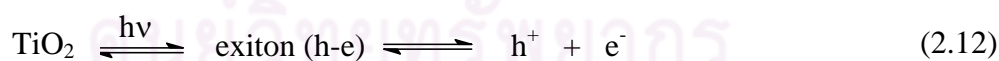


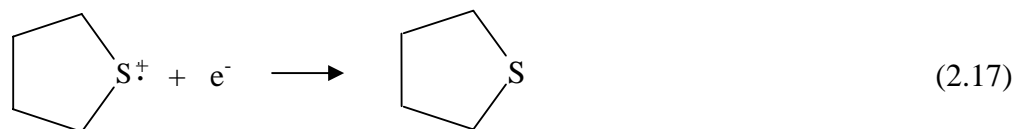
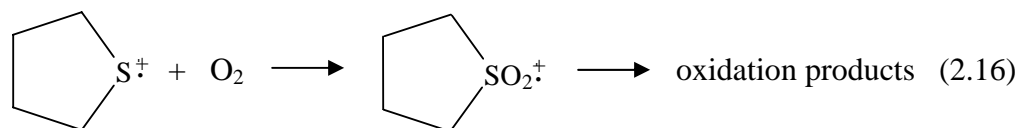
The detailed mechanism of the photocatalytic process on the TiO₂ surface is still not completely clear, particularly the initial steps involving the reaction of reactive oxygen species and organic molecules. The separately monitoring of oxidation and reduction reactions is employed for a simple macroscopic model that can be used to simulate individual particles (Carp et al., 2004). The following mechanism is widely accepted as the mechanism of photodegradation of organics by a ultraviolet (UV)/TiO₂ system (Konstantinou and Albanis, 2004). Photogenerated e_{cb}^- and h_{vb}^+ are produced when TiO₂ particles are irradiated by UV light (Eq. 2.5). Hydroxyl radicals are mainly formed by the oxidation of OH⁻ or H₂O via these photogenerated holes (Eq. 2.6 and 2.7), and hydroxyl radicals are principally responsible for destruction of organic species. Oxygen primarily acts as an efficient electron trap (Eq. 2.8), preventing recombination of electrons and photogenerated holes. The hydroperoxyl radical (HO₂[•]) are generated from the free radical activity of the superoxide radical anion reacts with hydrogen ion in reaction (Eq. 2.9). Hydroperoxide ion (OH₂⁻) are formed by electrons and superoxide radical anion react with H⁺ ions in solution (Eq. 2.10). The hydroperoxide ion reacts with H⁺ ions to form the hydrogen peroxide (Eq. 2.11). If oxygen is limited, rapid recombination of photoproduced electrons and holes in TiO₂ significantly reduces the efficiency of photocatalytic reactions; consequently, such a system has limited practical application.



2.8.3 Mechanisms of Photocatalytic Desulfurization

Abdel-Wahab and Gaber (1998) studied the TiO₂-photocatalytic oxidation of selected heterocyclic sulfur compounds in the presence of light. The polynuclear-heterocyclic sulfides such as benzothiophene or dibenzothiophene were dominantly oxidized to the corresponding sulfoxides and sulfones via TiO₂-mediated photocatalytic oxidation in aerated acetonitrile (Fox and Abdel-Wahab, 1990 and Davison and Bratt, 1983). The mechanism of photocatalytic desulfurization of heterocyclic sulfur compounds is shown in Eq. 2.12 - 2.18. The adsorption of light with energy equal to or greater than the band gap energy of TiO₂ (i.e., 3.23 eV) will result in the electron ejection from the valence band to the conduction band generating a reactive electron (e⁻) and a positive hole (h⁺) (Eq. 2.12) (Fox, Serpone, and Pelizzetti, 1990; Fox, 1987). The photogenerated holes can oxidize the heterocyclic sulfur compounds to form sulfur radical cation (Eq. 2.13). The photogenerated electrons react with electron acceptor such as O₂ adsorbed on the TiO₂-surface, reducing it to superoxide radical anion (O₂⁻) (Eq. 2.14). The heterocyclic sulfur cationic radical readily reacts with superoxide radical anion (Eq. 2.15) or oxygen molecule to form oxidation products (Eq. 2.16). Sulfones could be directly accomplished via a secondary conversion to sulfoxide (Fox and Abdel-Wahab, 1990). Thus, co-adsorbed oxygen acts as an electron trap, preventing recombination of electrons reacts with heterocyclic sulfur cationic radical (Eq. 2.17) and photogenerated holes reacts with superoxide radical anion (Eq. 2.18).





2.9 Literature Reviews

Hirai, Ogawa, and Komasaawa (1996) investigated the desulfurization process for DBT and its derivatives such as 4-MDBT and 4,6-DMDBT by combination of photochemical reaction and liquid-liquid extraction. In this process, the DBTs dissolved in tetradecane were quantitatively photodecomposed by the use of a high-pressure mercury lamp and were removed to the water phase as SO_4^{2-} at room temperature and atmospheric pressure. The order of reactivity for the DBTs was $\text{DBT} < 4\text{-MDBT} < 4,6\text{-DMDBT}$ indicating a different tendency from that reported for the hydrodesulfurization method. However, the desulfurization yield of commercial light oil proposed method was only 22% at 30 h of irradiation possibly due to the large amount of aromatic compounds in the commercial light oil.

Shiraishi, Harai, and Komasaawa (1998) investigated deep desulfurization process of light oil via combination of photochemical reaction and liquid-liquid extraction. The first stage related to the photo-oxidation to decompose sulfur-containing compounds from the light oil under UV irradiation generated by a high-pressure mercury lamp. The operations were carried out under room temperature and atmospheric pressure. The oxidized sulfur-containing compounds were then transferred into the aqueous soluble polar solvent. It was found that acetonitrile was the most suitable polar solvent for the extraction stage. In acetonitrile, dibenzothiophene (DBT) was converted to DBT 5-monoxide and then to DBT 5,5-dioxide, dibenzoxathiin 6-oxide and aromatic sulfonate or sulfinate anion under UV irradiation. These products were highly polarized resulting in the difficulty to distribute into the nonpolar light oil phase. The desulfurization yield for commercial

light oil (CLO) and for straight-run light gas oil (LGO) was drastically improved by the present process. The sulfur contents of CLO and LGO were reduced from 0.2 to 0.05 wt% within 2 h and 1.4 to 0.05 wt% within 10 h under irradiation; respectively. The separation of the coextracted aromatics from the acetonitrile was successfully carried out by using light paraffinic hydrocarbon stripping agents.

Shiraishi et al. (1999) studied the desulfurization of benzothiophenes (BTs) and dibenzothiophenes (DBTs) via new photochemical desulfurization process, in the presence of organic liquid-liquid extraction. The acidic products were converted to their corresponding methyl esters by reaction with diazomethane. In acetonitrile, BT was firstly converted to benzothiophene-2,3-dione followed by hydrolysis to release carbon monoxide. The oxidized sulfur atom was finally converted to 2-sulfobenzoic acid. 3-Methyl BT and 2,3-dimethyl BT produced 2-sulfobenzoic acid and two other products: benzenesulfonic acid and 2-acetylbenzenesulfonic acid. DBT was firstly photooxidized to DBT sulfoxide, which was then further oxidized to form DBT sulfone or dibenz[*c,e*][1,2]-oxathiin-6-oxide. The latter was then oxidized and finally converted to 2-sulfobenzoic acid via dibenz[*c,e*][1,2]oxathiin-6,6-dioxide. Benzothiophene-2,3-dicarboxylic acid was directly formed by the oxidation of DBT using a singlet oxygen generated by photosensitization with DBT sulfone. 4-Methyl DBT and 4,6-dimethyl DBT finally produced the corresponding sulfobenzoic acid, dicarboxylic acid, and sulfone. The yields of these products were seriously affected by the presence of methyl substituents.

Ibrahim, Xian, and Wei (2003) studied a deep desulfurization process for FCC light gasoline. The process was comprised of liquid-liquid extraction using acetonitrile, and photooxidation under ultraviolet light generated from a high-pressure mercury lamp. After the extraction, the sulfurcontaining compounds were transferred from the oil into the extracting solvent. Then, the solvent containing these sulfur compounds was photoirradiated under ultraviolet light obtained from a high pressure mercury lamp at 300 W with 200–300 nm of wavelength. The system was also under extremely stirring during the irradiation. The resulting oil in the solvent was then recovered by using water. An azeotropic mixture (containing 86% acetonitrile and 14% water) was successfully recovered with one distillation column and could be reused. The total sulfur content in this gasoline decreased from 309 to 68 ppm within

8 h of photo-irradiation period. The total yield of the oil was varied between 90–96%. The main sulfur compounds of this gasoline were alkyl substituted thiophenes.

Robertson and Bandosz (2006) prepared a new titanium(IV)oxide–hectorite nanofilm photocatalyst deposited on quartz slides. Its reactivity was evaluated by photo-oxidation of dibenzothiophene (DBT) in nonpolar organic solution (tetradecane) which was used as a model for diesel fuel. The sulfur removal system was consisting of catalytic photo-oxidation followed by adsorption of products on silica gel. Photo-oxidation of DBT was performed with and without catalyst, at 254 and 300 nm of UV wavelength. Comparison was made with a commercially available TiO_2 catalyst, Degussa P25. The catalyst was analyzed by nitrogen adsorption, XRD, SEM, and TGA-DTA. The DBT concentrations remaining in the system were measured by HPLC and UV spectrophotometry. Preliminary qualitative analysis of products was performed by UV and HPLC. The results indicated that this process was effective to reduce the sulfurous content to below 10 ppm.

Yu and Wang (2010) developed TiO_2 nanotube arrays (TNs) by electrochemical anodization of titanium foil in a mixed electrolyte solution of glycerol and ammonium fluoride (NH_4F) and then calcined at various temperatures. The prepared samples were characterized by using X-ray diffraction, scanning electron microscopy and transmission electron microscopy. The photocatalytic activity was also evaluated by photocatalytic degradation of methyl orange (MO) in aqueous solution under UV light irradiation. The production of hydroxyl radicals ($\text{OH}\cdot$) on the surface of UV-irradiated samples was detected by a photoluminescence (PL) technique using terephthalic acid (TA) as a probe molecule. The transient photocurrent response was measured by several on–off cycles of intermittent irradiation. The results showed that the reaction temperatures below 600°C had no great influence on surface morphology and architecture of the TNs sample. Thus, the prepared TNs could be stable in the temperature up to ca. 600°C . At 800°C , the nanotube arrays were completely destroyed and only dense rutile crystallites were observed. For the photocatalytic activity, the formation rate of hydroxyl radicals and photocurrent of the TNs increased with increasing temperatures from 300 to 600°C due to the enhancement of crystallization. At 600°C , the sample showed the highest photocatalytic activity due to its bi-phase composition, good crystallization and

remaining tubular structures. With further increase in the calcination temperature to 800°C, the photocatalytic activity rapidly decreased due to the vanishing of anatase phase, collapse of nanotube structures and decrease of surface areas.



ศูนย์วิทยทรัพยากร
จุฬาลงกรณ์มหาวิทยาลัย

CHAPTER III

EXPERIMENT AND CHARACTERIZATION

The present research work focused on the photocatalytic desulfurization of waste tire pyrolysis oil using commercial titanium dioxide (TiO_2 or Degussa-P-25) at mild reaction condition. The experiment was divided into four steps:

1. Preparation and characterization of waste tire powder
2. Pyrolysis of waste tire powder and characterization of its products
3. Investigation of the effect of reaction conditions used in the photocatalytic desulfurization of pyrolysis oil derived from waste tire on the level of sulfur removal.
4. Characterization of oxidized pyrolysis oil properties and sulfurous compounds after the photocatalytic desulfurization process.

3.1 Materials

The waste tire powder ($\phi = 355\text{-}425 \mu\text{m}$) was received from Union Commercial Development Co., Ltd. (Samutprakarn, Thailand). TiO_2 was commercial grade Degussa P-25 with BET surface area of ca. $65 \text{ m}^2/\text{g}$ from J.J. Degussa Hüls Co., Ltd. (Bangkok, Thailand). Analytical grade methanol (CH_3OH) was obtained from QRëC (New Zealand), acetonitrile (CH_3CN) was purchased from Fisher Scientific (Leicestershire, UK). 30 wt% of hydrogen peroxide (H_2O_2) was received from Merck (Germany). Tetradecane ($\text{C}_{14}\text{H}_{30}$), thiophene ($\text{C}_4\text{H}_4\text{S}$), thianaphthene ($\text{C}_8\text{H}_6\text{S}$) and dibenzothiophene ($\text{C}_{12}\text{H}_8\text{S}$) were purchased from Sigma-Aldrich, Co., Ltd. (USA). Air with 99.98% purity was received from Praxair Co.,Ltd. (Samutprakarn, Thailand).

3.2 Experimental Procedures

3.2.1 Pyrolysis Process

The 100 g of dried waste tire powder contained in a stainless steel tubular fixed bed reactor was pyrolyzed in a tubular furnace at 400°C with $10^\circ\text{C}/\text{min}$ of

heating rate under nitrogen atmosphere with a flow rate of 0.1 L/min for 15 min or until no further significant release of oil was observed (Bunthid, Prasassarakich, and Hinchiranan, 2010). The pyrolysis oil was collected via vapor condensation during pyrolysis process in a series of erlenmeyer flasks which were immersed in an ice bath. The pyrolysis process was shown in Figure 3.1.

3.2.2 Photocatalytic Desulfurization

Figure 3.2 shows a diagram of experimental apparatus for photocatalytic desulfurization. The pyrex glass photoreactor (max. volume = 100 mL) was placed in the water bath which stood on a magnetic stirrer in an aluminium box. A 400 W high-pressure mercury lamp was used as the light source for photo-oxidation. The reaction temperature was controlled at target by using a water-cooling system. Air was introduced into the reaction solution from a gas cylinder at a desired flow rate.

The waste tire pyrolysis oil (10 ml) obtained from condensable fraction during pyrolysis was mixed with the extracting solvent at various volume ratio and then transferred into the photoreactor. The desired amount of TiO_2 (1-10 g/L of pyrolysis oil) used as the photocatalyst was added into the reaction mixture under 0-150 mL/min of air flow rate. The reaction temperature was varied in the range of 30-70°C for 1-7 h.

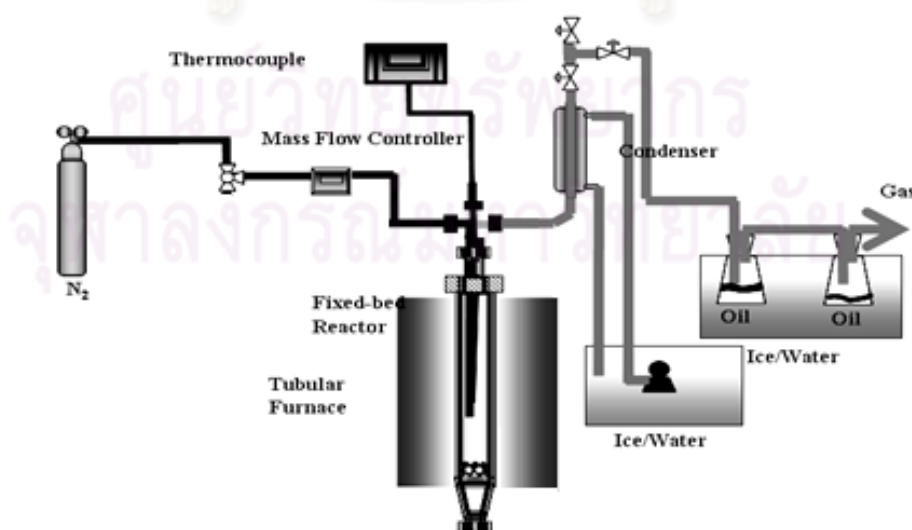


Figure 3.1 Schematic diagram of the fixed bed reactor for pyrolysis process.

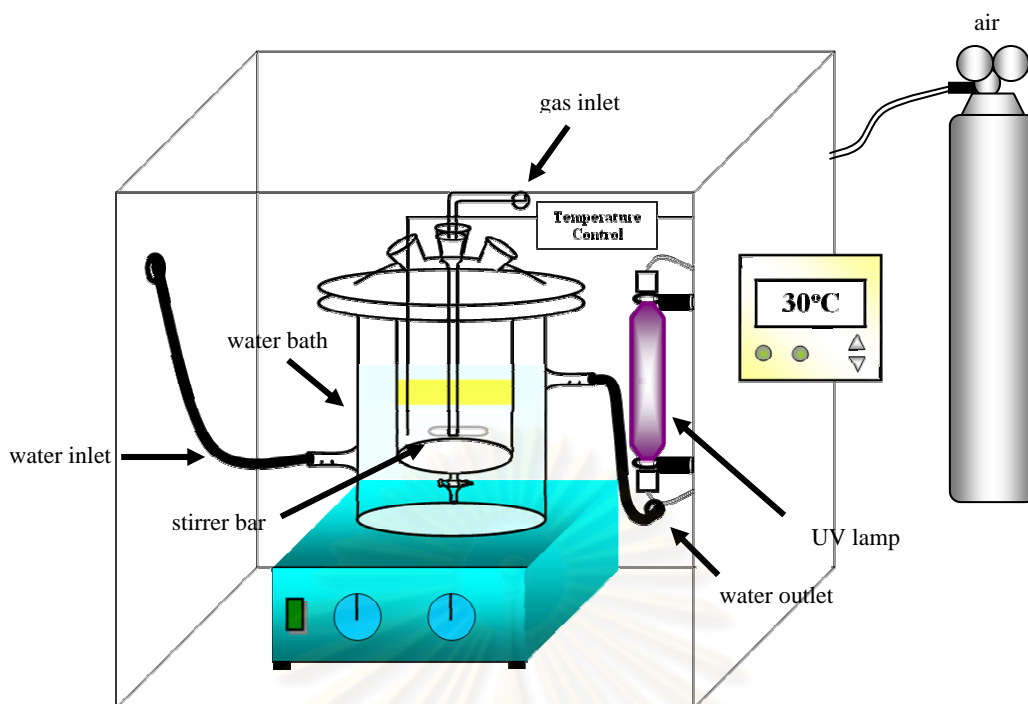


Figure 3.2 Diagram of experimental apparatus for photocatalytic desulfurization of pyrolysis oil.

When the reaction was terminated, TiO_2 particles and solvent-extraction phase were completely removed from the oxidized pyrolysis oil by centrifugation. The detail and range of reaction parameters are presented in Table 3.1. For the type of extracting solvent, the pyrolysis oil after photocatalytic desulfurization in the presence of methanol or acetonitrile used as extracting solvents was then transferred into the distilled water to separate the oxidized oil and extracting solvents.

Table 3.1 Parameters and range of study for photocatalytic desulfurization of the waste tire pyrolysis oil using TiO_2

Parameters	Range of study
TiO_2 dosage (g/L of pyrolysis oil)	1-10
Calcinations temperature of TiO_2 ($^\circ\text{C}$)	400-800
Temperature reaction ($^\circ\text{C}$)	30-70
Pyrolysis oil/extracting solvent (v/v)	1/1-1/5
Type of extracting solvent	Distilled water, methanol, acetonitrile
Air flow rate (mL/min)	0-150
H_2O_2 concentration (wt%)	0-30
Stage of reaction	1-3

3.3 Analytical Method

3.3.1 Characterization of Waste Tire Powder

The proximate analysis of waste tire powder was evaluated following ASTM D3173-D3175 to detect moisture, volatile matter, ash and fixed carbon. The total carbon, hydrogen and nitrogen contents of waste tire were determined by dry combustion using a LECO CHN-2000 analyzer. No more than 0.2 g of sample was placed in a tin foil capsule and combusted in a resistance furnace at 950°C using oxygen (O₂) as a carrier gas. The resulting gases were equilibrated in a ballast chamber followed by infra-red detection for carbondioxide (CO₂) and water (H₂O). Nitrogen (N₂) was determined by a thermal conductivity detector after reduction of nitrogen oxides and removal of CO₂ and H₂O. Calibration curves were validated on a daily basis by using a LECO standard (EDTA-C₁₀H₁₆N₂O₈-LECO Corp.) and quality control assured by running an EDTA standard for every ten samples (Graves et al., 2006). The total sulfur content was analyzed following ASTM D3172 Method B: Bomb washing method. The oxygen content was then calculated by the percentage difference. The gross calorific values of waste tire were also investigated following ASTM D2015.

3.3.2 Characterization of TiO₂

3.3.2.1 X-Ray Diffractometry (XRD)

The TiO₂ samples before and after calcinations were analyzed for XRD diffractometry using a Bruker AXS model D8 Discover with CuK α radiation at a scan rate (2 θ) of 5°/min to identify their phase type and crystallite size. The accelerating voltage and applied current were 40 kV and 30 mA; respectively. The average size of anatase and rutile crystallite was determined based on XRD peak broadening using the Scherrer equation ($t = 0.9\lambda/(B \cos \theta)$), where t is the average crystallite size, B is the broadening of the diffraction line measured at half maximum intensity ([1 0 1] and [1 1 0] reflections for anatase and rutile respectively), λ is the

wavelength of the X-ray radiation (0.15418 nm) and θ is the Bragg angle (Klug and Alexander, 1954).

3.3.2.2 Scanning Electron Microscopy (SEM)

The dried TiO₂ powder before and after calcinations was sputter-coated with gold and observed under the SEM (JEOL JSM-5800 LV) at an accelerating voltage of 15 kV.

3.3.3 Type and Content of Sulfurous Compounds in the Pyrolysis Oil

3.3.3.1 Total Sulfur Content

Total sulfur content of pyrolysis oil before and after photocatalytic desulfurization were determined by using the LECO SC-132 Sulfur Determinator (LECO Corporation, St Joseph, Michigan). The range of this instrument was 0.001 to 5% S for organic and inorganic materials. The weight of each sample analyzed was in the range 0.09-0.30 g and it was mixed with combustion accelerators in a ceramic boat and combusted in a resistance furnace at 1370°C in an O₂ atmosphere. The LECO SC-132 was calibrated using the 1% S content dibenzothiophene standard.

3.3.3.2 Gas Chromatography–Flame Photometric Detector (GC-FPD)

The type and content of sulfurous compounds in the pyrolysis oil before and after photodesulfurization were diluted in acetonitrile (1 wt%) and performed on an Agilent 6890N gas chromatography equipped with a flame photometric detector. The samples were injected at 250°C using the split/splitless mode. A HP-5 capillary column (30 m x 0.32 mm inner diameter (ID), 0.25 µm film thickness) was used for sulfur compound separation. The gas chromatograph oven temperature was programmed to rise from 35°C (hold 10 min) to 130°C at a heating rate of 15°C/min, and thereafter to 220°C at a heating rate of 10°C/min. The carrier gas was nitrogen (45.7 mL/min). The detector operated at 250°C with an air/hydrogen flame, for which the air and hydrogen gas pressures were 0.75 and 1 kg/cm; respectively.

3.3.3.3 High Performance Liquid Chromatography (HPLC)

The standard sulfur compounds and pyrolysis oil before and after photocatalytic desulfurization using acetonitrile as an extracting solvent were analyzed by HPLC to detect the products from their polarity compared to the raw materials. The standard sulfur compounds were thiophene, benzothiophene and dibenzothiophene. These samples were analyzed on a Agilent 1100, high performance liquid chromatograph equipped with Lichrospher C-18 bonded packing. The mobile phase was the mixture of acetonitrile and distilled water (90/10 v/v) at flow rate of 0.8 mL/min and detected by UV detector at 245 nm. This solution was injected using an injection loop with injection volume of 20 μ l.

3.3.4 Quality of Pyrolysis Oil

The analysis of kinematic viscosity and the copper strip corrosion in pyrolysis oil after photocatalytic desulfurization followed ASTM D 445 and ASTM D 130; respectively. The gross calorific values of the oxidized pyrolysis oil were also investigated following ASTM D2015.

ศูนย์วิทยทรัพยากร
จุฬาลงกรณ์มหาวิทยาลัย

CHAPTER IV

RESULTS AND DISCUSSION

4.1 Characterization of Waste Tire

Table 4.1 showed the proximate analysis data of waste tire powder. This indicated that the waste tire powder had high volatile content as 62.4 wt% with 27.6 wt% of fixed carbon, 8.73 wt% of ash and 1.22 wt% of moisture contents. From the ultimate analysis (Table 4.2), it showed that the waste tire powder had a large amount of carbon as 80.1 wt% with high hydrogen content (7.48 wt%). Thus, the waste tire powder had higher calorific value (35.7 MJ/kg) than the biomass which had lower hydrogen/carbon ratio (Cao et al., 2009). However, the waste tire powder contained 1.54 wt% of sulfur content obtained from vulcanizing agents in the vulcanization process of tire production.

Table 4.1 Composition of waste tire feedstock

Analytical	wt%
<u>Proximate Analysis</u>	
Volatiles	62.4
Fixed carbon	27.6
Ash	8.73
Moisture	1.22
<u>Ultimate Analysis</u>	
C	80.1
H	7.48
N	0.42
S	1.54
O	10.5

Table 4.2 Gross calorific values of various materials

Material	Gross calorific value (MJ/kg)	Reference
Waste tire	35.7	-
Rice husk	13-15	Jenkins, B.M. (1989)
Cocoa	13.2	Anno et al. (2006)
Palm	18-20	Vijaya et al. (2004)
Corn-shells	19.7	John, W.B. (2004)

4.2 Products Derived from Waste Tire Pyrolysis

The 100 g of waste tire powder was pyrolyzed in a stainless steel fixed bed reactor under nitrogen atmosphere which was fed at a flow rate of 0.1 L/min. The pyrolysis temperature was kept constant at 400°C with 20-25°C/min of heating rate for 15 min. The pyrolysis light oil was obtained from the condensable pyrolysis vapor; whilst, the heavy fraction trapped in the pyrolysis char and the reactor was collected using THF. The gas fraction was then calculated by the percentage difference. This pyrolysis condition gave pyrolysis light oil, pyrolysis heavy oil, char and gas fractions at a composition of 39.6, 14.0, 38.2 and 8.12 wt%; respectively (Table 4.3). Due to the highest content of pyrolysis light oil with high gross calorific values (43 MJ/kg) as much as commercial diesel (45 MJ/kg) and gasoline (47 MJ/kg) (Rose and Cooper, 1977), this fraction was used as a raw material for further experiment. The total sulfur content in the pyrolysis light oil was evaluated as ca. 0.84 wt%.

Table 4.3 Yield of waste tire pyrolysis products

Pyrolysis products	Yield (wt%)
Light oil fraction	39.6 ± 3.29
Heavy oil fraction	14.0 ± 2.52
Char	38.2 ± 1.97
Gas	8.12 ± 1.78

4.3 Photocatalytic Desulfurization of Pyrolysis Oil Derived from Waste Tire

4.3.1 Influence of TiO₂ Dosage on Degree of Sulfur Removal

The effect of TiO₂ content on the sulfur reduction in the pyrolysis oil was presented in Figure 4.1. The dosage of TiO₂ was varied from 1-10 g of TiO₂/L of pyrolysis oil at 30°C. The extracting solvent was distilled water at 1/1 (v/v) of pyrolysis oil/distilled water. It was found that the increase in the TiO₂ dosage from 1 to 7 g/L of pyrolysis oil enhanced the level of sulfur removal throughout the period of reaction time. The highest %sulfur removal was 27.9% when 7 g of TiO₂/L of pyrolysis oil was loaded into the system at 7 h of reaction time. Above TiO₂ content, the agglomeration of TiO₂ could be occurred to reduce its catalytic efficiency (Ku and Hsieh, 1992). It was also observed the formation of gas bubble with increasing the TiO₂ content. It was possibly due to the enhancement of surface tension at pyrolysis oil-water interface. The effect of bubble produced during photo-oxidation was also reported in the previous literature that the air bubbles in the TiO₂-suspension system inhibited the absorption of UV light resulting to the reduction of the sulfur removal efficiency of TiO₂ (Nam, Kim, and Han, 2002).

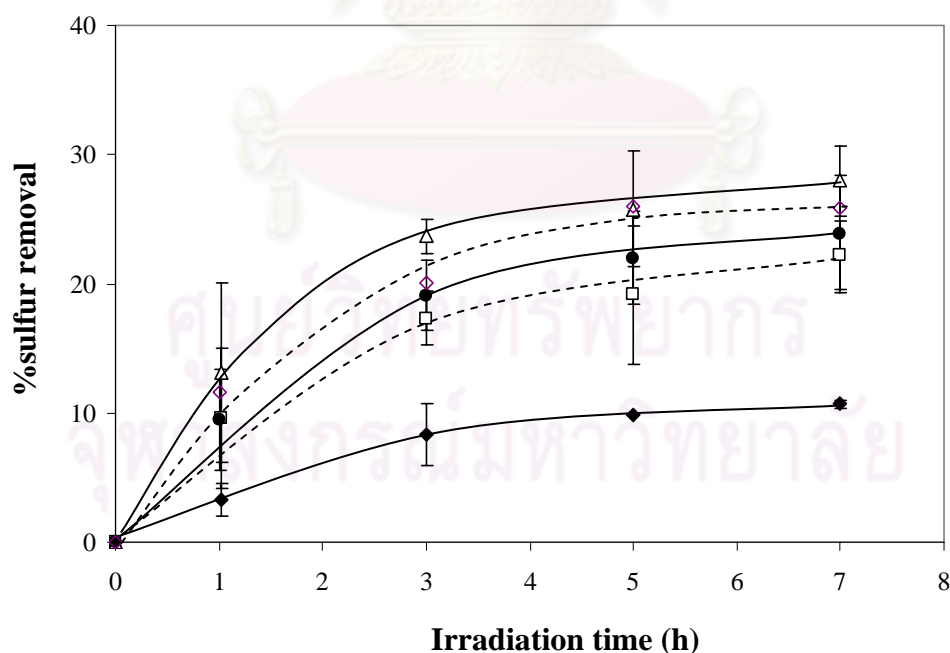


Figure 4.1 Effect of TiO₂ dosage on sulfur removal of pyrolysis oil derived from waste tire: 1 g/L (●); 3 g/L (◻); 5 g/L (●); 7 g/L (◻) and 10 g/L (◻) (pyrolysis oil/distilled water = 1/1 (v/v); air flow rate = 150 mL/min and T = 30°C).

4.3.2 Influence of Calcination Temperature on Degree of Desulfurization

The morphology of TiO_2 was also an important factor which affected the photocatalytic efficiency of TiO_2 for sulfur removal. The calcination temperature was the key parameter to change the crystallite phase of TiO_2 . In this research work, the calcination temperature was varied in the range of 400-800°C. The effect of calcination temperature on the photocatalytic efficiency of TiO_2 for sulfur removal was shown in Figure 4.2. When 7 g of TiO_2/L of pyrolysis oil was applied to the system in the presence of distilled water (pyrolysis oil/distilled water = 1/1 (v/v)), the higher calcination at high temperature decreased the photocatalytic efficiency of TiO_2 for desulfurization by reduction of surface area resulting from the growth of TiO_2 particle (Figure 4.3) (Youji et al., 2007).

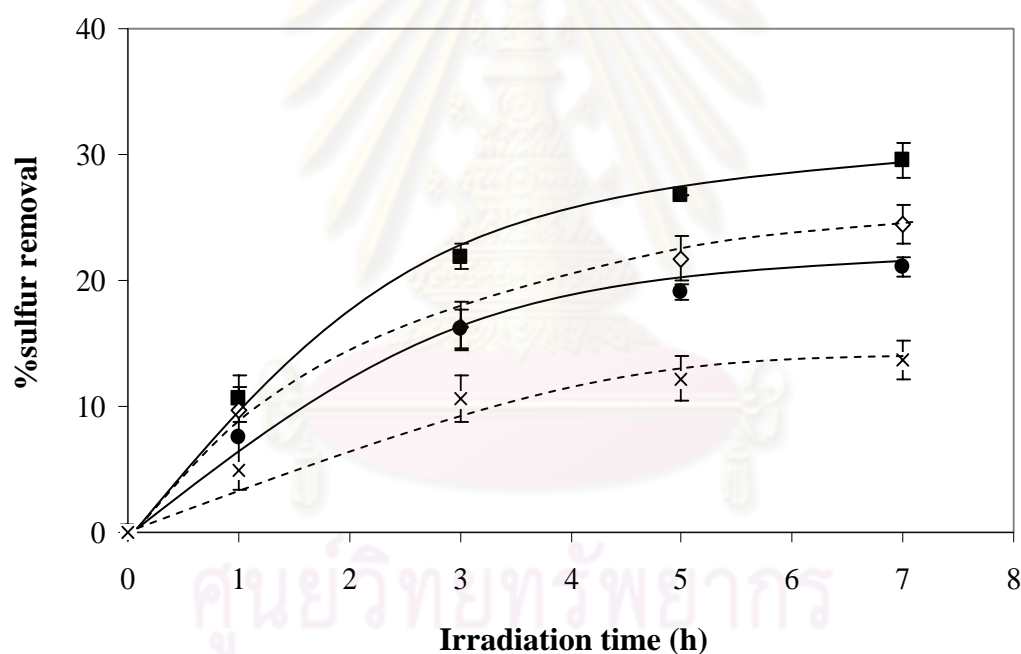


Figure 4.2 Effect of calcination temperature on sulfur removal of waste tire pyrolysis oil: no calcined (—■—); 400°C (-◇-); 600°C (-●-) and 800°C (-×-) ($\text{TiO}_2/\text{pyrolysis oil} = 7 \text{ g/L}$; pyrolysis oil/distilled water = 1/4 (v/v); air flow rate = 150 mL/min and $T = 30^\circ\text{C}$).

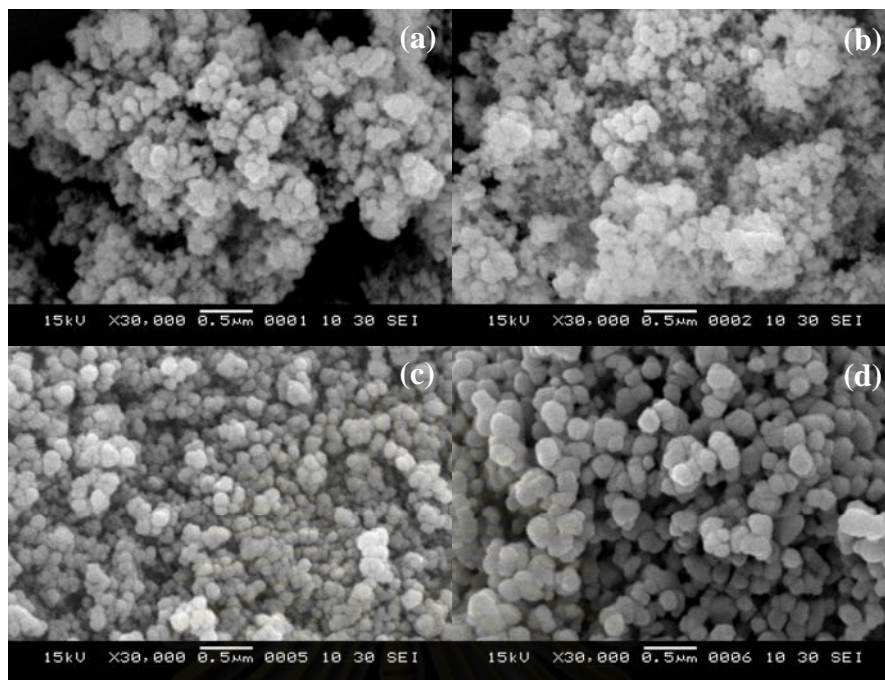


Figure 4.3 SEM morphology of TiO_2 (a) before and after calcination at (b) 400°C ; (c) 600°C and (d) 800°C .

Moreover, the XRD pattern (Figure 4.4) also indicated the formation of rutile phase during calcination which had lower catalytic efficiency for desulfurization. Before calcination, TiO_2 had ratio of anatase to rutile phase (A/R) as 80/20. The anatase phase was shifted to rutile phase when calcination temperature increased (Yu, Su, and Cheng, 2007). At 800°C , the crystallite phase of TiO_2 was only rutile. Some previous research works revealed that the anatase was suitable form for desulfurization than rutile (Yu et al., 2007). For this research, the commercial TiO_2 (Degussa P-25) without calcination containing 70-75% of anatase and 25-30% of rutile had highest potential to decrease the sulfur content in the waste tire pyrolysis oil when it was compared to pure anatase (Basca and Kiwi, 1998; Muggli and Ding, 2001; Ohno et al., 2001)

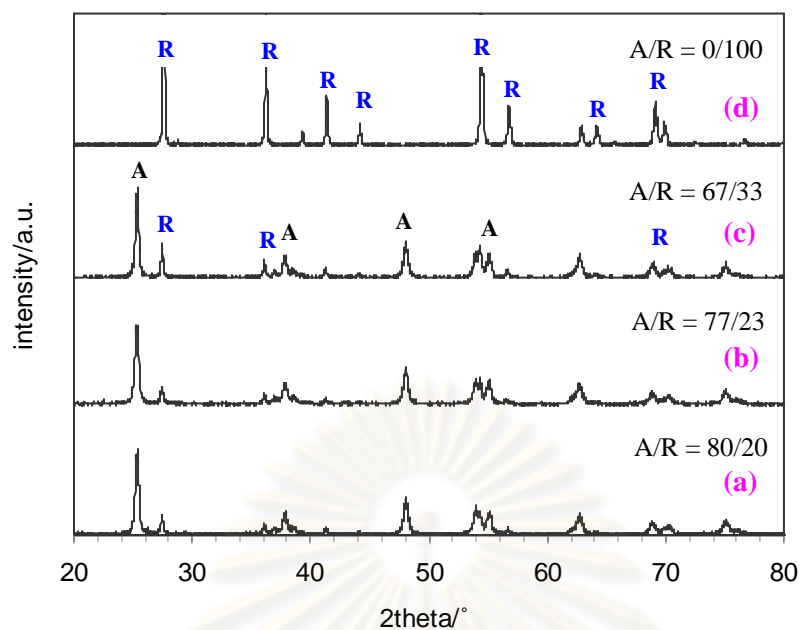


Figure 4.4 XRD patterns of TiO₂ (a) before and after calcination at (b) 400°C; (c) 600°C and (d) 800°C (A = anatase form and R = rutile form)

4.3.3 Influence of Reaction Temperature on Degree of Sulfur Removal

The effect of reaction temperature (30-70°C) on the sulfur reduction of pyrolysis oil in the presence of distilled water at 1/1 (v/v) catalyzed by 7 g of TiO₂/L of pyrolysis oil was shown in Figure 4.5. At 7 h of reaction time, the increase in the reaction temperature from 30 to 70°C slightly increased the %sulfur removal from 27.9 to 31.0%, respectively. It has been well known that the changes of reaction temperature in the range of 21-75°C do not affect the rate of photocatalytic oxidation due to the low activation energy as 0.8 kJ/mol (Fox and Dulay, 1993). At this range of reaction temperature, the thermal energy ($k_T=0.026$ eV) is not enough to activate the electron transfer in the wide band gap of TiO₂ (Matthews, 1987).

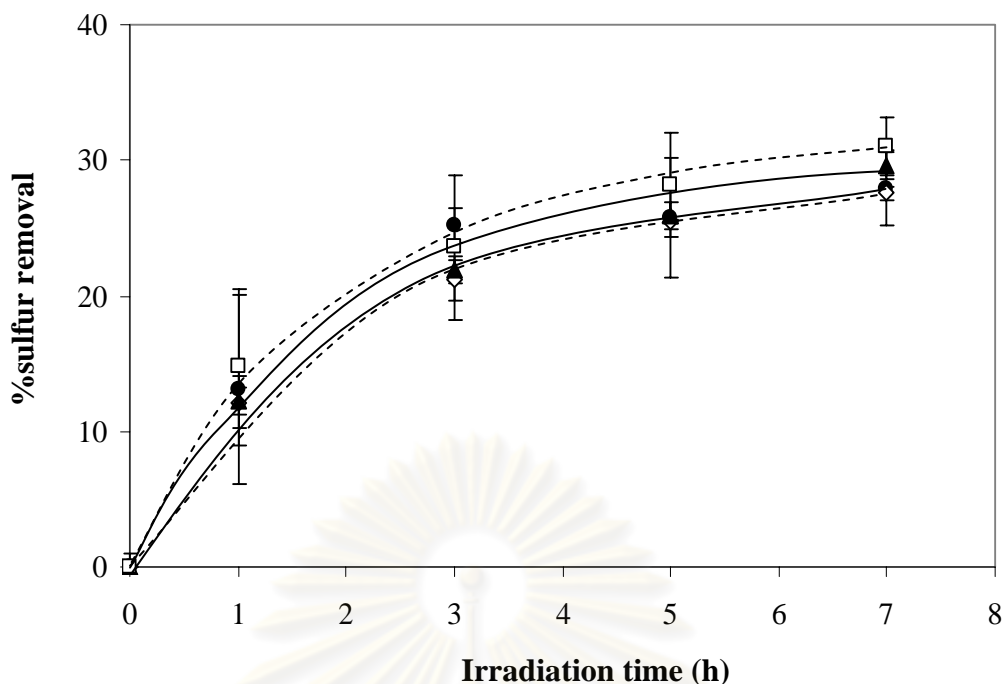


Figure 4.5 Effect of reaction temperature on sulfur reduction of waste tire pyrolysis oil: 30°C (---◇---); 40°C (—●—); 50°C (—▲—) and 70°C (---□---) (TiO_2 /pyrolysis oil = 7 g/L; pyrolysis oil/distilled water = 1/4 (v/v); air flow rate = 150 mL/min).

4.3.4 Influence of Air Flow Rate on Degree of Sulfur Removal

The effect of air flow on the sulfur reduction of pyrolysis oil via photocatalytic desulfurization at 50°C was shown in Figure 4.6. At 1/4 (v/v) of pyrolysis oil/ distilled water catalyzed by 7 g of TiO_2 /L of pyrolysis oil, the air flow rate was varied from 0-150 mL/min. Without the introduction of air into the reaction, the degree of desulfurization was only 3.2%. This indicated that the sulfur compounds in pyrolysis oil could not be oxidized itself by irradiation. The level of photocatalytic desulfurization of pyrolysis oil could be increased when air was supplied into the system. The increase in the air flow rate to 150 mL/min enhanced the %sulfur removal to reach the maximum value as 34.5%. However, the use of air flow rate higher than this point yielded the reduction of sulfur removal efficiency due to the extra volatilization of pyrolysis oil (Zhao et al., 2007). Furthermore, the effect of bubble produced during photocatalytic desulfurization also inhibited TiO_2 to absorb UV light resulting to the reduction of the sulfur removal efficiency (Nam et al., 2002).

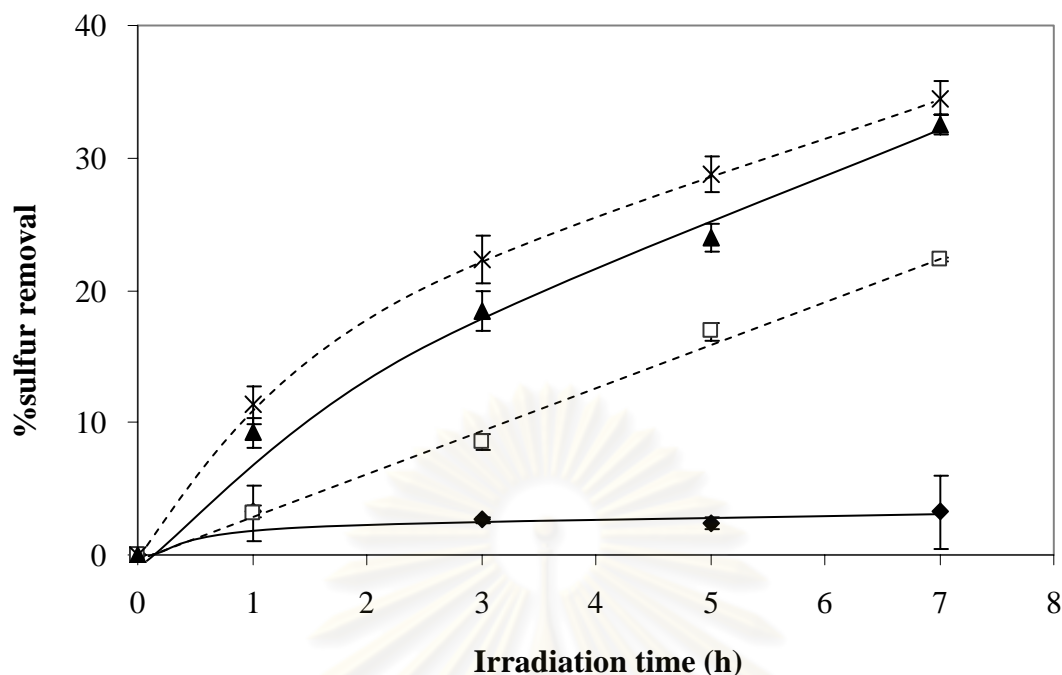


Figure 4.6 Effects of air flow rate on sulfur reduction of waste tire pyrolysis oil: 0 mL/min (—◆—); 50 mL/min (-□-); 100 mL/min (—▲—) and 150 mL/min (-×-) (TiO_2 /pyrolysis oil = 7 g/L; pyrolysis oil/distilled water = 1/4 (v/v) and $T = 50^\circ\text{C}$).

4.3.5 Influence of H_2O_2 Concentration on Degree of Sulfur Removal

The effect of the H_2O_2 concentration on the sulfur reduction of pyrolysis oil at 1/4 (v/v) of pyrolysis oil/ distilled water catalyzed by 7 g of TiO_2 /L of pyrolysis oil for 7 h was presented in Figure 4.7. The concentration of H_2O_2 in the distilled water used as the extracting solvent for photocatalytic desulfurization was varied in the range of 0-30 wt%. Without the introduction of air into the system, H_2O_2 could strongly enhance the photocatalytic efficiency of TiO_2 to remove sulfur compounds in the pyrolysis oil. It was found that the %sulfur removal increased from 3.22 % to 32.7% when the H_2O_2 concentration increased from 0 to 30 wt%, respectively. It could be explained that H_2O_2 was the source of hydroxyl free radicals ($\cdot\text{OH}$), which had strong oxidizing property. Thus, the increase in the H_2O_2 concentration increased the number of $\cdot\text{OH}$ via H_2O_2 photo-dissociation (Eq. 4.1) (Legrini, Oliveros, and Braun, 1993) and the reaction between H_2O_2 and photogenerated electrons on TiO_2 surface (e^-_{cb}) (Eq. 4.2) (Legrini et al., 1993) to enhance the %sulfur removal.

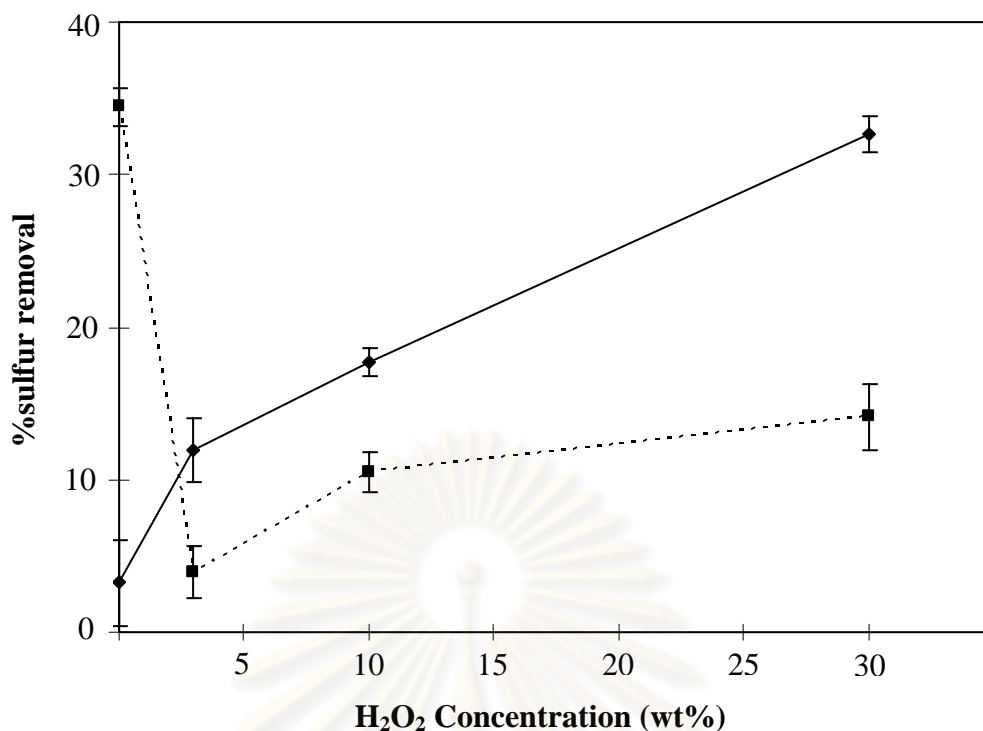
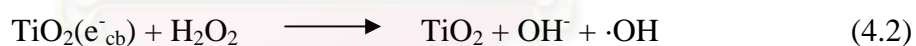


Figure 4.7 Effect of adding H₂O₂ on sulfur reduction of waste tire pyrolysis oil: with air flow rate 150 mL/min (—■—) and no air (---●---) (TiO₂/pyrolysis oil = 7 g/L; pyrolysis oil/distilled water = 1/4 (v/v); T = 50°C and reaction time = 7h).



To compare the system having introduction of air (150 mL/min), the formation of air bubbles was observed. The amount of air bubbles increased with increasing H₂O₂ concentration. These air bubbles inhibited TiO₂ to absorb UV light and be difficult to transfer oxidized sulfur compounds from pyrolysis oil to distilled water phase resulting to the higher amount of remaining sulfur compounds in the oxidized pyrolysis oil.

4.3.6 Influence of Extracting Solvent on Degree of Desulfurization

In this experimental section, the amount and type of extracting solvent affected the ability to remove the sulfone of sulfoxide compounds produced during photocatalytic desulfurization. The extracting solvent used in this section was distilled water, methanol and acetonitrile. To investigate the appropriate content of extracting solvent for this system, distilled water was selected due to its low cost and practicability. Figure 4.8 shows the effect of distilled water content on the degree of photocatalytic desulfurization. The volume ratio of pyrolysis oil to distilled water ($V_{\text{pyrolysis oil}}/V_{\text{distilled water}}$) was varied in the range of 1/1 to 1/5. The reaction was catalyzed by 7 g of TiO_2/L of pyrolysis oil at 50°C . It was observed that the increase in the distilled water content enhanced the %sulfur removal and reached to the maximum point at 34.5% when $V_{\text{pyrolysis oil}}/V_{\text{distilled water}}$ was 1/4 or 1/5 at 7 h of reaction time. The use of lower content of distilled water had lower efficiency to remove oxidized sulfur compounds from the pyrolysis oil after photocatalytic desulfurization possibly due to the saturation of sulfurous compounds in the extracting phase.

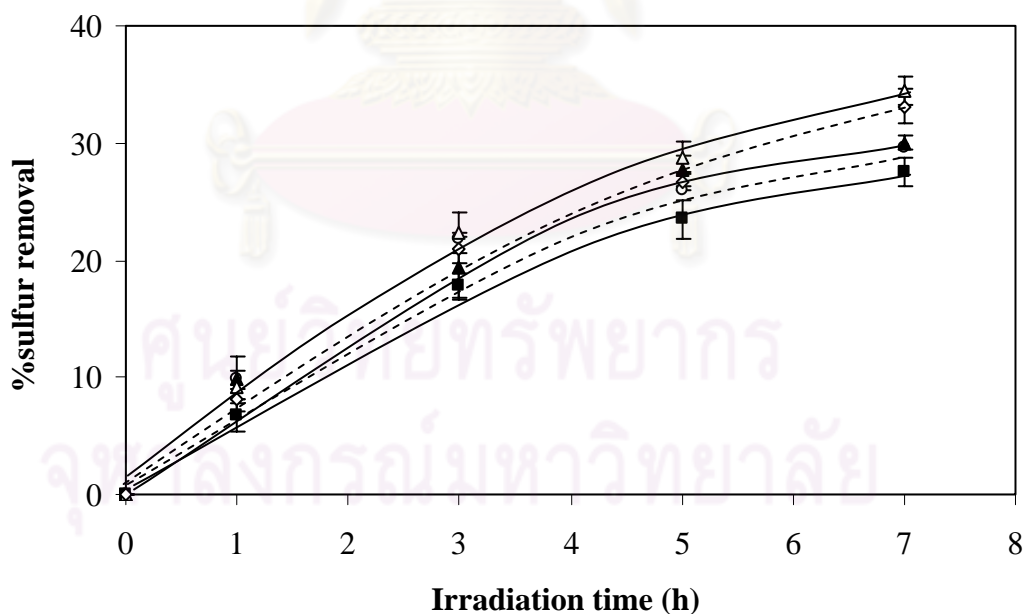


Figure 4.8 Effects of the pyrolysis oil/distilled water (v/v) on sulfur reduction of waste tire pyrolysis oil: 1/1 (—■—); 1/2 (---○---); 1/3 (—▲—); 1/4 (---◆---) and 1/5 (---◻---) ($\text{TiO}_2/\text{pyrolysis oil} = 7 \text{ g/L}$; air flow rate = 150 mL/min and $T = 50^\circ\text{C}$).

The effect of extracting solvent type was shown in Figure 4.9. At $V_{\text{pyrolysis oil}}/V_{\text{distilled water}} = 1/4$ with the similar reaction condition as described before, the results indicated that the photocatalytic desulfurization of the pyrolysis oil in the presence of acetonitrile gave the maximum %sulfur removal at 43.6%, whilst, methanol and distilled water could extract the oxidized sulfurous compounds from the pyrolysis oil 36.7% and 34.5%; respectively when reaction time was 7 h. It could be explained by using polarity of these extracting solvents. The polarity of these extracting solvents was put in the order as followed: distilled water (10.2) > acetonitrile (5.8) > methanol (5.1) (Sivasankar, 2005). Before photocatalytic desulfurization, the appearance of the pyrolysis oils in the presence of each extracting solvent was shown in Figure 4.10. It was observed that the level of homogeneity of the pyrolysis oil in the extracting solvents was highest for acetonitrile. This implied that the polarity of the pyrolysis oil was similar to that of acetonitrile resulting to the higher solubility of pyrolysis oil in acetonitrile than in methanol or distilled water. The color of the pyrolysis oil in acetonitrile was also paler resulting to be easier for UV light penetration. This was advantage for photocatalytic desulfurization to convert sulfurous compounds in the pyrolysis oil to sulfones or sulfoxides which were easier to be removed by distilled water in the next step. Furthermore, the use of acetonitrile also promoted the higher solubility of oxygen in the reaction mixture to enhance the efficiency of sulfur removal (Moeini-Nombel and Matsuzawa, 1998).

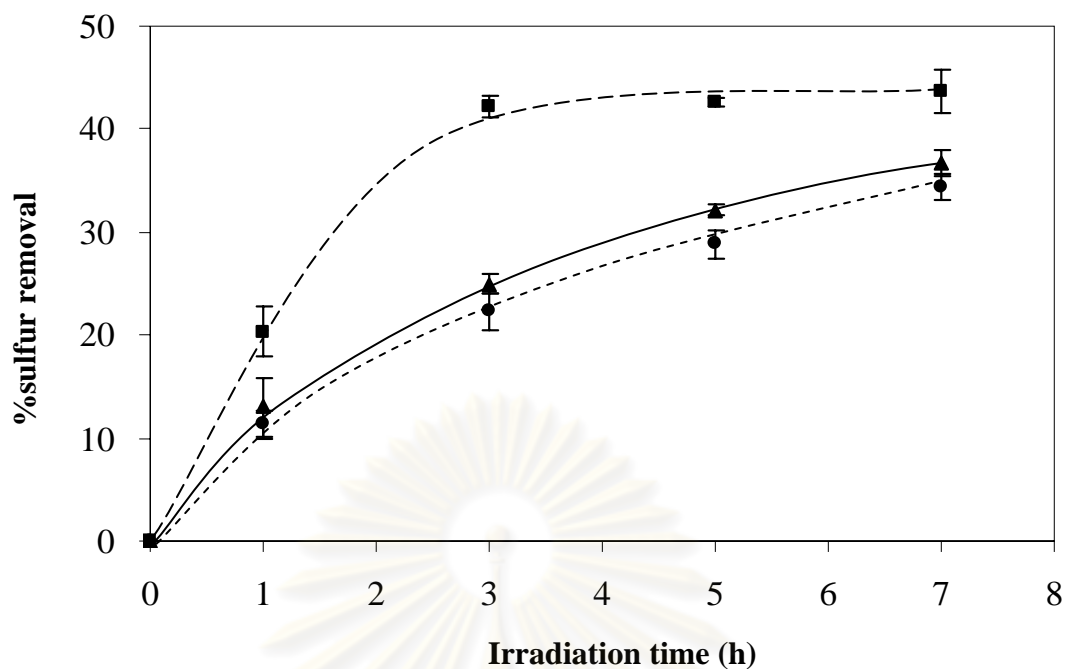


Figure 4.9 Effects of type used as extracting solvent on sulfur reduction of waste tire pyrolysis oil: distilled water (---●---); methanol (—▲—) and acetonitrile (—■—) (TiO_2 / pyrolysis oil = 7 g/L; pyrolysis oil/extracting solvent = 1/4 (v/v); air flow rate = 150 mL/min and $T = 50^\circ\text{C}$).

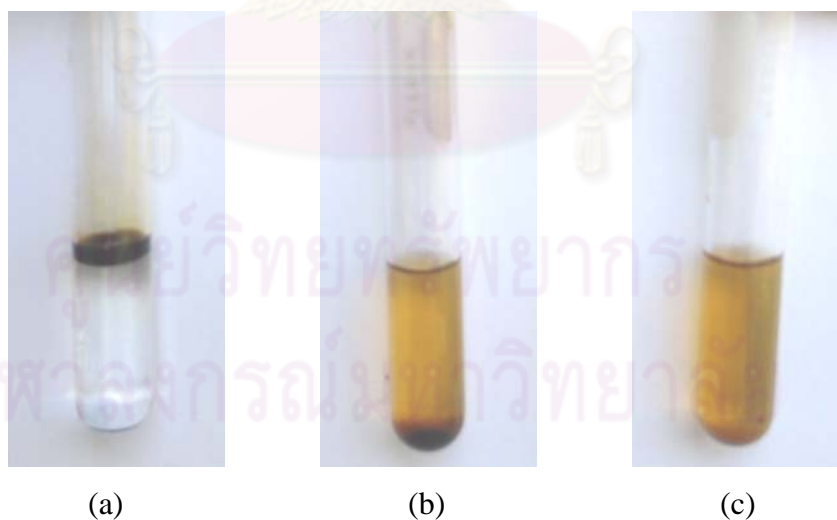


Figure 4.10 Appearance of pyrolysis oil in various extracting solvents: (a) distilled water; (b) methanol and (c) acetonitrile.

4.3.7 Influence of the Stage on Degree of Desulfurization

Table 4.4 shows the effect of photocatalytic desulfurization stages on the level of sulfur removal for waste tire pyrolysis oil. Under the optimum condition: using 7 g of TiO₂/L of pyrolysis oil in the presence of 1/4 (v/v) of pyrolysis oil/acetonitrile at 50°C with 150 mL/min of air flow rate for 7 h, The increase in the number of reaction stages enhanced the %sulfur removal from 40.3% to 42.8% and 47.5% as the number of stages increased from 1 to 2 or to 3; respectively. The first stage exhibited the highest reduction of sulfur compounds possibly due to a large amount of sulfur compounds such as thiophene and its derivatives, including benzothiophenes and its derivatives (Bunthid, Prasassarakich, and Hinchiranan, 2010) in the raw pyrolysis oil derived from waste tire. Thus, it was easier to decompose sulfur compounds in the earlier stage. The reactivity of sulfur compounds for oxidation also increased with increasing the electron density of a sulfur atom in a sulfur-containing compound. For example, the oxidation rate of sulfide was higher than thiophenic compounds (Ford and Young, 1965) because the electron density of sulfur atom in sulfide was higher than that of thiophenic compounds. The other sulfur compounds with higher electron densities could be easier to be oxidized to sulfones.

Table 4.4 Effect of stage of reaction on sulfur reduction of waste tire pyrolysis oil

Stage	%sulfur removal
1	40.3
2	42.8
3	47.5

4.4 Characterization of Sulfurous Compounds Containing in Pyrolysis Oil

Figure 4.11 shows GC-FPD chromatograms of pyrolysis oil derived from waste tire before and after photocatalytic desulfurization. From Figure 4.11(a), it was observed a large amount of sulfurous compounds in the pyrolysis oil. It could be classified type of sulfurous compounds in the pyrolysis oil from the elution time obtained from GC-FPD as 3.57 min for thiophenes, 19.32 min for benzothiophenes,

and 25.01 min for dibenzothiophenes. Thus, this means that the most sulfurous compounds in the pyrolysis oil from waste tire were benzothiophenes, dibenzothiophenes and larger sulfurous molecules.

After photocatalytic desulfurization in the presence of acetonitrile following the extraction by using distilled water, Figure 4.11 (b) shows the reduction of peak intensity of sulfurous compounds in the oxidized pyrolysis oil. It was observed that the peak intensity of sulfides, benzothiophenes, dibenzothiophenes and larger sulfurous molecules were decreased. However, the peak intensity of thiophenes was more difficult to be reduced by this method possibly due to the lower electron density of thiophenes resulting to the lower reactivity for photooxidation (Matsuzawa et al., 2002). The electron density of a sulfur atom in a sulfur-containing compounds decreased in the order: sulfides (5.915) > dibenzothiophene (5.758) > benzothiophene (5.739) > thiophene (5.696) (Otsuki et al., 2000).

To monitor the conversion of sulfurous compounds after photoirradiation, the oxidized pyrolysis oil obtained from photocatalytic desulfurization in the presence of acetonitrile for 7 h before extraction step by using distilled water was subjected to the high performance chromatographer (HPLC) at 245 nm of wavelength. The results were also compared with the standard sulfurous compounds: thiophene, benzothiophene, and dibenzothiophene which were photo-oxidized by the similar process as shown in Figure 4.12. Before photocatalytic desulfurization (Figure 4.12 a), the HPLC signals of standard sulfurous compounds were eluted at 1.99, 2.47 and 4.26 min for thiophene, BT and DBT; respectively; while the pyrolysis oil indicated the broader signal. This means that the sulfurous compounds in the pyrolysis oil had various sizes of sulfur molecules. This result was similar to that obtained from GC-FPD.

After photocatalytic desulfurization (Figure 4.12 b), the new signals of oxidized standard sulfurous compounds were appeared at earlier elution time (1.2-1.9 min) indicating the higher polarity. The products of standard sulfurous compounds after photoirradiation might be sulfone, sulfoxide, and sultine (Vignier et al., 1983).

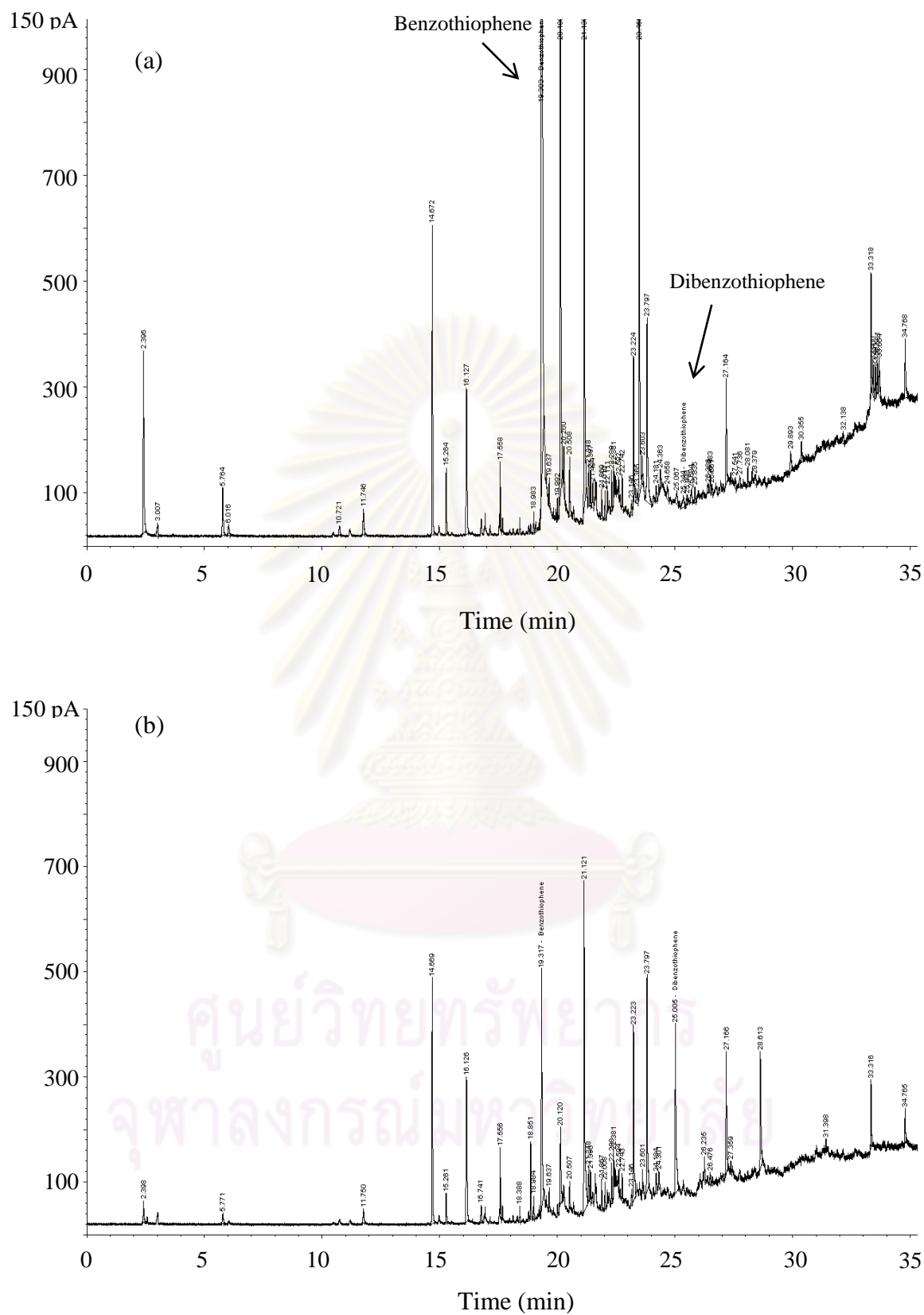


Figure 4.11 GC-FPD Chromatograms of (a) pyrolysis oil and (b) photo-oxidized pyrolysis oil.

For the oxidized pyrolysis oil, the HPLC signal was narrower and also appeared at the earlier stage of elution time same as the oxidized standard sulfurous compounds. This implied that the most of sulfurous compounds in the pyrolysis oil was converted as sulfurous species with higher polarity after photocatalytic desulfurization.

After extraction of the oxidized pyrolysis oil by using distilled water, the results obtained from GC-FPD as presented in Figure 4.11 (b) showed the new signals at 18.85, 26.23, and 28.61 min which were in the region of benzothiophenes and dibenzothiophenes. It was possible that the new sulfurous compounds were generated during photocatalytic desulfurization as shown in Figure 4.13 and 4.14 which proposed the conversion of 3-methyl BT and DBT via photoirradiation; respectively (Shiraishi et al., 1999).

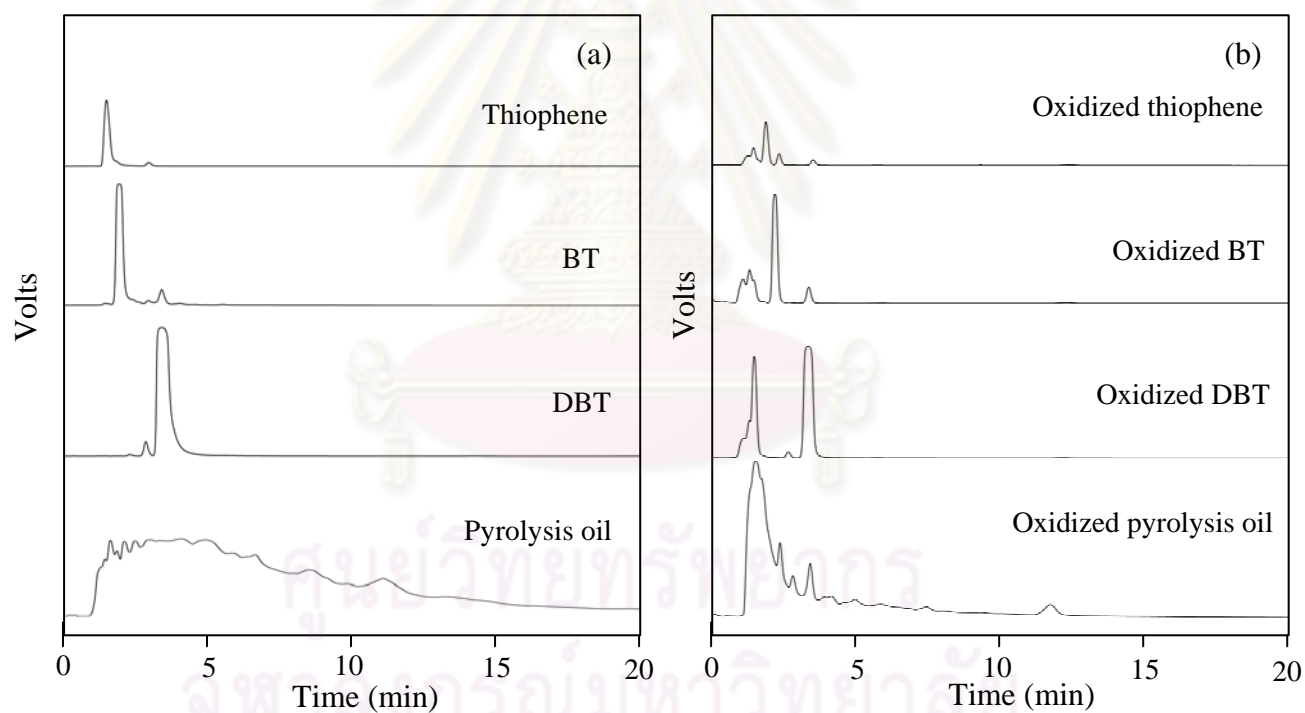


Figure 4.12 HPLC Chromatograms of standard sulfur compounds and pyrolysis oil (a) before and (b) after photocatalytic desulfurization.

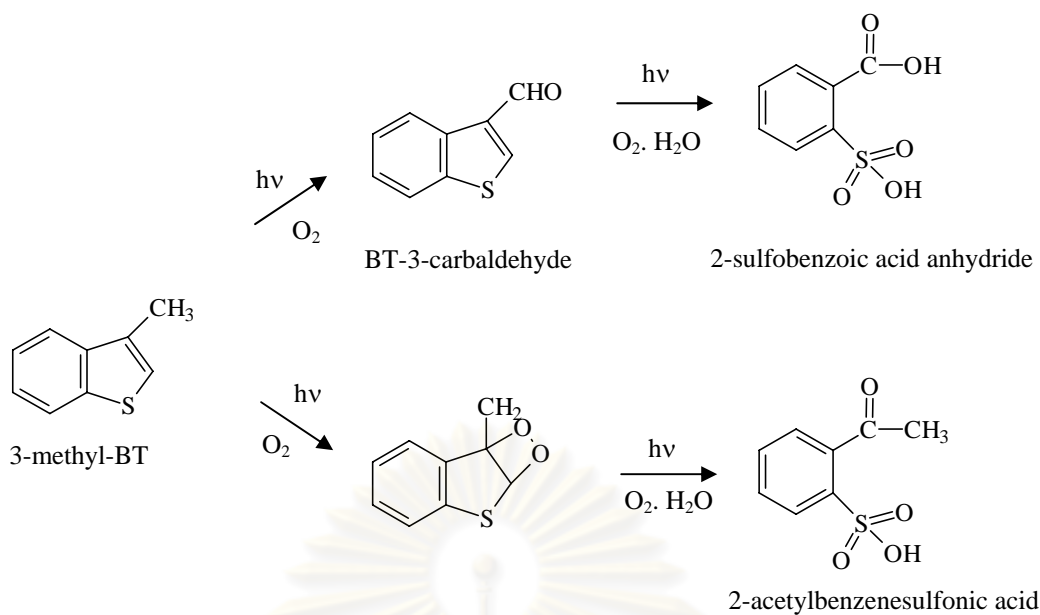


Figure 4.13 Reaction pathway for 3-methyl BT in acetonitrile by photoirradiation (Shiraishi et al., 1999).

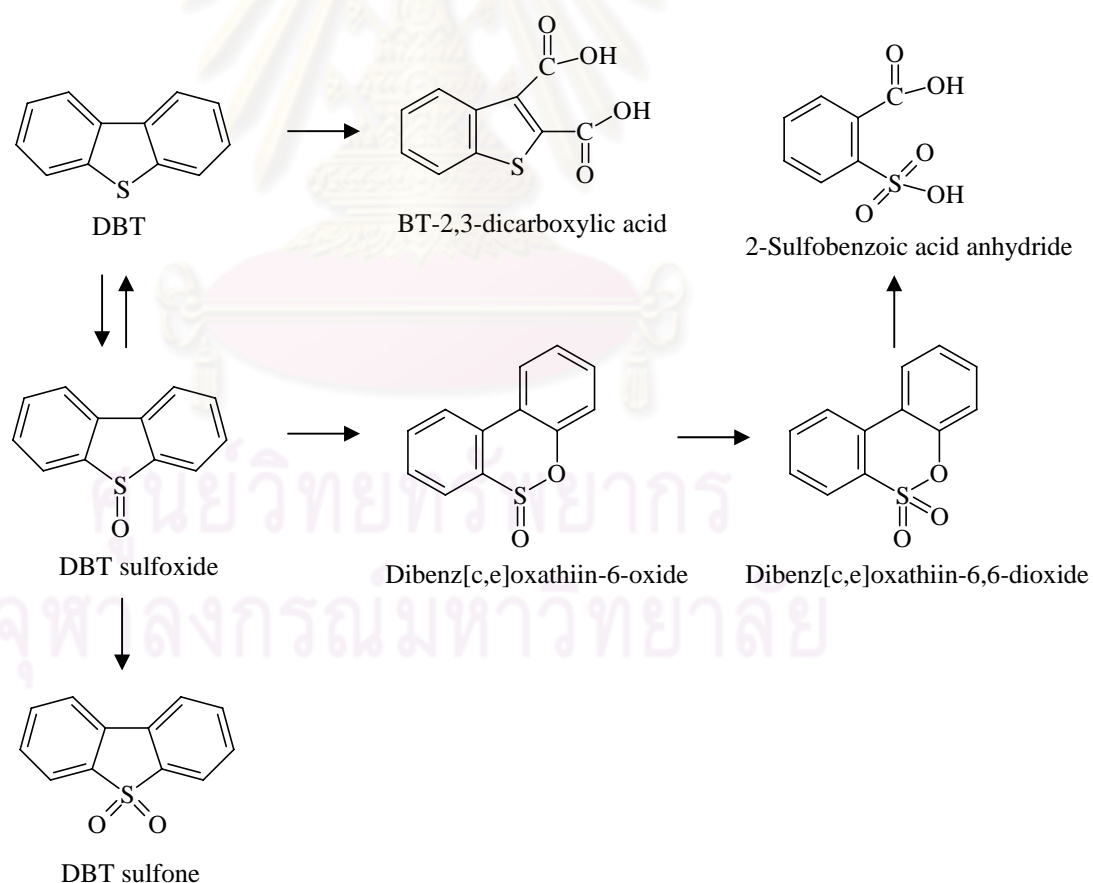


Figure 4.14 Reaction pathway for DBT in acetonitrile by photoirradiation (Shiraishi et al., 1999).

4.5 Quality of Oxidized Pyrolysis Oil

Gross calorific heating value of pyrolysis oil after photocatalytic desulfurization by using 7g/L of TiO_2 for 1-7 h was determined following ASTM D 2015 and shown in Table 4.5. It was found that the increase in the TiO_2 dosage enhanced the level of sulfur removal throughout the period of reaction time. The highest %sulfur removal at 27.9% was achieved when 7 g of TiO_2 /L of pyrolysis oil was loaded into the system and allowed for 7 h of reaction time. The gross calorific heating value of all samples obtained from the photocatalytic desulfurization of pyrolysis oil at various reaction time was ca. 43 MJ/kg. This means that this process did not affect the gross calorific heating value of product.

The other oil properties such as viscosity (ASTM D 445) and corrosive property (ASTM D 130) were determined and compared to commercial diesel and gasoline as shown in Table 4.6. The viscosity of pyrolysis oil was 2.66 Sct. which was in the range of viscosity of the commercial diesel (1.8 to 4.1 Sct.), but it was higher than that of gasoline fuel (0.53 Sct.). After photocatalytic desulfurization, the viscosity of the oxidized pyrolysis oil was higher than that of pyrolysis oil possibly due to the polymerization of organic matters during desulfurization process. From the test of the copper strip corrosion, it was found that the oxidized pyrolysis oil had no effect on the corrosion and the color of copper strip. This result indicated that the oxidized pyrolysis oil could be applied for equipments made from copper. The gross calorific heating value of the oxidized pyrolysis oil (43 MJ/kg) was also close to that of diesel. Thus, it is possible to apply this oil as an alternative fuel for replacing the conventional one after treating with the higher effective desulfurization process.

Table 4.5 Gross calorific heating value of photocatalytic oxidation of sulfur in pyrolysis oil using TiO₂ dosage 7 g/L

Irradiation time (h)	Sulfur removal (%)	Remaining sulfur contents (wt%)	Gross calorific heating value(MJ/kg)
0	0	0.7850	43.2
1	13.1	0.6823	43.2
3	25.2	0.5872	42.8
5	25.8	0.5827	43.1
7	27.9	0.5655	43.2

Table 4.6 Viscosity, copper strip corrosion and gross calorific heating value of oils

Products	Viscosity (Sct)	Copper strip corrosion	Gross calorific heating value(MJ/kg)
Diesel	2.0-5.0 ^a	Not worse than No.1 ^a	45
Gasoline	0.53	Not more than No.1 ^a	47
Pyrolysis oil	2.66 [*]	Not change	42-43
Oxidized pyrolysis oil	2.85	Not change	43

^a Standard for diesel and gasoline quality (USEPA, 1996)

^{*} Obtained from pyrolysis at 400°C for 15 min.

ศูนย์วิทยทรัพยากร
จุฬาลงกรณ์มหาวิทยาลัย

CHAPTER V

CONCLUSIONS

5.1 Conclusions

5.1.1 Characterization of Waste Tire and Its Pyrolysis Products

The waste tire powder had high content of volatile matter with low amount of moisture. However, it also contained a large amount of sulfurous compounds (1.54 wt%). Due to the high carbon content, the calorific value of waste tire powder was also high (35.7 MJ/kg). After pyrolysis process, the pyrolysis yields derived from waste tire was consisted of pyrolysis light oil, pyrolysis heavy oil, char and gas fractions at a composition of 39.6, 14.0, 38.2 and 8.12 wt%, respectively. According to the large amount of light oil fraction, the pyrolysis light oil was used as the raw material for further experiment. The pyrolysis light oil had gross calorific value as 42 MJ/kg with 0.84 wt% of sulfur content.

5.1.2 Photocatalytic Desulfurization of Pyrolysis Oil Derived from Waste Tire

From the results of photocatalytic desulfurization of the light oil fraction obtained from waste tire pyrolysis, it was found that the increase in the TiO_2 content, air flow rate and reaction temperature enhanced the sulfur reduction of pyrolysis oil. Whereas, the increase in the calcination temperature decreased the catalytic activity of TiO_2 by promoting the formation of rutile structure. The increase in the H_2O_2 concentrate without the introduction of air into the system also gave higher the sulfur removal efficiency. It could be explained that H_2O_2 was the source of hydroxyl radicals ($\cdot\text{OH}$), which had strong oxidizing property. The use of acetonitrile as an extracting solvent for photocatalytic desulfurization showed the maximum %sulfur removal efficiency as 43.6% due to the polarity of the pyrolysis oil was similar to that of acetonitrile resulting to the higher solubility of pyrolysis oil in acetonitrile. The

color of the pyrolysis oil in acetonitrile was also paler resulting to be easier for UV light penetration. It could be concluded that the maximum %sulfur removal at 47.5% was achieved when 7 g/L of uncalcined TiO_2 was loaded in the presence of 1/4 (v/v) of pyrolysis oil/acetonitrile at 50°C for 7 h after 3 stages of reaction.

The oxidation of sulfurous compounds in the pyrolysis oil before and after photocatalytic desulfurization was determined by using GC-FPD and HPLC. Its results indicated that the most sulfurous compounds in the pyrolysis oil from waste tire were benzothiophenes, dibenzothiophene and the larger molecules of sulfurous compounds molecules. After photocatalytic desulfurization, the sulfurous compounds in pyrolysis oil were reduced; especially, benzothiophenes by converting as sulfones or sulfoxides with higher polarity which was easier to be dissolved into the extracting phase.

5.1.3 Quality of the Photo-Oxidized Pyrolysis Oil

The viscosity of the pyrolysis oil was close to the commercial diesel and higher than that of gasoline. The photocatalytic desulfurization produced the lower sulfurous content in the pyrolysis oil without the effect on the heating value and corrosive property.

5.2 Recommendations

5.2.1 Enhancement of Titanium Dioxide Efficiency

Due to the limitation for oxidizing sulfurous compounds of TiO_2 (Degussa P-25) via photocatalytic desulfurization, TiO_2 properties should be improved by increasing the adsorption efficiency to increase the surface area. The doping with some metal such as manganese (Mn) on the surface of TiO_2 is also recommended. The electrons from TiO_2 can be transferred to change Mn^{4+} as Mn^{3+} ($\text{Mn}^{4+}/\text{Mn}^{3+}$). The electrons trapped on the $\text{Mn}^{4+}/\text{Mn}^{3+}$ sites are subsequently transferred to O_2 adsorbed on the surface to generate superoxide radical anions, which can oxidize sulfur compounds. Thus, Mn serves as an electron acceptor to effectively inhibit the charge recombination of TiO_2 .

5.2.2 Preparation of TiO₂ Photocatalyst on Various Rigid Supports

The use of TiO₂ powder as photocatalyst normally requires the separation step to isolate from products. The impregnation or coating of TiO₂ on rigid supports with transparency property such as poly(methyl methacrylate) or glass beads is easier to separate and reuse TiO₂ for several times. The transparency of supports is expected to enhance the efficiency of TiO₂ to catalyze the reaction.



ศูนย์วิทยทรัพยากร
จุฬาลงกรณ์มหาวิทยาลัย

REFERENCES

- Abdel-Wahab, A. M. A., and Gaber, A. A. M. (1998). TiO₂-photocatalytic oxidation of selected heterocyclic sulfur compounds. Journal of Photochemistry and Photobiology A 114: 213-218.
- Ali, M. F., Al-Malki, A., and Ahmed, S. (2009). Chemical desulfurization of petroleum fractions for ultra-low sulfur fuels. Fuel Processing Technology 90: 536–544.
- Babich, I. V., and Moulijn, J. A. (2003). Science and technology of novel processes for deep desulfurization of oil refinery streams: a review. Fuel 82: 607–31.
- Basca, R. R., and Kiwi, J. (1998). Effect of rutile phase on the photocatalytic properties of nanocrystalline titania during the degradation of p-coumaric acid. Applied Catalysis B: Environmental 16: 19-29.
- Bernard, J. R. (1980). Hydrocarbons aromatization on platinum alkaline zeolites. In L. W. Rees (ed.), Proceedings of the 5th International Conference Zeolites, pp. 686-695. London: Heyden.
- Berrueco, C., Esperanza, E., Mastral, F. J., Ceamanos, J., and Garc´a-Bacaicoa, P. (2005). Journal of Analytical and Applied Pyrolysis 73: 65–73.
- Boxiong, S., Chunfei, W., Cai, L., Binbin, G., and Rui, W. (2007). Pyrolysis of wastes tyres: The influence of USY catalyst/tyre ratio on products. Journal of Analytical and Applied Pyrolysis 78: 243–249.
- Bunthid, D., Prasassarakich, P., and Hinchiranan, N. (2010). Oxidative desulfurization of tire pyrolysis naphtha in formic acid/H₂O₂/pyrolysis char system. Fuel 89: 2617-2622.
- Cao, Q., Jin, L. E., Bao, W. R., and Lv, Y. K. (2009). Investigations into the characteristics of oils produced from co-pyrolysis of biomass and tire. Fuel Processing Technology 90: 337–342.
- Carp, O., Huisman, C. L., and Reller, A. (2004). Photoinduced reactivity of titanium dioxide. Progress in Solid State Chemistry 32: 33–177.
- Dall'Orso, M., San Miguel, G., Fowler, G. D., and Sollars, C. J. (1999). Pneumatici usati alternative di utilizzo ed opzioni di smaltimento. RS Rifiuti Solidi XIII 1: 12–25.
- Davidson, R. S., Bratt, J. E. (1983). The titanium dioxide sensitised photo-oxidation of sulphides. Tetrahedron Letters 24: 5903.

- De Marco Rodriguez, I., et al (2001). Pyrolysis of scrap tires. Fuel Processing Technology 72: 9–22.
- Dick, J. S. (2001). Rubber Technology: compounding and testing for performance, pp. 381-382. Munich, Germany: Hanser Gardner.
- Dodds, J., et al (1983). Scrap tyres: A resource and technology evaluation of tyre pyrolysis and other selected alternative technologies, EGG-2214. Washington, DC: US Department of Energy.
- Edward, L., Mui, K., Danny C. K. Ko, and Gordon McKay (2004). Production of chars from waste tyres-a review. Carbon 42: 2789–2805.
- Eriksen, J., Foote, C. S., and Parker, T. L. (1977). Photosensitized oxygenation of alkenes and sulfides via a non-singlet-oxygen mechanism. Journal of The American Chemical Society 99: 6455.
- Erman, B., Mark, J. E., and Eirich, F. R. (2005). Vulcanization: Science and technology of rubber, p. 678. Amsterdam: Elsevier Academic Press.
- Ford, J. F., and Young, V. O. (1965). Effect of structure on the rate of reaction of organo-sulfur compounds with peracetic acid and t-butyl hydroperoxide. Preprints Division of Petroleum Chemistry, American Chemical Society 10: C-111.
- Fox, M. A. (1987). Selective formation of organic compounds by photoelectrosynthesis at semiconductor particles. Topics in Current Chemistry 142: 21.
- Fox, M. A. (1990). In N. Serpone and E. Pelizzetti (eds.), Photocatalysis: Fundamentals and Applications, p.421. New York: Wiley.
- Fox, M. A., and AbdeI-Wahab, A. A. (1990). Photocatalytic oxidation of multifunctional organic molecules: The effect of an intramolecular aryl thioether group on the semiconductor-mediated oxidation/dehydrogenation of a primary aliphatic alcohol. Journal of Catalysis 126: 693.
- Fox, M. A., and AbdeI-Wahab, A. A. (1990). Selectivity in the TiO₂-mediated photocatalytic oxidation of thioethers. Tetrahedron Letters 31: 4533.
- Fox, M. A., and Dulay, M. T. (1993). Heterogeneous photocatalysis. Chemical Reviews 95: 341-357.
- Fujishima, A., Hashimoto, K., and Watanabe, T. (1999). TiO₂ Photocatalysis: Fundamental and Applications. Tokyo: BKC Industrial Company.

- Galvagno, S., Casu, S., Casabianca, T., Calabrese, A., and Cornacchia, G. (2002). Pyrolysis process for the treatment of scrap tyres: Preliminary experimental results. Waste Management 22: 917.
- Grassie, N. (1971). Thermal Degradation. In H. F. Mark et al. (eds.), Encyclopedia of Polymer Science and Technology 14: 651.
- Hernandez-Maldonado, A. J., Stamatis, S. D., and Yang, R. T. (2004). New sorbents for desulfurization of diesel fuels via π complexation: layered beds and regeneration. Industrial and Engineering Chemistry Research 43: 769–776.
- Hernandez-Maldonado A. J., Yang, F. H., Qi, G., and Yang, R. T. (2005). Desulfurization of transportation fuels by π -complexation sorbents: Cu(I)-, Ni(II)-, and Zn(II)-zeolites. Applied Catalysis B: Environmental 56: 111-126.
- Hernandez-Maldonado, A. J., and Yang, R. T. (2003). Desulfurization of Liquid Fuels by Adsorption via π -complexation with Cu(I)-Y and Ag-Y Zeolites. Industrial and Engineering Chemistry Research 42: 123-129.
- Hernandez-Maldonado, A. J., and Yang, R. T. (2004). Denitrogenation of transportation fuels by zeolites at ambient temperature and pressure. Angewandte Chemie International Edition 43: 1004–1006.
- Hernandez-Maldonado, A. J., and Yang, R. T. (2004). Desulfurization of diesel fuels by adsorption via π -complexation with vapor-phase exchanged Cu(I)-Y zeolites. Journal of the American Chemical Society 126: 992-993.
- Hernandez-Maldonado, A. J., and Yang, R. T. (2004). Newsorbents for desulfurization of diesel fuels via π complexation. AIChE Journal 50: 791–801.
- Hirai, T., Ogawa, K., and Komasa, I. (1996). Desulfurization process for dibenzothiophenes from light oil by photochemical reaction and liquid-liquid extraction. Industrial and Engineering Chemistry Research 35: 586-589.
- Huang, D., Wang, Y. J., Cui, Y. C., and Luo, G. S. (2008). Direct synthesis of mesoporous TiO_2 and its catalytic performance in DBT oxidative desulfurization. Microporous and Mesoporous Materials 116: 378-385.
- Ibrahim, A., Xian, S. B., and Wei, Z. (2003). Desulfurization of FCC gasoline by solvent extraction and photooxidation. Petroleum Science and Technology 21: 1555-1573.
- Ito, E., and Rob van Veen, J. A. (2006). On novel processes for removing sulphur from refinery streams. Catalysis Today 116: 446–60.

- Jayne, D., Zhang, Y., Haji, S., and Erkey, C. (2005). Dynamics of removal of organosulfur compounds from diesel by adsorption on carbon aerogels for fuel cell application. International Journal of Hydrogen Energy 30: 1287-1293
- Jenkins, B. M. (1989). Physical properties of biomass. In O. Kitani and C.W. Hall (eds.), Biomass Handbook. New York: Gordon and Breach Science.
- Juma, M. Korenova, Z., Markos, J., Annus, J., and Jelemensky, L. (2006). Pyrolysis and combustion of scrap tire. Petroleum and Coal 48: 15-26.
- Kim, I. K., Huang, C. P., and Chiu, P.C. (2001). Sonochemical decomposition of dibenzothiophene in aqueous solution. Water Research 35: 4370–4378.
- Kim, J. H., Ma, X., Zhou, A., and Song, C. (2006). Ultra-deep desulfurization and denitrogenation of diesel fuel by selective adsorption over three different adsorbents: a study on adsorptive selectivity and mechanism. Catalysis Today 111: 74–83.
- King, D. L., Faz, C., and Flynn T. (2000). Desulfurization of Gasoline Feedstocks for Application in Fuel Reforming. SAE paper 2000-01-0002, Society of Automotive Engineers. Detroit, MI.
- Klug, H. P., and Alexander, L. E. (1954). X-Ray diffraction procedures for polycrystalline and amorphous materials, p. 491. London: John Wiley.
- Konstantinou, I. K., and Albanis, T. A. (2004). TiO₂-assisted photocatalytic degradation of azo dyes in aqueous solution: kinetic and mechanistic investigations—a review. Applied Catalysis B: Environmental 49: 1–14.
- K.Rajeshwar, J. (1995). Photoelectrochemistry and the environment. Journal of Applied Electrochemistry 25: 1067.
- Ku, Y., and Hsieh, C.B. (1992). Photocatalytic decomposition of 2,4-dichlorophenol in aqueous TiO₂ suspensions. Water Research 26: 1451-1456.
- Laresgoiti, M. F., et al (2004). Characterization of the liquid products obtained in tyre pyrolysis. Journal of Analytical and Applied Pyrolysis 71: 917–934.
- Laresgoiti, M. F., et al (2000). Chromatographic analysis of the gases obtained in tyre pyrolysis. Journal of Analytical and Applied Pyrolysis 55: 43-54.
- Legrini, O., Oliveros, E., and Braun, A. M. (1993). Photochemical process for water treatment. Chemical Review 93: 671–698.
- Liang, J. -J., Gu, C. L., Kacher, M. L., and Foote, C. S. (1983). Chemistry of singlet oxygen. Journal of the American Chemical Society 105: 4717.

- Litter, M. I. (1999). Heterogeneous photocatalysis: Transition metal ions in photocatalytic systems. Applied Catalysis B: Environmental 23: 89-114.
- Matthews, R. W. (1987). Photooxidation of organic impurities in water using thin films of titanium dioxide. Journal of Physical Chemistry 91: 3328-3333.
- Meille, V., Shulz, E., Vrinat, M., and Lemaire, M. (1998). A new route towards deep desulfurization: selective charge transfer complex formation. Chemical Communications 3: 305.
- Muggli, D. S., and Ding, L. (2001). Photocatalytic performance of sulfate TiO₂ and Degussa P-25 TiO₂ during oxidation of organics. Applied Catalysis B: Environmental 32: 181-194.
- Moeini-Nombel, L., and Matsuzawa, S. (1998). Effect of solvents and a substituent group on photooxidation of fluorene. Journal of Photochemistry and Photobiology A: Chemistry 119: 15-23.
- Ma, X., Sun, L., and Song, C. (2002). A new approach to desulfurization of gasoline, diesel fuel and jet fuel by selective adsorption for ultra-clean fuels and fuel cell applications. Catalysis Today 77: 107-116.
- Ma, X., Sun, L., Yin, Z., and Song, C. (2001). New approaches to deep desulfurization of diesel fuel, jet fuel, and gasoline by adsorption for ultra-clean fuels and for fuel cell applications. Preprints Division of Petroleum Chemistry, American Chemical Society 46: 648.
- Ma, X., Velu, S., Kim, J. H., and Song, C. (2005). Deep desulfurization of gasoline by selective adsorption over solid adsorbents and impact of analytical methods on ppm-level sulfur quantification for fuel cell applications. Applied Catalysis B: Environmental 56: 137-147.
- Madorsky, S. L. (1964). Thermal Degradation of Organic Polymers. New York: Wiley InterScience.
- Matsuzawa, S., Tanaka, J., Sato, S., and Ibusuki, T. (2002). Photocatalytic oxidation of dibenzothiophenes in MeCN using TiO₂: Effect of hydrogen peroxide and ultrasound irradiation, Journal of Photochemistry and Photobiology A 149: 183-189.
- McNeill, I. C. (1989). Thermal Degradation. In G.C. Eastmond et al. (eds.), Comprehensive Polymer Science. Oxford: Pergamon Press.

- Milenkovic, A., et al. (1999). Selective elimination of alkyldibenzothiophenes from gas oil by formation of insoluble charge-transfer complexes. Energy and Fuels 13: 881.
- Mirmiran, S., Pakdel, H., and Roy, C. (1992). Characterization of used tire vacuum pyrolysis oil: nitrogenous compounds from the naphtha fraction. Journal of Analytical and Applied Pyrolysis 22: 205.
- Murugan, S., Ramaswamy, M. C., and Nagarajan, G. (2006). Production of tyre pyrolysis oil from waste automobile tyres. Proceedings of National Conference on Advances in Mechanical Engineering, pp. 899–906.
- Nam, W. S., Kim, J. M., and Han, G. Y., (2002). Photocatalytic oxidation of methyl orange in a three- phase fluidized bed reactor. Chemosphere 47: 1019.
- Natarajan, E., Nordin, A., and Rao, A. N. (1998). Overview of combustion and gasification of rice husk in fluidized bed reactors. Biomass Bioenergy 14: 533-546.
- Ohno, T., Sarukawa, K., Tokieda, K., and Matsumura, M. (2001). Morphology of a TiO₂ photocatalyst (Degussa, P-25) consisting of anatase and rutile crystalline phases. Journal of Catalysis 203: 82-86.
- Otsuki, S., et al (2000). Oxidative desulfurization of light gas oil and vacuum gas oil by oxidation and solvent extraction. Energy and Fuels 14: 1232-1239.
- Pakdel, H., Pantea D. M., and Roy, C. (2001). Production of dl-limonene by vacuum pyrolysis of used tires. Journal of Analytical and Applied Pyrolysis 57: 91-107.
- Pandey, A. (2008). Handbook of plant-based biofuels, p. 35. USA: CRC Press.
- Pavlik, J. W., and Tanlayanon, S. (1981). Photocatalytic oxidation of lactams and N-acylamines. Journal of the American Chemical Society 103: 6755.
- Robertson, J., and Bendosz, T. (2006). Photooxidation of dibenzothiophene on TiO₂/hectorite thin films layered catalyst. Journal of Colloid and Interface Science 299: 125-135.
- Rose, J. W., and Cooper, J. R. (1977). British National Committee of the World Energy Conference, London 56: 463.
- Roy, C., Labrecque, B., and Caumia, B. D. (1990). Recycling of scrap tires to oil and carbon black by vacuum pyrolysis. Resources, Conservation and Recycling 4: 203-213.
- Salem, A. B. S. H., and Hamid, H. S. (1997). Removal of sulphur compound from

- naphtha solutions using solid adsorbents. Chemical Engineering and Technology 20: 342-347.
- Savage, D. W., Kaul, B. K., Dupre, G. D., and O'Bara, J. T. (1995). Deep desulfurization of distillate fuels. U.S patent 5 454: 933.
- Schwartz, P. F., Turro, N. J., Bossmann, S. H., Braun, A. M., Abdel-Wahab, A. A., and Durr, H. (1997). A new method to determine the generation of hydroxyl radicals in illuminated TiO₂ suspensions. Journal of Physical Chemistry 101: 7127.
- Schnecko, H. (1994). Rubber recycling. Kautschuk Gummi Kunststoffe 47: 885.
- Shiraishi, Y., Hirai, T., and Komasaawa, I. (1998). A deep desulfurization process for light oil by photochemical reaction in an organic two-phase liquid-liquid extraction system. Industrial and Engineering Chemistry Research 37: 203-211.
- Shiraishi, Y., Hirai, T., and Komasaawa, I. (1999). Identification of desulfurization products in the photochemical desulfurization process for benzothiophenes and dibenzothiophenes from light oil using an organic two-phase extraction system. Industrial and Engineering Chemistry Research 38: 3300-3309.
- Sivasankar, B. (2005). Bioseparations: Principles and Techniques, p. 203. New Delhi: Prentice-Hall of India.
- Snyder, R. H. (1998). Enhancement of cytotoxicity and clastogenicity of L-DOPA and dopamine by manganese and copper. Society of Automotive Engineering 405: 1-8.
- Song, C. (2003). An overview of new approaches to deep desulfurization for ultra-clean gasoline, diesel fuel and jet fuel. Catalysis Today 86: 211-63.
- Song, C., and Ma, X. (2003). New design approaches to ultra-clean diesel fuels by deep desulfurization and deep dearomatization. Applied Catalysis B: Environmental 41: 207-38.
- Takahashi, A., Yang, F. H., and Yang, R.T. (2002). New sorbents for desulfurization by π -complexation: Thiophene/benzene adsorption. Industrial and Engineering Chemistry Research 41: 2487-2496.
- Topsoe, H., Clausen, B. S., and Massoth, F. E. (1996). Hydrotreating Catalysis. Science and Technology 11: 310.

- United States Environmental Protection Agency. (1996). Motor vehicles: Environmental standards, pp. 27-31. Cite in Central pollution control board, Ministry of Environment & Forests (2000). Environmental standards for ambient air, automobiles, fuel, industries and noise. New Delhi: Creative Graphics.
- Vignier, F., Berthou, F., and Picart, D. (1983). Influence of injection systems on the gas chromatographic analysis of oxygenated dibenzothiophenes. Journal of High Resolution Chromatography and Chromatography Communications 6: 661-665.
- Vijaya, S., Chow, M. C., and Ma, A. N. (2004). Energy database of the oil palm. MPOB Palm Oil Engineering Bulletin 70: 15-22.
- Wauquier, J. P. (1995). Petroleum Refining, 1 vol. Crude Oil, Petroleum Products, and Process Flowsheets, p. 315. Paris: Technip.
- Weitkamp, J., Schwark, M., and Ernest, S. (1991). Removal of thiophene impurities from benzene by selective adsorption in zeolite ZSM-5. Journal of the Chemical Society, Chemical Communications 16: 1133.
- Williams, P. T., and Bottrill, R. P. (1995). Sulfur-polycyclic aromatic hydrocarbons in tyre pyrolysis oil. Fuel 74: 736-742.
- Williams P. T., and Brindle A. J. (2003). Temperature selective condensation of tyre pyrolysis oils to maximise the recovery of single ring aromatic compounds. Fuel 82: 1023-1031.
- Williams P. T., and Taylor D. T. (1993). Aromatization of tyre pyrolysis oil to yield polycyclic aromatic hydrocarbons. Fuel 72: 1469-1474.
- Williams P. T., and Taylor D. T. (1994). Molecular weight range of pyrolytic oils derived from tyre waste. Journal of Analytical and Applied Pyrolysis 29: 111-128.
- Wolfson, D. E., Beckman, J. A., Walters, J. G., and Bennett, D. J. (1969). Destructive distillation of scrap tyres. US Department of the Interior Bureau of Mines Report of Investigations 7302.
- Yang, R. T., Hernandez-Maldonado, A. J., and Yang, F. H. (2003). Desulfurization of transportation fuels with zeolites under ambient conditions. Science 301: 79-81.

- Youji, L., Shiyong, Z., Qumin, Y., and Wenbin, Y. (2007). The effects of activated carbon supports on the structure and properties of TiO₂ nanoparticles prepared by a sol-gel method. Applied Surface Science 253: 9254–9258.
- Yu, J., and Wang, B. (2010). Effect of calcination temperature on morphology and photoelectrochemical properties of anodized titanium dioxide nanotube arrays. Applied Catalysis B: Environmental 94: 295-302.
- Yu, J. G., Su, Y. R., and Cheng, B. (2007). Template-Free Fabrication and enhanced photocatalytic activity of hierarchical macro-/mesoporous titania. Advanced Functional Materials 17: 1984-1990.
- Yu, J. G., Zhang, L. J., Cheng, B., and Su, Y. R. (2007). Hydrothermal preparation and photocatalytic activity of hierarchically sponge-like macro-/mesoporous titania, Journal of Physical Chemistry C 111: 10582-10589.
- Zabaniotou, A., et al. (2004). Activated carbon from used tires using industrial pyrolyser and pilot activation furnace. Journal of Analytical and Applied Pyrolysis 72: 289-297.
- Zhang, H., and Banfield, J. F. (1998). Thermodynamic analysis of phase stability of nanocrystalline titania. Journal of Materials Chemistry 8: 2073.
- Zhang, H., and Banfield, J. F. (2000). Understanding polymorphic phase transformation behavior during growth of nanocrystalline aggregates: Insights from TiO₂. Journal of Physical Chemistry B 104: 3481.
- Zhao, D., Li, F., Han, J., and Li, H. (2007). Photochemical oxidation of thiophene by O₂ in an organic two-phase liquid-liquid extraction system. Petroleum Chemistry 47: 448–451.
- Zhou, L. (2007). Adsorption. Progress in Fundamental and Application Research Selected Reports at the 4th Pacific Basin Conference on Adsorption Science and Technology, pp. 241-242. Singapore: World Scientific.



APPENDICES

ศูนย์วิทยทรัพยากร
จุฬาลงกรณ์มหาวิทยาลัย

APPENDIX A

CALCULATION OF PRODUCT YIELDS

The total conversion and product yields were calculated by the following expressions:

$$\% \text{Liquid yield} = 100 \times \left[\frac{W_{\text{Liq}}}{W_{\text{Daf}}} \right]$$

$$\% \text{Solid yield} = 100 \times \left[\frac{W_{\text{R}}}{W_{\text{Daf}}} \right]$$

$$\% \text{Gas yield} = 100 - \% \text{Liquid yield} - \% \text{Solid yield}$$

where:

W_{Daf} = weight of dry-ash free waste tire

W_{R} = weight of dry-ash free residue remained after THF solvent washing and drying

W_{Liq} = weight of liquid

Example:

Pyrolysis condition:

- Reaction temperature: 400°C
- Reaction time: 10 min
- N₂ flow rate: 0.1 L/min

Calculation:

Weight of initial waste tire = 100 g

Weight of dry-ash free waste tire = 92.46 g

Weight of pyrolysis light oil = 36.61 g

Weight of pyrolysis heavy oil = 12.94 g

Weight of liquid = 49.55 g

Weight of dry-residue solid = 39.47 g

Weight of dry-ash free residue solid = 35.31 g

$$\% \text{Liquid yield} = 100 \times \left[\frac{49.55}{92.46} \right] = 53.59$$

$$\% \text{Solid yield} = 100 \times \left[\frac{35.31}{92.46} \right] = 38.19$$

$$\% \text{Gas yield} = 100 - 53.59 - 38.19 = 8.22$$

ศูนย์วิทยพัชกร
จุฬาลงกรณ์มหาวิทยาลัย

APPENDIX B

CALCULATION OF GROSS CALORIFIC HEATING VALUE

Gross calorific heating value of solid was determined following Standard Test Method for Gross Calorific Value of Coal and Coke by Adiabatic Bomb Calorimeter (ASTM D2015)

Summary of Test Method

The heat capacity of the calorimeter is determined by burning a specified mass of benzoic acid in oxygen. A comparable amount of the analysis sample is burned under the conditions in the calorimeter. The calorific value of the analysis sample is computed by multiplying the corrected temperature rise, adjusted for extraneous heat effects, by the heat capacity and dividing by the mass of the sample.

Apparatus

1. Oxygen Bomb Calorimeter

Reagents

1. Distilled Water
2. Standard benzoic acid available from the National Institute of Standards and Technology (NIST)
3. Oxygen 99.5%
4. Methyl orange
5. Sodium carbonate (Na_2CO_3) (Dissolve 3.57 g of sodium carbonate, dried for 24 h at 105°C in deionized water, and diluted to 1L).
6. Water for washing of the bomb interior (1 mL of methyl orange is diluted in 1L of deionized water).

Determination of the heat capacity of the calorimeter

1. Weigh 0.8-1.2 g of benzoic acid into a sample holder. Record sample weight to the nearest 0.0001g.
2. Connect a measured fuse in accordance with manufacturer's guidelines.

3. Rinse the bomb with water to wet internal seals and surface areas of the bomb or precondition the calorimeter according to the manufacturer's instructions. Add 1.0 mL of water to the bomb before assembly.
4. Assemble the bomb. Admit oxygen to the bomb to a consistent pressure of between 30 atm. The same pressure is used for each heat capacity run. Control oxygen flow to the bomb so as not to blow material from the sample holder.
5. Fill the calorimeter vessel with water at a temperature not more than 2°C below room temperature and place the assembled bomb in the calorimeter. Check that no oxygen bubbles are leaking from the bomb.
6. Allow 5 min for the temperature of the calorimeter vessel to stabilize.
7. Fire the charge.
8. For adiabatic calorimeters adjust the jacket temperature to match that of the calorimeter vessel temperature during a period of the rise. Record the first reading after the rate of change has stabilized the final temperature.
9. Open the calorimeter and remove the bomb.

Follow the procedures as described in 1-9 for determination of heat capacity of waste tire and pyrolysis oil. Calculate the gross calorific value using the following equation:

$$Q_v(\text{gross}) = \frac{[(TE) - e_1 - e_2 - e_3]}{g}$$

where:

$Q_v(\text{gross})$ = gross calorific value at constant volume as determined (J/g)

E = the heat capacity of the calorimeter (J/°C)

T = corrected temperature rise (°C)

e_1 = volume of the titrant (sodium carbonate) (mL)

e_2 = the length of fuse consumed during combustion (cm) x the heat of combustion the firing fuse (J/cm)

e_3 = 25×10^3 (J) x wt% sulfur in the sample x mass of sample (g)

g = mass of the sample (g)

APPENDIX C

CALCULATION OF %SULFUR REMOVAL

The influence of extracting solvent on the degree of photocatalytic desulfurization of the pyrolysis oil derived from waste tire can be calculated as shown below:

Condition:

TiO ₂ dosage:	7 g/L of pyrolysis oil
Reaction temperature:	50°C
Pyrolysis oil/extracting solvent:	1/4 v/v
Type of extracting solvent:	acetonitrile
Air flow rate:	150 ml/min

% Sulfur removal was calculated using the following equation:

$$X = \frac{(C_0 - C_1)}{C_0} \times 100$$

Where:

X	=	%Sulfur removal
C ₀	=	initial sulfur concentration (wt%)
C ₁	=	sulfur concentration after t hours reaction (wt%)

Table C-1 The influence of extracting solvent on degree of desulfurization

Extracting solvent	Irradiation time (h)	C ₀ (wt%)	C ₁ (wt%)	% Sulfur removal
acetonitrile	0	0.7665	0.7665	0
	1	0.7665	0.611	20.29
	3	0.6765	0.391	42.20
	5	0.7665	0.4395	42.66
	7	0.6765	0.3815	43.61

% Sulfur removal of pyrolysis oil after photocatalytic desulfurization for 7 h was calculated as followed:

$$\begin{aligned}\% \text{Sulfur removal} &= \frac{(C_0 - C_1)}{C_0} \times 100 \\ \% \text{Sulfur removal} &= \frac{(0.6765 - 0.3815)}{0.6765} \times 100 \\ &= 43.61 \%\end{aligned}$$



ศูนย์วิทยทรัพยากร
จุฬาลงกรณ์มหาวิทยาลัย

APPENDIX D

DATA OF SULFUR REMOVAL EFFICIENCY

Table D-1 Influence of TiO₂ dosage on the degree of sulfur removal

TiO ₂ dosage (g/L)	Irradiation time (h)	C ₀ * (wt%)	C ₁ ** (wt%)	% Sulfur removal
1	0	0.8174	0.8174	0
	1	0.8174	0.7906	3.27
	3	0.8174	0.7491	8.35
	5	0.8174	0.7366	9.88
	7	0.8174	0.7301	10.7
3	0	0.8511	0.8511	0
	1	0.8511	0.7694	9.60
	3	0.9705	0.8021	17.4
	5	0.8511	0.6884	19.1
	7	0.7772	0.6049	22.2
5	0	0.6855	0.6855	0
	1	0.6855	0.6207	9.45
	3	0.6855	0.5547	19.1
	5	0.6855	0.5348	22.0
	7	0.6855	0.5219	23.9
7	0	0.7850	0.7850	0
	1	0.7850	0.6823	13.1
	3	0.7850	0.5872	25.2
	5	0.7850	0.5827	25.8
	7	0.7850	0.5655	28.0
10	0	0.9642	0.9642	0
	1	0.9642	0.8525	11.6
	3	0.9272	0.7415	20.0
	5	0.9642	0.7140	26.0
	7	0.9642	0.7155	25.8

* C₀ = initial sulfur concentration (wt%)

** C₁ = sulfur concentration after t hours reaction (wt%)

Table D-2 Influence of calcination temperature of TiO₂ on degree of sulfur removal

Calcination temperature (°C)	Irradiation time (h)	C ₀ (wt%)	C ₁ (wt%)	% Sulfur removal
Degussa P-25	0	0.8479	0	0
	1	0.8479	0.7444	12.2
	3	0.8479	0.6623	21.9
	5	0.8479	0.6280	25.9
	7	0.8911	0.6275	29.6
400°C	0	0.8096	0	0
	1	0.8096	0.7195	11.1
	3	0.8372	0.7000	16.4
	5	0.8372	0.6479	22.6
	7	0.8096	0.6116	24.5
600°C	0	0.8339	0	0
	1	0.8339	0.7598	8.89
	3	0.8491	0.7120	16.1
	5	0.8491	0.6869	19.1
	7	0.8491	0.6702	21.1
800°C	0	0.8409	0	0
	1	0.8409	0.7803	7.20
	3	0.8409	0.7511	10.7
	5	0.8409	0.7382	12.2
	7	0.8409	0.7260	13.7

Table D-3 Influence of reaction temperature on degree of sulfur removal

Reaction temperature (°C)	Irradiation time (h)	C ₀ (wt%)	C ₁ (wt%)	% Sulfur removal
30°C	0	0.7850	0	0
	1	0.7850	0.6823	13.1
	3	0.7850	0.5872	25.2
	5	0.7850	0.5827	25.8
	7	0.7850	0.5655	28.0
40°C	0	0.8372	0	0
	1	0.8372	0.7354	12.2
	3	0.8372	0.6599	21.2
	5	0.8372	0.6242	25.4
	7	0.8372	0.6066	27.5
50°C	0	0.8479	0	0
	1	0.8479	0.7444	12.2
	3	0.8479	0.6623	21.9
	5	0.8479	0.6280	25.9
	7	0.8911	0.6275	29.6
70°C	0	0.7239	0	0
	1	0.7239	0.6084	16.0
	3	0.7239	0.5533	23.6
	5	0.7239	0.5298	26.8
	7	0.7239	0.4994	31.0

Table D-4 Influence of air flow rate on degree of sulfur removal

Air flow rate (mL/min)	Irradiation time (h)	C ₀ (wt%)	C ₁ (wt%)	% Sulfur removal
0	0	0.8375	0	0
	1	0.8375	0.8095	3.34
	3	0.8375	0.8155	2.63
	5	0.8375	0.8175	2.39
	7	0.8375	0.8105	3.22
50	0	0.8305	0	0
	1	0.8305	0.8045	3.13
	3	0.8305	0.7595	8.55
	5	0.8305	0.6900	16.9
	7	0.8305	0.6450	22.3
100	0	0.8395		
	1	0.8395	0.7620	9.23
	3	0.8395	0.6850	18.4
	5	0.8395	0.6385	23.9
	7	0.8395	0.5665	32.5
150	0	0.8385	0	0
	1	0.8385	0.7435	11.3
	3	0.8385	0.6515	22.3
	5	0.8385	0.5970	28.8
	7	0.8385	0.5495	34.5

Table D-5 Influence of H₂O₂ concentration on degree of sulfur removal

	H ₂ O ₂ concentration (wt%)	C ₀ (wt%)	C ₁ (wt%)	% Sulfur removal
Air (flow rate 150 mL/min)	0	0.8385	0.5495	34.5
	3	0.7055	0.6775	3.97
	10	0.7055	0.6315	10.5
	30	0.7055	0.6060	14.1
Without of Air	0	0.8375	0.8105	3.22
	3	0.7055	0.6215	11.9
	10	0.7055	0.5805	17.7
	30	0.7055	0.4750	32.7

ศูนย์วิทยทรัพยากร
จุฬาลงกรณ์มหาวิทยาลัย

Table D-6 Influence of pyrolysis oil/extracting solvent on degree of sulfur removal

Pyrolysis oil/ extracting solvent (v/v)	Irradiation time (h)	C ₀ (wt%)	C ₁ (wt%)	% Sulfur removal
1/1	0	0.8479	0	0
	1	0.8479	0.7444	12.2
	3	0.8479	0.6623	21.9
	5	0.8479	0.6280	25.9
	7	0.8911	0.6275	29.6
1/2	0	0.944	0	0
	1	0.944	0.8555	9.38
	3	0.944	0.7750	17.9
	5	0.944	0.7225	23.5
	7	0.944	0.6840	27.5
1/3	0	0.729	0	0
	1	0.729	0.6425	11.9
	3	0.729	0.5870	19.5
	5	0.729	0.5275	27.6
	7	0.729	0.5100	30.0
1/4	0	0.8385	0	0
	1	0.8385	0.7435	11.3
	3	0.8385	0.6515	22.3
	5	0.8385	0.5970	28.8
	7	0.8385	0.5495	34.5
1/5	0	0.929	0	0
	1	0.929	0.8285	10.8
	3	0.929	0.7350	20.9
	5	0.929	0.6805	26.8
	7	0.929	0.6215	33.1

Table D-7 Influence of extracting solvent on degree of sulfur removal

Type of extracting solvent	Irradiation time (h)	C ₀ (wt%)	C ₁ (wt%)	% Sulfur removal
Distilled water	0	0.8385	0	0
	1	0.8385	0.7435	11.3
	3	0.8385	0.6515	22.3
	5	0.8385	0.5970	28.8
	7	0.8385	0.5495	34.5
Methanol	0	0.8385	0	0
	1	0.8385	0.5885	13.0
	3	0.8385	0.5075	25.0
	5	0.8385	0.4595	32.1
	7	0.8385	0.4280	36.7
Acetonitrile	0	0.7665	0	0
	1	0.7665	0.6110	20.3
	3	0.6765	0.3910	42.2
	5	0.7665	0.4395	42.7
	7	0.6765	0.3815	43.6

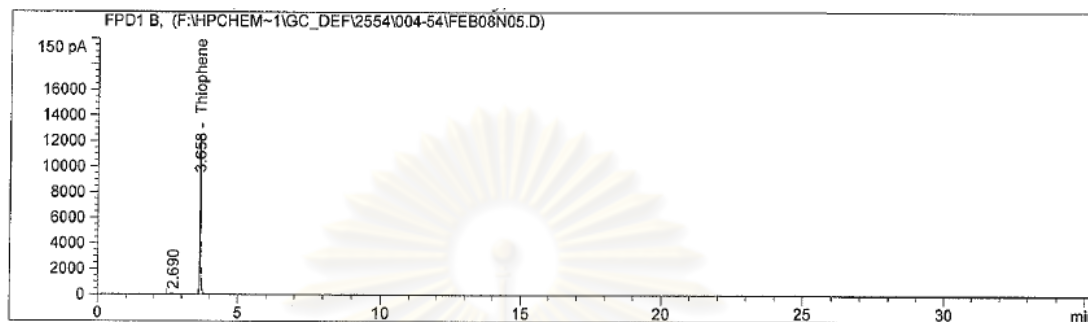
ศูนย์วิทยทรัพยากร
จุฬาลงกรณ์มหาวิทยาลัย

Table D-8 Influence of the stage on degree of sulfur removal

Stage of the reaction	Irradiation time (h)	C ₀ (wt%)	C ₁ (wt%)	% Sulfur removal
Stage 1	7	0.7145	0.4725	40.2
		0.7145	0.4390	38.6
		0.7145	0.4190	41.4
		0.7145	0.4185	41.4
		0.7145	0.4305	39.8
Stage 2	7	0.7145	0.4095	42.7
		0.7145	0.4075	43.0
Stage 3	7	0.7145	0.3750	47.5

ศูนย์วิทยทรัพยากร
จุฬาลงกรณ์มหาวิทยาลัย

APPENDIX E

GC-FPD CHROMATOGRAMS OF STANDARD SULFUR
COMPOUNDS, PYROLYSIS OIL AND OXIDIZED PYROLYSIS OIL

Area Percent Report

Sorted By : Signal
 Calib. Data Modified : 15/2/2011 15:14:15 PM
 Multiplier : 1.0000
 Dilution : 1.0000
 Use Multiplier & Dilution Factor with ISTDs

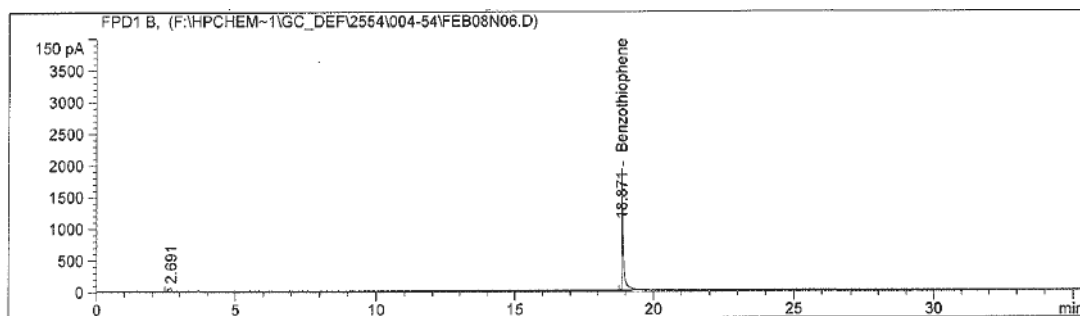
Signal 1: FPD1 B,

Peak #	RetTime [min]	Type	Width [min]	Area 150 pA*s	Area %	Name
1	2.690	BBA	0.0948	367.79865	1.44656	?
2	3.658	BB S+	0.0310	2.50579e4	98.55344	Thiophene
3	18.870	+	0.0000	0.00000	0.00000	Benzothiophene
4	24.998	+	0.0000	0.00000	0.00000	Dibenzothiophene

Totals : 2.54257e4

Figure E-1 GC-FPD Chromatogram of thiophene.

ศูนย์วิทยทรัพยากร
จุฬาลงกรณ์มหาวิทยาลัย



=====
 Area Percent Report
 =====

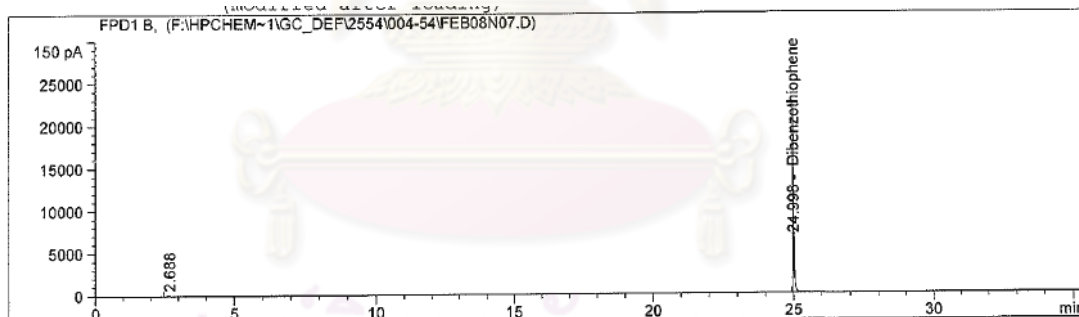
Sorted By : Signal
 Calib. Data Modified : 15/2/2011 15:14:15 PM
 Multiplier : 1.0000
 Dilution : 1.0000
 Use Multiplier & Dilution Factor with ISTDs

Signal 1: FPD1 B,

Peak #	RetTime [min]	Type	Width [min]	Area 150 pA*s	Area %	Name
1	2.691	BB	0.0902	352.08899	4.37481	?
2	3.657	+	0.0000	0.00000	0.00000	Thiophene
3	18.871	BB +	0.0549	7696.01318	95.62519	Benzothiophene
4	24.998	+	0.0000	0.00000	0.00000	Dibenzothiophene

Totals : 8048.10217

Figure E-2 GC-SPD Chromatogram of benzothiophene.



=====
 Area Percent Report
 =====

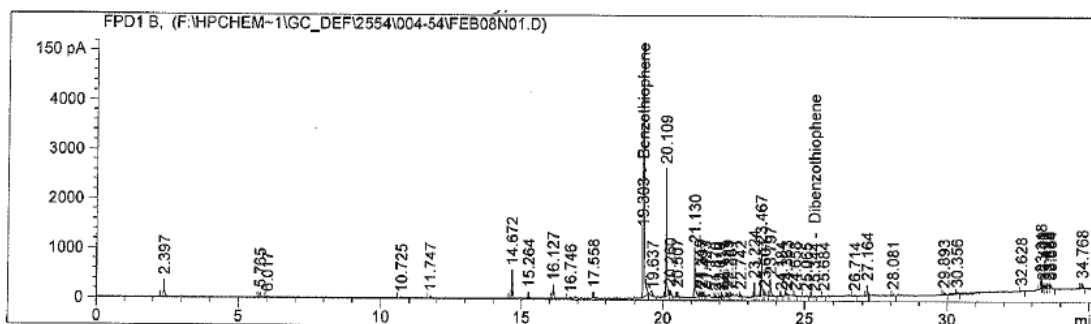
Sorted By : Signal
 Calib. Data Modified : 15/2/2011 15:14:15 PM
 Multiplier : 1.0000
 Dilution : 1.0000
 Use Multiplier & Dilution Factor with ISTDs

Signal 1: FPD1 B,

Peak #	RetTime [min]	Type	Width [min]	Area 150 pA*s	Area %	Name
1	2.688	BBA	0.0971	372.17386	0.82587	?
2	3.657	+	0.0000	0.00000	0.00000	Thiophene
3	18.870	+	0.0000	0.00000	0.00000	Benzothiophene
4	24.998	BB S+	0.0299	4.46921e4	99.17413	Dibenzothiophene

Totals : 4.50643e4

Figure E-3 GC-SPD Chromatogram of dibenzothiophene.



=====
 Area Percent Report
 =====

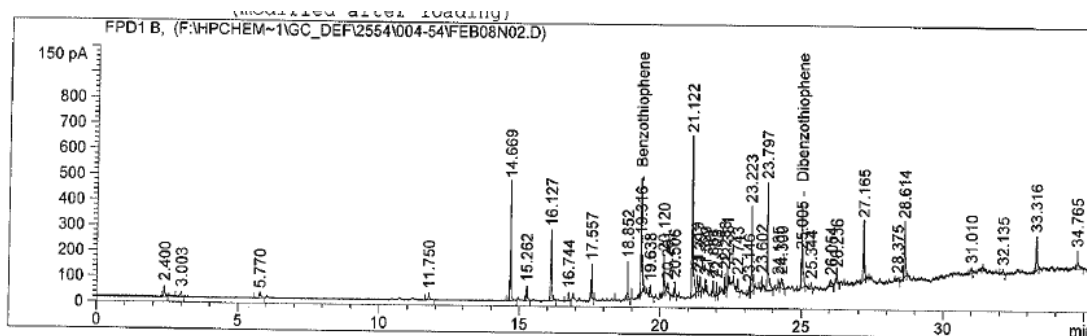
Sorted By : Signal
 Calib. Data Modified : 15/2/2011 15:14:15 PM
 Multiplier : 1.0000
 Dilution : 1.0000
 Use Multiplier & Dilution Factor with ISTDs

Signal 1: FPD1 B,

Peak #	RetTime [min]	Type	Width [min]	Area 150 pA*s	Area %	Name
1	2.397	BB	0.0419	988.63104	1.48845	?
2	3.657	+	0.0000	0.00000	0.00000	Thiophene
3	5.765	BB	0.0448	274.49982	0.41328	?
4	6.017	BB	0.0523	77.06835	0.11603	?
5	10.725	BB	0.0665	82.99491	0.12495	?
6	11.747	BB	0.0585	189.15665	0.28479	?
7	14.672	BB	0.0329	1237.51562	1.86317	?
8	15.264	BB	0.0293	249.33667	0.37539	?
9	16.127	BB	0.0452	783.79687	1.18006	?
10	16.746	BB	0.0469	85.75585	0.12911	?
11	17.558	BB	0.0203	154.94948	0.23329	?
12	19.303	BB S+	0.0251	4.69237e4	70.64686	Benzothiophene
13	19.637	BB	0.0323	109.95228	0.16554	?
14	20.109	BB	0.0283	4856.82520	7.31229	?
15	20.260	BB	0.0384	200.79262	0.30231	?
16	20.507	BB	0.0277	199.62366	0.30055	?
17	21.130	BB	0.0387	2587.16626	3.89516	?
18	21.319	BB	0.0368	181.81657	0.27374	?
19	21.397	BB	0.0282	117.63087	0.17710	?
20	21.493	BB	0.0324	107.97620	0.16257	?
21	21.870	BB	0.0276	97.85920	0.14733	?
22	22.010	BB	0.0278	93.00357	0.14002	?
23	22.111	BB	0.0268	88.75854	0.13363	?
24	22.289	BB	0.0275	135.13925	0.20346	?
25	22.381	BB	0.0230	86.87179	0.13079	?
26	22.742	BB	0.0275	114.27282	0.17205	?
27	23.224	BB	0.0268	461.13141	0.69427	?
28	23.467	BB	0.0322	2072.94214	3.12096	?
29	23.601	BB	0.0355	124.61573	0.18762	?
30	23.797	BB	0.0368	878.62378	1.32283	?
31	24.184	BB	0.0383	72.34771	0.10892	?
32	24.363	BB	0.0441	108.21837	0.16293	?
33	24.658	BB	0.0529	94.03298	0.14157	?
34	25.065	BB	0.0621	108.30693	0.16306	?
35	25.344	BB +	0.0717	117.09983	0.17630	Dibenzothiophene
36	25.684	BB	0.0436	89.25237	0.13438	?
37	26.714	BB	0.0668	97.34534	0.14656	?
38	27.164	BB	0.0328	439.18588	0.66122	?
39	28.081	BB	0.0413	104.05874	0.15667	?
40	29.893	BB	0.0574	168.86597	0.25424	?
41	30.356	BB	0.0394	100.41531	0.15118	?
42	32.628	BB	0.0554	82.48135	0.12418	?
43	33.318	BB	0.0294	442.19479	0.66576	?
44	33.400	BB	0.0359	130.66440	0.19672	?
45	33.492	BB	0.0386	126.89476	0.19105	?
46	33.580	BB	0.0360	144.41901	0.21743	?
47	33.664	BB	0.0408	172.41708	0.25959	?
48	34.768	BB	0.0353	259.46109	0.39064	?

Totals : 6.64200e4

Figure E-4 GC-SPD Chromatogram of pyrolysis oil.



=====
 Area Percent Report
 =====

Sorted By : Signal
 Calib. Data Modified : 15/2/2011 15:14:15 PM
 Multiplier : 1.0000
 Dilution : 1.0000
 Use Multiplier & Dilution Factor with ISTDs

Signal 1: FPD1 B,

Peak #	RetTime [min]	Type	Width [min]	Area 150 pA*s	Area %	Name
1	2.400	BB	0.0413	128.76469	1.05399	?
2	3.003	BB	0.0487	76.58017	0.62684	?
3	3.657	+	0.0000	0.00000	0.00000	Thiophene
4	5.770	BBA	0.0529	78.45624	0.64219	?
5	11.750	BB	0.0579	107.61383	0.88086	?
6	14.669	BB	0.0334	1009.67273	8.26454	?
7	15.262	BB	0.0337	124.52573	1.01929	?
8	16.127	BB	0.0469	804.56757	6.58568	?
9	16.744	BB	0.0462	100.90537	0.82595	?
10	17.557	BB	0.0208	168.23999	1.37711	?
11	18.852	BB	0.0269	259.42654	2.12350	?
12	19.316	+	0.0347	1070.47766	8.76225	Benzo thiophene
13	19.638	BB	0.0381	113.24374	0.92694	?
14	20.120	BB	0.0360	372.16516	3.04631	?
15	20.261	BB	0.0455	95.46056	0.78138	?
16	20.506	BB	0.0279	103.57001	0.84776	?
17	21.122	BB	0.0362	1601.50098	13.10888	?
18	21.319	BB	0.0380	154.46274	1.26433	?
19	21.397	BB	0.0278	100.35621	0.82145	?
20	21.599	BB	0.0261	70.31157	0.57553	?
21	21.868	BB	0.0280	108.85940	0.89105	?
22	22.008	BB	0.0256	85.48880	0.69976	?
23	22.288	BB	0.0279	136.13994	1.11436	?
24	22.381	BB	0.0229	88.41621	0.72372	?
25	22.743	BB	0.0284	93.08406	0.76193	?
26	23.146	BB	0.0380	75.84673	0.62083	?
27	23.223	BB	0.0315	693.42914	5.67597	?
28	23.602	BB	0.0256	71.08342	0.58184	?
29	23.797	BB	0.0344	1008.69067	8.25651	?
30	24.185	BB	0.0410	101.73309	0.83272	?
31	24.300	BB	0.0605	162.95212	1.33382	?
32	25.005	BB	0.0396	887.21631	7.26219	Dibenzo thiophene
33	25.344	BB	0.0482	87.45048	0.71581	?
34	26.054	BB	0.0464	91.18525	0.74638	?
35	26.236	BB	0.0311	92.03606	0.75335	?
36	27.165	BB	0.0346	541.03845	4.42860	?
37	28.375	BB	0.0646	82.84483	0.67812	?
38	28.614	BB	0.0404	580.73810	4.75356	?
39	31.010	BB	0.0532	90.13110	0.73776	?
40	32.135	BB	0.0571	80.18832	0.65637	?
41	33.316	BB	0.0333	296.71469	2.42872	?
42	34.765	BB	0.0441	221.35135	1.81184	?

Totals : 1.22169e4

Figure E-5 GC-SPD Chromatogram of oxidized pyrolysis oil.

VITA

Miss Phakakrong Trongkaew was born on September 18, 1982 in Nakhon Si Thammarat, Thailand. She graduated Bachelor's degree of Science (first-class honor) from Department of Chemistry, Faculty of Science and Technology, Yala Rajabhat University in 2005. She has been a graduate student studying in the program of Petrochemistry and Polymer Science at Faculty of Science, Chulalongkorn University and finished her study in 2010.

Articles in peer-reviewed conference proceedings

Trongkaew, P., Utisthum, T., and Hinchiranan, N. (2010). Desulfurization of Waste Tire Pyrolysis Oil via Photo-oxidation Catalyzed by Titanium Dioxide. Proceeding of the GMSTEC 2010: International Conference for a Sustainable Greater Mekong Subregion, August 26-27, Bangkok, Thailand.



ศูนย์วิทยทรัพยากร
จุฬาลงกรณ์มหาวิทยาลัย